UNIVERSITAT POLITÈCNICA DE VALÈNCIA

INSTITUTO INTERUNIVERSITARIO DE RECONOCIMIENTO MOLECULAR Y DESARROLLO TECNOLÓGICO

Optical detection of chemical species of environmental and biological relevance using molecular sensors and hybrid materials

PhD. THESIS

Submitted by

Maria Lo Presti

PhD. Supervisors:

Prof. Ramón Martínez Máñez
Dr. José Vicente Ros Lis

Valencia, July 2021

RAMÓN MARTÍNEZ MÁÑEZ, PhD in Chemistry and Professor at the *Universitat Politècnica de València*, and JOSÉ VICENTE ROS-LIS, PhD in Chemistry and Associate Professor at the *Universitat de València*.

CERTIFY:

That the work *"Optical detection of chemical species of environmental and biological relevance using molecular sensors and hybrid materials"* has been developed by Maria Lo Presti under their supervision in the Instituto Interuniversitario de Investigación de Reconocimiento Molecular y Desarrollo Tecnológico (IDM) of the *Universitat Politècnica de València*, as a Thesis Project in order to obtain the degree of PhD in Chemistry at the *Universitat Politècnica de València.*

Valencia, July 5th 2021.

Prof. Ramón Martínez Máñez Dr. José Vicente Ros-Lis

A mia madre, per sostenermi e amarmi in ogni momento della mia vita.

“Siempre estoy haciendo lo que no puedo hacer, para poder aprender cómo hacerlo”
Pablo Picasso

“Velle parum est; cupias, ut re potiaris, oportet”
Ovidio

“Many of life's failures are people who did not realize how close they were to success when they gave up”
Thomas Edison

Έτσι, δεν γνωρίζω’Σωκράτης

Acknowledgements

Agradecimientos

En primer lugar, quiero agradecer a mis directores de tesis, Ramón, Félix y José Vicente, por haberme acompañada en este camino tan importante y significativo.

Gracias Ramón, por haberme dado la oportunidad de ser parte de tu grupo, un grupo que en todo momento me ha dado orgullo. Pocas personas tienen la suerte de ser parte de un grupo tan prestigioso e internacional como el tuyo; gracias por ser siempre tan profesional y por seguir creyendo en mí durante estos años. Gracias también por elegirme para representar a nuestro grupo en el congreso de Dijon, un evento que nunca olvidaré en mi vida, también porque me dio el honor de conocer personalmente el Premio Nobel Jean-Pierre Sauvage. Gracias, de corazón.

Gracias Félix, por haber estado siempre a mi lado desde el primer día que volví a Valencia, por ayudarme en los primeros pasos de mi tesis, por tu inmensa disponibilidad en todo momento. Fuiste tú mi primer contacto y fuiste tú el que me comunicó que había ganado la beca, que me cambió la vida. Sin ti todo esto no hubiera sido posible.

Gracias José Vicente, por ayudarme y animarme en el período más difícil de mi tesis, los últimos años, por ayudarme a ver las cosas desde la perspectiva correcta con tu calma, ayudándome a desenredar los nudos más complicados que han surgido, con tu forma de simplificar los problemas que a veces me parecían irresolubles.

Me gustaría agradecer también a Margarita Parra y a todo el grupo del IDM de la Universitat de València, donde desarrollé mi trabajo de fin de grado durante mi Erasmus en 2012, que me introdujo en el fascinante mundo de la química supramolecular.

Gracias a todo el grupo del Prof. Werner Nau, que me recibió en su laboratorio durante mi estancia en la Jacobs University de Bremen y especialmente a Andreas, por enseñarme a ser tan crítica y escrupulosa en cada momento.

Gracias a Manuela Raposo y su grupo de la Universidad de Braga, por la colaboración que tuvimos, sin la cual parte de esta tesis no existiría.

Gracias a todos mis compañeros de laboratorio con los que hemos compartido largos años de éxitos, fracasos, glorias y derrotas.

Gracias Luis Enrique, por enseñarme mucho con tu increíble alegría y pasión por la química. Gracias Sameh, por su tenacidad y tu ser incansable y sus valiosos consejos, tanto con respecto a la química como a la vida.

Acknowledgements

Gracias Toni, por tu amistad, por estar siempre ahí, por tu ayuda, tus consejos, tu apoyo, dentro y fuera del laboratorio. Has sido uno de mis pilares en Valencia y sigues siéndolo incluso ahora que ambos estamos lejos de allí.

Gracias Tania, por tu sonrisa, tu felicidad y tu forma de ver la vida con tanta positividad y por los viajes que compartimos.

Gracias Andy, por tu amabilidad, por ser tan alegre y sobre todo humilde, a pesar de ser uno de los químicos más valiosos que he conocido en este camino.

Gracias Hazem, por darme el honor de guiarte en los primeros momentos en que entraste, por tu amistad, educación y por todos los buenos momentos juntos.

Muchas gracias a todos los demás que habéis compartido conmigo no solamente un laboratorio, si no también momentos importantes de mi vida: Cris Marín, María, Lluís, Mar, Santi, Amelia, Cris de la Torre, Luis, Ángela, Adrián, Bea Lozano, Mónica, Alba, Elisa, Lorena, Irene, Borja, Xente, Ismael, Marta, Eva, Bea de Luis, Carol, Édgar, Andrea, Elena, Loles, Quique, Eva, Pablo, Luis Villascusa.

Arianna, Manoharan, Anita, Mirka, Muthu, Asha, gracias por los buenos momentos que hemos compartido durante vuestras estancias.

Gracias a mis amigos de baile latinos de la UPV, por permitirme conocer una parte de mí que no conocía, por vuestro apoyo, amistad y la felicidad que me habéis dado durante estos años.

Gracias a mis compañeros de Jijona, por todos los consejos y las sonrisas; gracias sobre todo a María y a Isabel, compañera, “madre” y amiga, por escucharme cuando conciliar trabajo y doctorado no fue fácil.

Gracias a la gente que me ha apoyado en Salamanca, sobre todo a Jesús por intentar ayudarme y por animarme en todo momento.

Gracias a todos mis amigos que me han apoyado en todos estos años largos, a veces difíciles.

Gracias también a todos los que, de una forma u otra, obstaculizaron mis pasos durante este viaje, me ayudó a ser más fuerte y a ser la persona que soy hoy.

Por supuesto gracias a mi familia, sobre todo a mi madre, a la que debo todo.

Resumen

La presente tesis doctoral titulada "Detección óptica de especies químicas de importancia ambiental y biológica utilizando sensores moleculares y materiales híbridos" se centra en el diseño, preparación, caracterización y evaluación de sensores químicos moleculares. El trabajo realizado se puede dividir en dos partes: (i) síntesis de sensores de cationes metálicos en disolución y (ii) síntesis y caracterización de nanopartículas híbridas orgánico-inorgánicas para el reconocimiento de especies químicas y biológicas.

En el primer capítulo se introduce el marco en el que se engloban los fundamentos teóricos de la química supramolecular en que se basan los estudios prácticos realizados durante la presente tesis doctoral. A continuación, en el capítulo dos, se presentan los objetivos generales de la tesis.

En el tercer capítulo se presenta un quimiodosímetro cromo-fluorogénico, capaz de detectar selectivamente cationes trivalentes entre cationes y aniones monovalentes y divalentes mediante una reacción de deshidratación en agua.

En el cuarto capítulo se presenta una unidad (BODIPY) conectada electrónicamente con un macrociclo dithia-dioxa-aza. Las soluciones de acetonitrilo y agua-acetonitrilo 95: 5 v / v de la sonda mostraron una banda ICT en la zona visible y son casi no emisivas. Cuando se utilizó acetonitrilo como disolvente, la adición de Hg (II) y cationes metálicos trivalentes indujo un cambio hipsocrómico de la banda de absorción y mejoras moderadas de la emisión. Se obtuvo una respuesta altamente selectiva al utilizar medios competitivos como agua-acetonitrilo 95:5 v/v. En este caso, sólo el Hg (II) indujo un cambio hipsocrómico de la banda de absorción y una mejora marcada de la emisión.

El quinto capítulo explora el desarrollo de sensores para berberina y amantadina. Dos moléculas de interés biológico por su uso como fármacos. Se han preparado tres sistemas de sensores basados en la aproximación de puertas moleculares. En concreto, sobre nanopartículas MCM-41 cargadas con rodamina B como unidad de señalización, se ha llevado a cabo la funcionalización con diversas aminas y el bloqueo de poros con cucurbituril CB7. Las aminas utilizadas son

ciclohexilamina, bencilamina y amantadina. Los materiales obtenidos se han caracterizado por técnicas de difracción de rayos X y microscopía electrónica de transmisión confirmando la estructura mesoporosa de las nanopartículas. Los materiales preparados muestran una respuesta a la berberina y la adamantina, quitando el tapón y liberando el tinte fluorescente al medio. La respuesta de los materiales a las dos sustancias de interés (berberina y amantadina) depende de la estructura química de cada uno de los materiales en función de las constantes de afinidad entre el analito y CB7. Los resultados obtenidos abren el camino al uso de puertas moleculares como sensores de berberina y amantadina.

Resum

La present tesi doctoral titulada "Detecció òptica d'espècies químiques d'importància ambiental i biològica utilitzant sensors moleculars i materials híbrids" se centra en el disseny, preparació, caracterització i avaluació de sensors químics moleculars. El treball realitzat es pot dividir en dues parts: (i) síntesi de sensors de cations metàl·lics en dissolució i (ii) síntesi i caracterització de nanopartícules híbrides orgànic-inorgànics per al reconeixement d'espècies químiques i biològiques.

En el primer capítol s'introdueix el marc en el qual s'engloben els fonaments teòrics de la química supramolecular en què es basen els estudis pràctics realitzats durant la present tesi doctoral. A continuació, en el capítol dos, es presenten els objectius generals de la tesi.

En el tercer capítol es presenta un quimiodosímetro crom-fluorogénic, capaç de detectar selectivament cations trivalents entre cations i anions monovalents i divalents mitjançant una reacció de deshidratació en aigua.

En el quart capítol es presenta una unitat (BODIPY) connectada electrònicament amb un macrocicle dithia-dioxa-aza. Les solucions de acetonitril i aigua-acetonitril 95:5 v/v de la sonda van mostrar una banda ICT a la zona visible i són gairebé no emisivas. Quan es va utilitzar acetonitril com a dissolvent, l'addició de Hg (II) i cations metàl·lics trivalents va induir un canvi hipsocròmic de la banda d'absorció i millores moderades de l'emissió. Es va obtenir una resposta altament selectiva a l'utilitzar mitjans competitius com aigua-acetonitril 95:5 v/v. En aquest cas, només el Hg (II) va induir un canvi hipsocròmic de la banda d'absorció i una millora marcada de l'emissió.

El cinquè capítol explora el desenvolupament de sensors per berberina i amantadina. Dues molècules d'interès biològic pel seu ús com a fàrmacs. S'han preparat tres sistemes de sensors basats en l'aproximació de portes moleculars. En concret, sobre nanopartícules MCM-41 carregades amb rodamina B com a unitat de senyalització, s'ha dut a terme la funcionalització amb diverses amines i el bloqueig de porus amb cucurbituril CB7. Les amines utilitzades són ciclohexilamina, bencilamina i amantadina. Els materials obtinguts s'han caracteritzat per tècniques

de difracció de raigs X i microscòpia electrònica de transmissió confirmant l'estructura mesoporosa de les nanopartícules. Els materials preparats mostren una resposta a la berberina i la adamantina, llevant el tap i alliberant el tint fluorescent a l'mig. La resposta dels materials a les dues substàncies d'interès (berberina i amantadina) depèn de l'estructura química de cada un dels materials en funció de les constants d'afinitat entre l'anàlit i CB7. Els resultats obtinguts obren el camí a l'ús de portes moleculars com a sensors de berberina i amantadina.

Summary

The present doctoral thesis entitled "Optical detection of chemical species of environmental and biological importance using molecular sensors and hybrid materials" focuses on the design, preparation, characterization and evaluation of molecular chemical sensors. The work carried out can be divided into two parts: (i) synthesis of metal cation sensors in solution and (ii) synthesis and characterization of hybrid organic-inorganic nanoparticles for the recognition of chemical and biological species.

The first chapter introduces the framework that encompasses the theoretical foundations of supramolecular chemistry on which the practical studies carried out during this doctoral thesis are based. Next, in chapter two, the general objectives of the thesis are presented.

In the third chapter, a chromium-fluorogenic chemodosimeter is presented, capable of selectively detecting trivalent cations by means of a dehydration reaction in water.

The fourth chapter presents a new compound containing a BODIPY unit electronically connected with a dithia-dioxa-aza macrocycle. Acetonitrile and water–acetonitrile 95:5 v/v solutions of the probe showed an ICT band in the visible zone and were nearly non-emissive. When acetonitrile was used as a solvent, addition of Hg(II) and trivalent metal cations induced an hypsochromic shift of the absorption band and moderate emission enhancements. A highly selective response was obtained when using competitive media such as water– acetonitrile 95:5 v/v. In this case only Hg(II) induced a hypsochromic shift of the absorption band and a marked emission enhancement.

The fifth chapter explores the development of sensors for berberine and amantadine; two molecules of biological interest due to their use as drugs. Three sensing systems based on a “molecular gate” approximation have been prepared. Specifically, MCM-41 nanoparticles were loaded with Rhodamine B as a signalling unit, functionalized with various amines and capped with cucurbituril CB7. The amines used are cyclohexylamine, benzylamine and amantadine., The materials obtained were characterized by X-ray diffraction techniques and transmission

electron microscopy, confirming the mesoporous structure of the nanoparticles. The prepared materials showed a response to berberine and adamantine, which induced release of the fluorescent dye to the medium. The response of the materials to the two substances of interest (berberine and amantadine) depends on the chemical structure of the capping ensemble and it is a function of the affinity constants between the analyte and CB7. The results obtained open the way to the use of gated materials as berberine and amantadine probes.

Publications

Results of this PhD Thesis and other contributions have resulted in the following scientific publications:

- **Maria Lo Presti,** Sameh El Sayed, Ramón Martínez-Máñez, Ana M. Costero, Salvador Gil, Margarita Parra and Félix Sancenón (2016). "Selective chromo-fluorogenic detection of trivalent cations in aqueous environments using a dehydration reaction". *New J. Chem.,* **2016**, 40, 9042-9045.
- **Maria Lo Presti,** Ramón Martínez-Máñez, José V. Ros-Lis, Rosa M. F. Batista, Susana P. G. Costa, M. Manuela M. Raposo and Félix Sancenón (2018) "A dual channel sulphur-containing macrocycle functionalised BODIPY probe for the detection of Hg(II) in mixed aqueous solution". *New J. Chem.*, **2018**, 42, 7863-7868.

Abbreviations and Acronyms

BODIPY	Boron-dipyrromethene
CB	Cucurbituril
CT	Charge tranfer
CTABr	Cetyltrimethylamonium bromide
CDCl3	Deuterated Chloroform
CIBER-BBN	Centro de Investigación Biomédica en Red en Bioingeniería, Biomateriales y Nanomedicina
DCM	Dichloromethane
DDQ	Dichloro Dicyano Benzoquinone
DMF	Dimethylformamide
DNA	Deoxyribonucleic Acid
DPA	Diphenylamine
EA	Elemental análisis
ELISA	Enzyme-Linked Immunosorbent Assay
ESI	Electronic Supporting Information
FEDER	European Fund for Regional Development
HOMO	Highest Occupied Molecular Orbital
HMBC	Heteronuclear multiple bond coherence
HMQC	Heteronuclear multiple quantum coherence
HPLC	High-performance liquid chromatography
HRMS	High Resolution Mass Spectra
ICT	Internal Charge Transfer
IR	Infrared
ISMEC	International Symposium on Metal Complexes
IUPAC	International Union of Pure and Applied Chemistry
LOD	Limit of detection
LUMO	Lowest Unoccupied Molecular Orbital
MCM	Mobile Composition of Matter
NAA	Nano-porous Anodic Alumina
NIR	Near-infrared
NMR	Nuclear magnetic resonance
PBS	Phosphate buffer saline

PhD	Doctor of Philosophy of Philosophy Doctorate
p-TsOH	p-Toluenesulfonic acid
RhB	Rhodamine B
TEM	Transmission electron microscopy
TEOS	Tetraethyl orthosilicate
TFA	Trifluoroacetic acid
THF	Tetrahydrofuran
TMOS	Tetramethyl orthosilicate
TMS	Trimethylsilyl
UPV	Universitat Politécnica de Valéncia
UV-vis	Ultraviolet-visible
XRD	X-ray diffraction
λ_{exc}	Excitation wavelength

Table of Contents

Chapter 1: General Introduction

1.1 Supramolecular chemistry

Supramolecular chemistry is the branch of chemistry that studies systems formed by two or more molecular species that interact with each other through noncovalent forces, i.e., weak interactions [1,2] (electrostatic, hydrophobic, hydrogen bonding, van der Waals, etc).

Nowadays, supramolecular chemistry, defined *"the chemistry beyond the molecules"* by the Nobel Laureate Jean- Marie Lehn, is a well stablished field inside the chemistry realm. While traditional chemistry deals with covalent bonds that form a molecule, supramolecular chemistry focuses on weak and reversible interactions between molecules.

In particular, this is a relatively young field of science, highly interdisciplinary and its roots go into organic and inorganic chemistry for molecular construction, coordination chemistry and metal-ligand interactions and physical chemistry and biochemistry.

The work presented in this PhD thesis is dedicated to the preparation of chemical probes and sensing hybrid organic-inorganic materials constructed bearing in mind some supramolecular chemistry principles. For this reason, main concepts related with supramolecular chemistry will be explained below.

---

[1] Lehn, J. M. "Supramolecular chemistry can help to understand better how to make efficient drugs". Universitat Autònoma de Barcelona, Spain. October **2012**. Lecture.

1.1.1. The origins of Supramolecular Chemistry

Although supramolecular chemistry established itself after the Nobel Prize in Chemistry 1987 of Charles Pedersen, Jean-Marie Lehn and Donald Cram, three of the pioneers of this new part of chemistry, the origins of supramolecular chemistry can be traced by the late nineteenth century, with the discovery of intermolecular forces in 1873 by Johannes van der Waals Diderik, Nobel Prize in Physics of 1910,[2] and the first isolation of cyclodextrins, made in 1891 by Antoine Villiers.

A big step forward was taken by Alfred Werner, Nobel Prize in Chemistry in 1913, for the theory of the octahedral configuration of transition metal complexes coordination presented in 1893. Another fundamental contribution was made by Hermann Emil Fischer, Nobel Prize in chemistry in 1902, who hypothesized the lock and key mechanism of enzyme-substrate interactions, presented in 1893.[3] As a consequence of these studies, the correlation between chemical and biological processes became increasingly important in the following years.

One of the pillars of supramolecular chemistry of the twenty-first century was the introduction of the concept of molecular receptor, suggested in 1906 by Paul Ehrlich, Nobel Prize in Physiology or Medicine of 1908.[4-6]

[2] a) J. D. Van der Waals, Nobel Lecture: Physics 1901-1921, **1967**, 255-265. b) J. D. Van der Waals, "On the continuity of the gaseous and liquid state", PhD Dissertation. Leiden University, 1873.
[3] a) A. Werner, Nobel Lecture: Chemistry 1901-1921, 1966, 256-269. b) K. Bowman-James, Acc. Chem. Res., 2005, 38, 671–678.
[4] F. Huang and E. V. Anslyn, Chem. Rev., **2015**, 115, 6999 —7000 CrossRef PubMed.
[5] J.-M. Lehn Angew. Chem., Int. Ed., **1988**, 27, 89 —112 CrossRef.
[6] L. Brunsveld, B. Folmer, E. W. Meijer and R. Sijbesma, Chem. Rev., **2001**, 101, 4071 —4098

The term supramolecule was introduced in 1937 by Karl Lothar Wolf, who used the term “übermoleküle” to describe hydrogen-bonded acetic acid dimers.[7] Two years later, Linus Pauling described in 1939 the hydrogen-bond.[8] However, it was only in 1987 when the discovery and study of the specific interactions of crown ethers and cryptands performed in 1967-1973 by the Nobel Prize in chemistry, Jean-Marie Lehn, Donald J. Cram and Charles J. Pedersen definitely established the specific field of supramolecular chemistry, a new and a solid branch of chemistry still growing. Moreover, in 2016, the Royal Swedish Academy of Sciences awarded the Nobel Prize in Chemistry "for the design and synthesis of molecular machines" to Jean-Pierre Sauvage, (who I was honoured to meet personally in Dijon, France, during ISMEC 2017), J. Fraser Stoddart and Bernard L. Feringa.

---

[7] K. L. Wolf, H. Frahm, H. Harms, Z Phys. Chem., Abt. B, **1937**, 36, 237-287.

[8] L. Pauling, The Nature of the Chemical Bond, Cornell University, Ithaca, NY, 1st ed., **1939**.

1.1.2. From molecular to supramolecular chemistry

For more than 100 years, chemistry has mainly focused on understanding the behavior of molecules and building them from the constituent atoms. While molecular chemistry, ''the chemistry of the covalent bond'' focuses itself on the structures, properties and reactions of individual molecules made up by atoms united by covalent and ionic bonds,[9] supramolecular chemistry studies the intermolecular interactions, with much larger length scales, for the creation of assemblies.[10]

The term supramolecular chemistry was first coined in 1978 by Jean-Marie Lehn, who defined it as "chemistry beyond the molecules" or "chemistry of non-covalent bond".[11-12] The difference between molecular and supramolecular chemistry was brilliantly explained by Prof. Lehn comparing the relationship between the individual family and the whole society (Figure 1).[1]

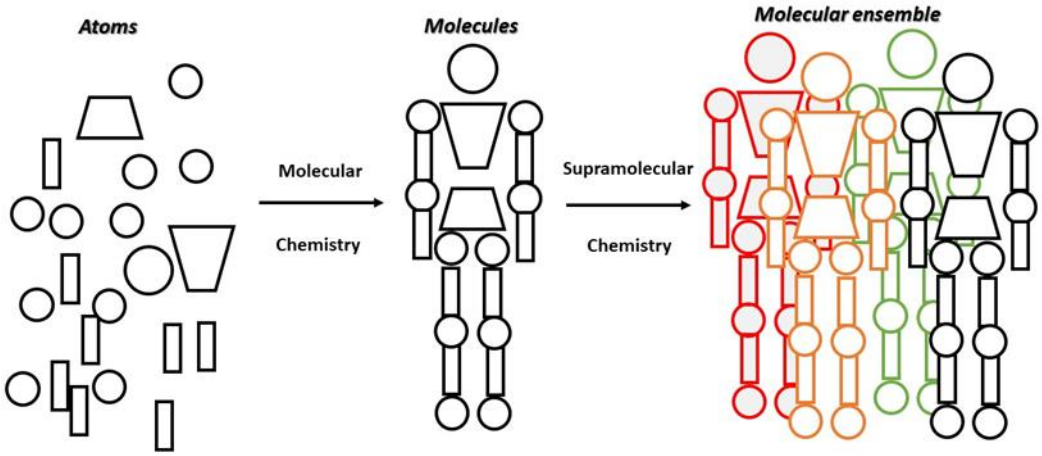

Figure 1. Schematic representation that illustrates the difference between molecular and supramolecular chemistry.

[9] K. Ariga, T. Kunitake, Supramolecular Chemistry-Fundamentals and application © Springer Verlag Berlin Heidelberg Edition **2006**.
[10] Lehn, J.-M. Supramolecular Chemistry; VCH: New York, **1995**.
[11] J. M. Lehn,Acc. Chem. Res., **1978**,11, 49–57
[12] J. M. Lehn, Angew. Chem., **1988**, 100, 91-116.

Molecules are like individual families, formed by persons who represents atoms. Each family has its special properties and the interaction between the members is controlled by molecular chemistry. However, the interaction between one family and others in the whole society to form bigger associations and alliances with different characteristics (supermolecule) are controlled by supramolecular chemistry.[13]

Supramolecular chemistry takes its origin in organic chemistry, which derives from studying the chemistry of living systems. It is precisely in nature that we can observe many examples of supramolecular interactions. One of the most important examples of biological supermolecule is DNA, whose structure was discovered by Francis Crick and James Watson, with the contributions of Maurice Wilkins and Rosalind Franklin. After many theories that DNA adopted a triple helix, they finally proposed the model of the "double helix" structure of DNA.

The helix conformation is obtained by combining two different types of supramolecular interactions namely (i) hydrogen bonds between the bases in different strands and (ii) π-π interactions between the aromatic rings of the nucleobases (Figure 2).

---

[13] J. M. Lehn, Supramolecular chemistry, Ed. VCH, **1995**.
[14] Pauling, L., Corey, R.B.: A proposed structure for the nucleic acids. PNAS39, 84–97, **1953**
[15] Watson, J.D., Crick, F.H.C.: A structure for deoxyribose nucleic acid. Nature171, 737–738, **1953**
[16] Wilkins, A.R., Stokes, A.R., Wilson, H.R.: Molecular structure of deoxypentose nucleic acids. Nature171, 738–740, **1953**
[17] Franklin, E.R., Gosling, R.G.: Molecular configuration in sodium thymonucleate. Nature171, 740–741, **1953**
[18] Franklin, E.R., Gosling, R.G.: Evidence for 2-chain helix in crystalline structure of sodium deoxyribonucleate. Nature172,156–157, **1953**
[19] Watson, J.D., Crick, F.H.C.: Genetical implications of the structure of deoxyribose nucleic acid. Nature171, 964–967, **1953**

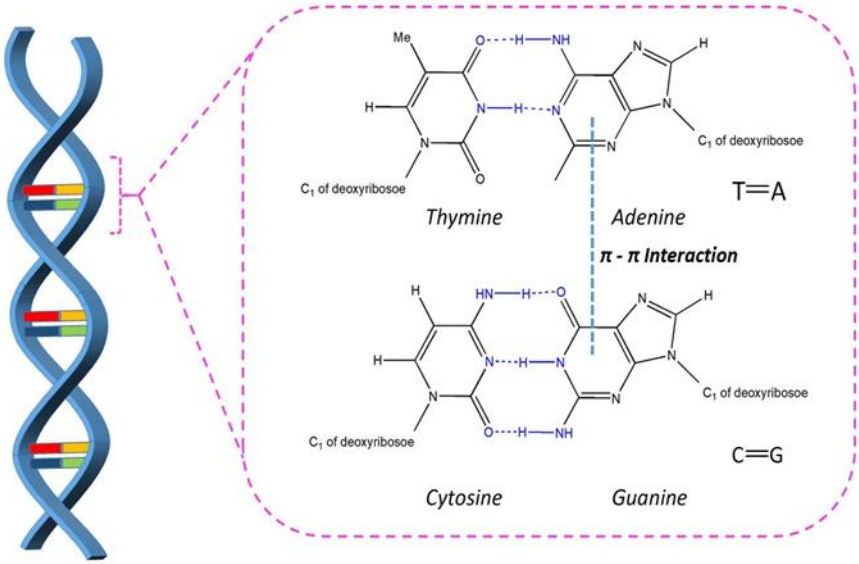

Figure 2: Hydrogen bonded complementary A-T and G-C base pairs in DNA helix. Sandwich π-staking interaction between aromatic rings and primary and secondary hydrogen bond interactions.

In the last decades the studies on supramolecular chemistry have been classified into three main areas:

- ***Molecular recognition,*** chemistry process associated with a molecule recognizing a partner compound, also defined as Host-Guest chemistry.

- ***Molecular self-assembly,*** chemistry process of spontaneous formation of supermolecules without guidance from an outside source.

- **Preparation of functional systems**, interdisciplinar applications of supramolecular chemistry to prepare functional systems such as chemical templated capsules, control release systems, nano superstructures or mechanically interlocked switchable scaffolds (molecular machines).

1.2 Molecular recognition

Molecular recognition forms the basis for supramolecular chemistry, because the construction of any supramolecular systems involves selective molecular combination. Only few molecules are able to interact with our bodies and to be recognized, since the host molecule must possess a high degree of complementarity with the guest, in terms of geometric and electronic features.

This process is called "molecular recognition" and it is the basis of Supramolecular Chemistry, it can be defined as the specific binding of a guest molecule to a host compound to form a supramolecular complex. The molecules that do the recognizing are called host molecules and those that are recognized through non-covalent bonding, molecules or ions, are known as guest molecules. For this reason, molecular recognition chemistry is sometimes called "host–guest" chemistry. The different non-covalent interactions between host and guest are hydrogen bonding, metal coordination, hydrophobic forces, van der Waals forces and π-π interactions[20] and they are the basis of many biological processes such as enzymatic catalysis, antigen-antibody interaction, the binding of a drug or a neurotransmitter to its receptor, etc.

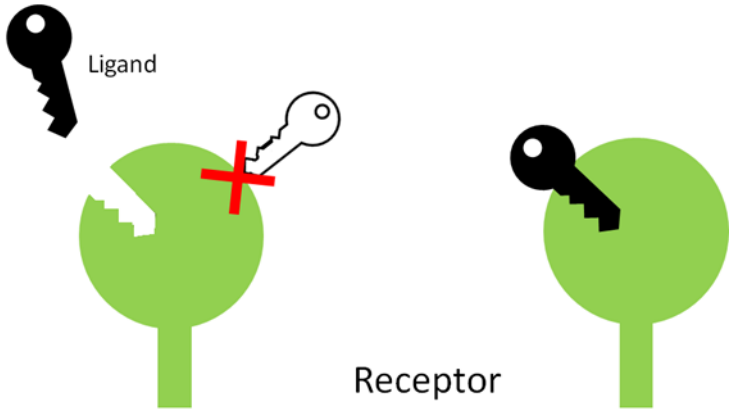

Figure 3: Schematic representation of lock-key principle.

[20] Schmidtchen, F. P. Chem. Soc. Rev., 2010, 39, 3916-3935; Smith, D. K. J. Chem. Edu., **2005**, 82, 393-400.

The first and simplest model of molecular recognition is the lock-key principle suggested in 1984 by Dr. Hermann Emil Fischer, who proposed this analogy as a means of understanding of natural receptors.[21] The receptor represents the lock and the analyte represents the key (See Figure 3). In this model, an enzyme (host) can discriminate among different substrates (guests) through the specific geometric complementarity between host and guest. Therefore, only one guest fit exactly into one host like only a key enter in a specific lock.

A chemical receptor is a particular molecule designed and optimized for molecular recognition of a given substrate, so during the design many factors need to be taken into account, such as size, shape, geometry, charge, hydrophilic/lipophilic character and other physical- chemical characteristics of guest-analyte to provide the best and largest number of intermolecular forces between the host and the guest. Moreover, the environment in which molecular recognition takes place is crucial when designing the chemical receptor, due to the influence of intermolecular processes such as solvation and electrostatic interactions between receptor, medium and analyte.[22]

Furthermore, the effectiveness of a chemical receptor is associated to the degree of complementarity between host and guest, which promotes the action of one or more intermolecular forces during the recognition process. Moreover, the receptor efficiency is determined by its ability to selectively recognize a specific guest, including on the presence of other substrates with similar features. Therefore, it is intended that the chemical receptor have more than one form of interaction type with the analyte (Figure 4), such as biological receptors whose complexity and complementarity with certain substrates ensures the activation of biological processes in a consistent and very specific manner.[23]

[21] Behr, J.-P., Ed. Perspectives In Supramolecular Chemistry 1; John Wiley & Sons: Chichester, **1994**.

[22] Oshovsky, G. V.; Reinhoudt, D. N. and Verboom, W. Angew. Chem. Int. Ed. 2007, 46, 2366 – 2393; Kubik, S. Chem. Soc. Rev., 2010, 39, 3648-3663.

[23] Joyce, L. A.; Shabbir, S. H. and Anslyn, E. V. Chem. Soc. Rev., 2010, 39, 3621–3632.

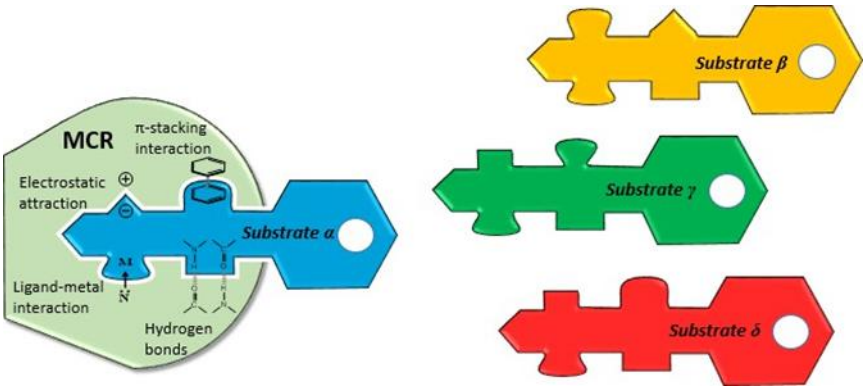

Figure 4. Schematic representation of host-guest complementarity to a specific receptor and a specific substrate α by multiple noncovalent interactions.

In 1932 it was found that polysaccharides, characterized as cyclodextrins after a while, are able to capture a guest molecule to form an inclusion solid, which is a kind of host-guest system based on a molecular recognition behavior.[24]

Selectivity is the key point in the host-guest interaction, it consists in the ability of the host to distinguish among different guests. This selectivity can arise from a number of different factors, such as complementarity between the guest and the host binding sites, cooperativity of the binding groups and preorganization of the host.[25]

- *Complementarity*: both the host and guest must have mutual spatially and electronically complementary binding sites to form the supermolecule.
- *Cooperativity*: a host molecule with multiple binding sites that are covalently connected forms a more stable host-guest complex than a similar system with sites that are not covalently connected (therefore acting separately from each other).
- *Preorganization*: a pre-organized host has a series of binding sites in a well-defined geometry within its structure and does not require a significant conformational change in order to bind to a specific guest in the most stable possible way.

[24] H. Pringsheim, The Chemistry of the Monosaccharides and of the Polysaccharides, McGraw-Hill, New York, **1932**.
[25] J. W. Steed, J. L. Atwood, Supramolecular Chemistry, © 2009, John Wiley & Sons, Ltd.

The complex formed from the host-guest interaction of two or more molecules by non-covalent bonds is an equilibrium process defined by a binding constant. Nowadays, the synthesis of new molecular receptors with enhanced selectivities toward selected guests is a field of research with increasing interest and attention. Design of selective molecular receptors is especially appealing for industrial, biomedical or environmental applications.

1.3 Molecular chemosensors

A molecular sensor, also called chemical sensor, chemosensor or probe, is a molecule composed by two subunits, a "binding site" and a "reporter", that can interact selectively with an analyte (guest) displaying a measurable signal as a consequence of the interaction. Thus, the molecular event of the coordination between the chemosensor and the analyte is reflected in a macroscopic signal that allowed the detection of the later. Signals widely used to detect the presence of certain guest molecules are changes in color,[26] fluorescence[27] or modulations in electrochemical properties.[28]

Chemosensors show up for their selectivity and specificity over others as they can be designed specifically for a particular analyte and their ideal form would be completely specific to a single analyte, recognizing no other.[29] This is the case of antibodies, aptamers, and enzymatic lock-and key or bioconjugation pairs such as streptavidin/biotin.[30, 31]

Very often, however, this ideal is not achievable, due to high similarity between analytes or a lack of tools for specific sensing of the target. Then, selective sensing is often the best that can be achieved.

[26] A. W. Czarnik, Acc. Chem. Res., **1994**, 27, 302.
[27] a) H. G. Löhr, F. Vögtle, Acc. Chem. Res., **1985**, 65. b) M. Takagi, K. Ueno, Top. Curr. Chem., **1984**, 121, 39
[28] a) P. D. Beer, Chem. Commun., **1996**, 689. b) P. D. Beer, Coord. Chem. Rev., **2000**, 205, 131.
[29] W. J. Peveler, M. Yazdani, V. M. Rotello ACS Sens. **2016**, 1, 11, 1282–1285.
[30] H.-P. Peng, K.H. Lee, J.-W. Jian, A.-S. Yang, *Proc. Natl. Acad. Sci. U. S. A.* **2014**, 111, E2656−E2665.
[31] O. Livnah, E. A. Bayer, M. Wilchek, J. L. Sussman, *Proc. Natl. Acad. Sci. U. S. A.* **1993**, 90, 5076−5080.

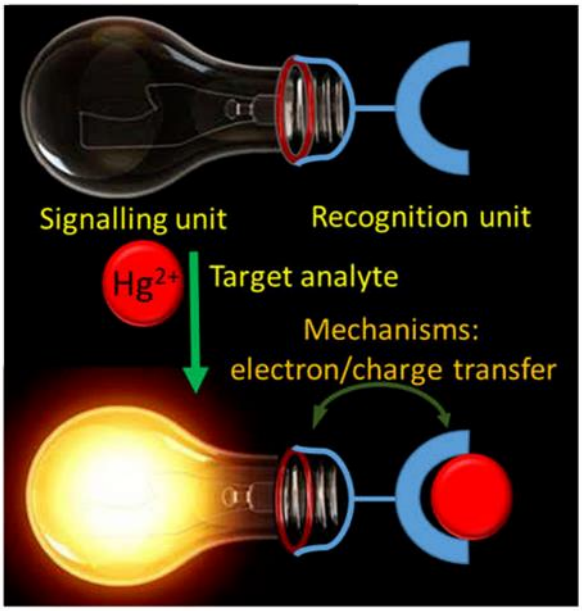

Figure 5. Schematic representation showing the design of a chemosensor.

The chromo-fluorogenic chemosensors are designed and developed by considering three important issues: (i) the signaling unit, (ii) the recognition unit, and (iii) the mechanism (Figure 5). The signaling unit may be an organic fluorophore, chromophore, or optically active nanoparticles.[32] When the recognition unit selectively recognizes the target analyte, some different mechanisms based on electron/charge/energy transfer, etc in the sensor can alter the electronic properties of the signaling unit, resulting in a detectable optical response.[33]

Three main approaches have been used in the design of optical chemosensors, (i) the ‘‘binding site-signaling subunit’’ protocol, (ii) the ‘‘displacement’’ approach and (iii) the ‘‘chemodosimeter’’ paradigm. The choice of one over the other depends largely on analyte affinity, binding selectivity, medium, synthetic effort of the chemosensor preparation (See Scheme 1).

[32] Bhardwaj, V.; Nurchi, V.M.; Sahoo, S.K. Mercury Toxicity and Detection Using Chromo-Fluorogenic Chemosensors. Pharmaceuticals **2021**, 14, 123.
[33] Houston, M.C. Role of Mercury Toxicity in Hypertension, Cardiovascular Disease, and Stroke. J. Clin. Hypertens. **2011**, 13, 621–627.14, 123.

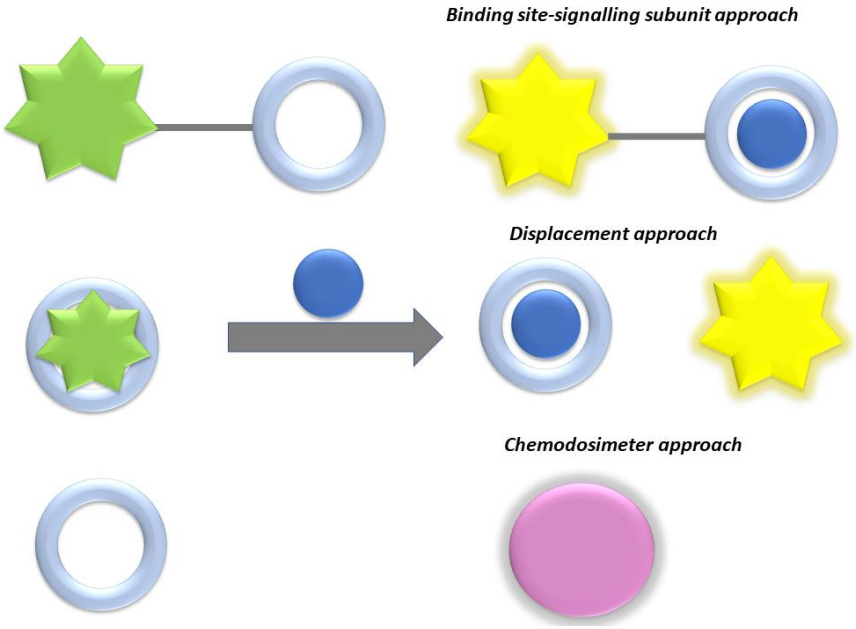

Scheme 1 Schematic representation of the three main paradigms used in the development of chemosensors.

1. ***Binding site-signalling subunit approach*:** In this approach the chemosensor is formed by "binding sites" and "signaling units" that are covalently linked. The coordination of the guest with the binding site changes physical properties of the signaling subunit giving rise to variations either in the color (chromogenic chemosensor) or in its fluorescence behavior (fluorogenic chemosensor).[34] Sometimes a spacer, able to modify the geometry of the system and tune the electronic interaction between the receptor and photoactive unit, is included in the system. An example is a colorimetric and fluorescent anion sensor based on urea substituted with a coumarin moiety and a pendant phenylazo unit, synthesized by Shao *et al* which used a binding site-signalling subunit approach.[35]

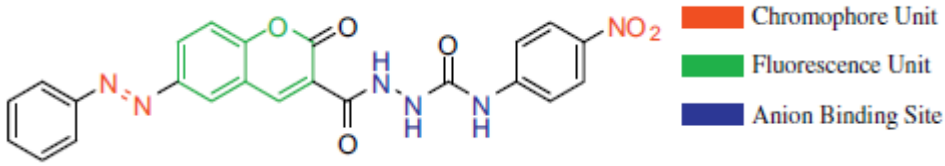

Figure 6. Structure of the sensor.

The azo group was exploited as a chromogenic signaling group, the urea moiety provides the anion binding site and the coumarin system is responsible for fluorescence. As such, the dye enables visual detection of acetate ion in DMSO with a color change from light yellow to red and displays significant fluorescence enhancement response to acetate because of complex formation. In solution, the N-N bond of the sensor could freely vibrate and rotate, which enabled vibrational and rotational relaxation modes of the non-radiative decay. As a consequence of the anion coordination, the rigidity of the formed complex increased rendering the non-radiative decay from the excited state less probable; consequently, the emission intensity increased. (Figure 7)

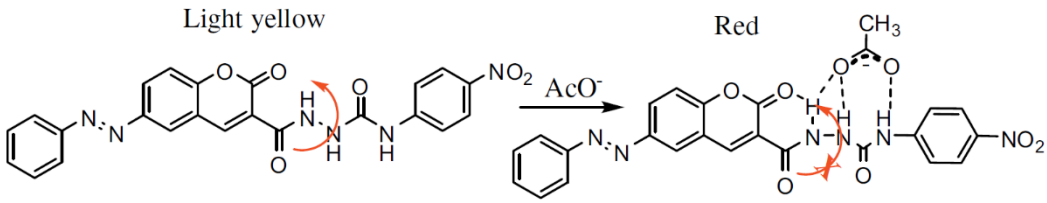

Figure 7. The proposed host-guest interaction mode in the solution.

2. ***The displacement approach*****:** This approach uses binding sites and signaling subunits forming a coordination complex (molecular ensemble), not covalently linked. This approach relies in a displacement reaction when the target molecule is coordinated with the binding site and the signaling subunit returns to the solution. A suitable signal is observed when the color or emission of the signaling subunit in the sensing ensemble is different than that present when it is free in solution.[36]

An example of this approach is a Cu^{2+} fluorescent probe employing BODIPY as fluorophore and DPA as Cu^{2+} chelator, synthesised by Wanga *et al*.[37] For this probe, alkyl chain -$CH_2CH_2CH_2$- was chosen as the linker connect BODIPY and DPA.

[34] R. A. Bissell, P. de Silva, H. Q. N. Gunaratne, P. L.M. Lynch, G. E. M. Maguire, K. R. A. S. Sandanayake, Chem. Soc.Rev., **1992**, 21, 187.
[35] J. Shao Dyes and Pigments 87, **2010**, 272-276.
[36] a) S. L. Wiskur, H. Ait-Haddou, J. J. Lavigne, E. V. Anslyn, Acc. Chem. Res., 2001, 34, 963. b) B. T. Nguyen, E. V. Anslyn, Coord. Chem. Rev., **2006**, 250, 3118.
[37] S. Wua, X. Mab, Y. Wang, J. Zhou, X. Li, X. Wanga, Spectrochimica Acta Part A: Molecular and Biomolecular Spectroscopy 249, **2021**, 119330.

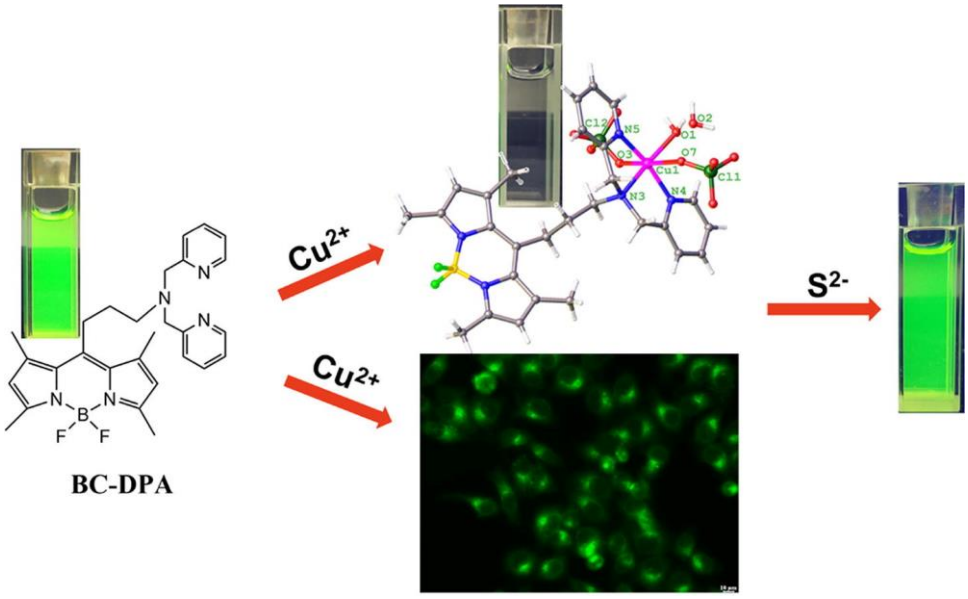

Figure 8. Schematic representation of the behaviour of the sensor in the presence of Cu^{2+} and S^{2-}. *Reprinted with permission from Spectrochimica Acta Part A: Molecular and Biomolecular Spectroscopy, Volume 249, 2021, 119330 (Copyright © 2021 Elsevier B.V.)*

The BODIPY-based compound successfully served as a fluorescent ‘‘turn OFF” probe for selective detection of Cu^{2+} among different cations in aqueous media at neutral pH. A significant decrease in fluorescence was observed upon addition of Cu^{2+}, indicating the generation of BCDPA-Cu^{2+} complex and the chelation enhanced fluorescence quenching effect, as shown in Figure 8.

The N-N bond within the sensor was able to move with no restrictions in solution, therefore allowing vibrational relaxation of the non-radioactive decay and rotational either. Since anion coordination happened as well, the so formed complex became more rigid making more unlikely decay from excited state; therefore, the emission was more intense.

Afterwards, on the basis of the *displacement approach*, the fluorescence of BC-DPA-Cu^{2+} was recovered in the presence of S^{2-}, which allowed the system to act as a sensitive ‘‘turn-on” sensor for hydrogen sulfide in acetonitrile solution without any interference from other common anions.

3. ***The "chemodosimeter" approach:*** This approach is related with the use of specific irreversible reactions involving hosts and guests, which are coupled to a color or emission variations.[38] If the chemical reaction is irreversible, the use of the term chemosensor cannot strictly be used and we will refer to these systems as chemodosimeters or chemoreactants. [39]

   For example, the "chemodosimeter" approach was explored by Ros-Lis and coworkers in the studies conducted on the specific reactivity of some water-soluble squaraine derivatives, shown in Scheme 2. [40]

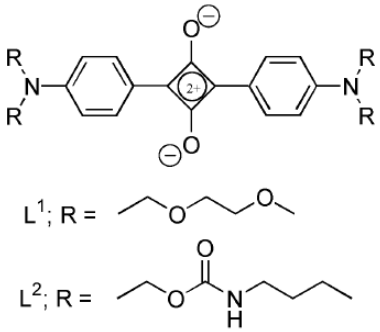

Scheme 2. Molecular Structure of the Squaraine Derivatives.

   It was observed a bleaching from blue to colorless in the presence of cysteine, with a concomitant complete fluorescence quenching, whereas alcohols, phenols, and amines (primary, secondary, and tertiary) or sulfides produced no color changes. The product shown an intense blue colour in solution. Upon exposition to nucleophilic compounds, it suffered an attack in the central four-member ring, destroying the delocalisation of the electrons. (See Scheme 3). This shows that specific fluoro-chromo chemodosimeters for thiol-containing compounds in aqueous environments were synthesized and they were able to selectively detect cysteine among different amino acids.

[38] a) M.-Y. Chae, A. W. Czarnik, J. Am. Chem. Soc., 1992, 114, 9704. b) V. Dujols, F. Ford, A. W. Czarnik, J. Am. Chem. Soc., **1997**, 119, 7386.
[39] Z. Xu, X. Chen, H. N. Kim, J. Yoon, Chem. Soc. Rev., **2010**, 39, 127.
[40] J. V. Ros-Lis, B. García, D. Jiménez, R. Martínez-Máñez, F. Sancenón, J. Soto, F. Gonzalvo, M. C. Valldecabres J. Am. Chem. Soc. **2004**, 126, 13, 4064–4065.

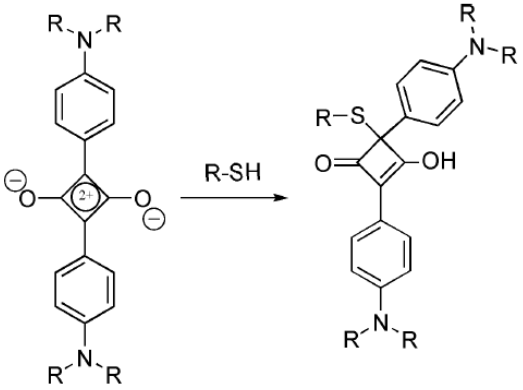

Scheme 3. Proposed Reaction between Squarine Derivatives and Thiol-Containing Compounds.

1.4 Mesoporous silica materials

Over the last decades, interest in porous materials has greatly increased, due to their large specific surface area and attending their potential applications in different fields such as catalysis,[41] adsorption,[42] sensing and drug delivery.[43] Porous materials are classified by the International Union of Pure and Applied Chemistry (IUPAC) according to the pore size as microporous (pore size < 2 nm), mesoporous (2-50 nm) and macroporous (>50 nm) materials.[44]

The first mesoporous solid synthetized were MCM mesoporous silica materials (where MCM stands for Mobil Composition of Matter), discovered in 1992 by Mobil Oil Company[45]. These materials showed a regular ordered pore arrangement and a very narrow pore-size distribution. Using different synthesis conditions such as solvent, pH, temperature, concentration, it is possible to obtained different silica solid, MCM-41 with a hexagonal arrangement of the mesopores, MCM-48 with a cubic arrangement of mesopores and MCM-50 with a lamellar structure (See Figure 9).

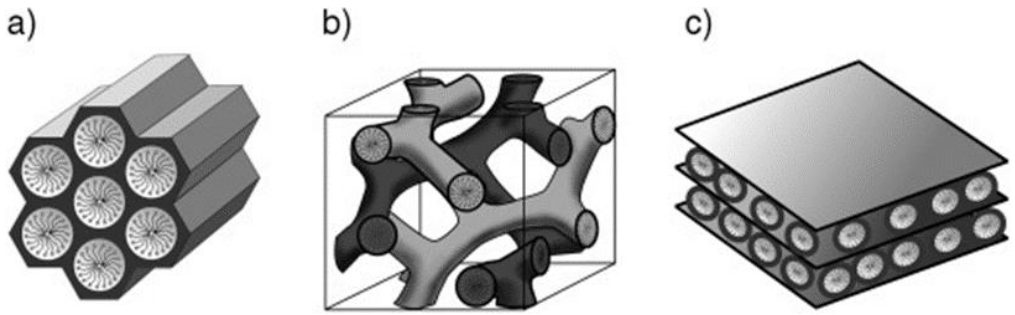

Figure 9. Structures of mesoporous M41S materials: a) MCM-41, b) MCM-48 and c) MCM-50. *Reprinted with permission from Angew Chem Int Ed*. 2006, 45, 3216 – 3251 (Copyright © 2006 WILEY-VCH Verlag GmbH & Co. KGaA, Weinheim).

[41] C. Perego, R. Millini, Chem. Soc. Rev. **2013**, 42, 3956.
[42] K. M. Thomas, Catal. Today **2007**, 120, 389.
[43] D. J. Wales, J. Grand, V. P. Ting, R. D. Burke, K. J. Edler, C. R. Bowen, S. Mintova, A. D. Burrows, *Chem. Soc. Rev.* **2015**, *44,* 4290.
[44] a) IUPAC, Pure appl. Chem. **1972**, 31, 578; b) X. S. Zhao, J. Mater. Chem. **2006**, 16, 623.
[45] J. S. Beck, J. C. Vartuli, W. J. Roth, M. E. Leonowicz, C. T. Kresge, K. D. Schmitt, C. T. W. Chu, D. H. Olson, E. W. Sheppard, S. B. McCullen, J. B. Higgins, J. L. Schlenker, J. Am. Chem. Soc. **1992**, 114, 10834-10843.

MCM-41 has been investigated more than other materials, which are thermally unstable or difficult to obtain, due to the relative simplicity of its synthesis and its particular honeycomb- like structure.[46]

Additionally, this material presents high chemical inertness and thermal stability features, it is biocompatible and its surface can be easily functionalized using alkoxysilane derivatives, which confers the final materials improved features and advanced functionalities.[47]

1.4.1. Synthesis of mesoporous silica materials

As a general protocol, the synthesis of mesoporous silica materials is based on the condensation of a silica precursor (tetraethyl orthosilicate, sodium silicate or tetramethylammonium silicate) in the presence of cationic surfactants under basic conditions.[48] It is considered a sol-gel process that involves the conversion of monomers in solution (sol) into an integrated solid network (gel), similar to the method described by Stöber in 1968 for obtaining silica nanoparticles, but performed in the presence of surfactants.[49]

The surfactant molecules act as a template or structure directing agent by forming supermicelles (supramolecular self- assemblies of individual micelles) over which the precursors molecules condensate. Selected conditions, such as temperature, pH, ionic force and surfactant nature and concentration, will determine the structure of the supermicelles. In general, at moderate temperatures, cylindrical micelles clump together forming first a hexagonal phase, which evolves towards a cubic phase and later to a laminar structure as the concentration of surfactant increases. Once the super-micelles have formed, the silica precursor is added to the reaction solution. In this step, the molecules of the siliceous precursor hydrolyze and form silanol groups (Si-OH), which polymerize through condensation and create a network of Si-O-Si (Figure10).

---

[46] J.C. Vartuli, K.D. Schmitt, C.T. Kresge, W.J Roth, M.E. Leonowicz, S.B. McCullen, S.D. Hellring, J.S. Beck, J.L. Schlenker, D.H. Olson, E.W. Sheppard, Chem. Mater. **1994**, 6, 2317–2326.
[47] J. G. Croissant, Y. Fatieiev, A. Almalik, N. M. Khashab, *Adv. Healthcare Mater.* **2018**, *7*, 1700831.
[48] M. C. Llinàs, D. Sánchez-García, Afinidad LXXI 2014, 565, 20-31.
[49] W. Stöber, A. Fink, E. J. Bohn, *J. Colloid Interf. Sci.* **1968**, *26*, 62.

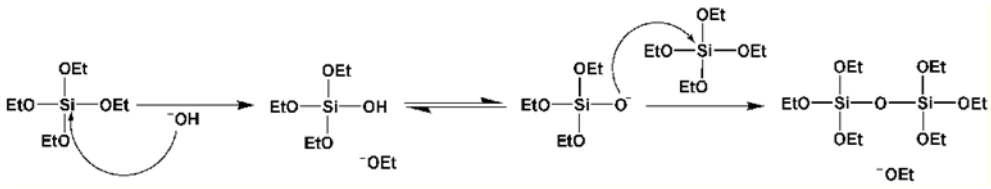

Figure 10. Mechanism of TEOS hydrolysis and condensation.

At this point, the presence of the super-micelles is crucial for the assembly of the silica on its surroundings and the formation of the pores. It is the positive charges of the cationic surfactant that attract the negative charges of the silica species, which concentrate around the micelles and form a tubular silica structure. The nanoparticles increase in size as the silica precursor condenses, until the net negative charge is so high that they stop growing. This entire process can be followed visually, since when the silica nanoparticles begin to form, the solution acquires an easily detectable white turbidity. Once the synthesis process is finished, the surfactant is removed by an extraction process under reflux in an acid medium or by a calcination process (heating the solid obtained in a muffle furnace at high temperatures for several hours).

Figure 11. Representative scheme of synthetic procedure for preparing MCM-41-type mesoporous silica nanoparticles. *Adapted with permission from Angew. Chem. Int. Ed. 2006, 45, 3216. Copyright © 2006 Wiley-VCH.*

- ***Functionalization of mesoporous silica materials***

Functionalization of inorganic materials is intended as the incorporation of organic groups on the surface of these mesoporous silica materials, giving rise to the mentioned organic-inorganic hybrid materials. Thanks to functionalization (which can occur on the surface of the inorganic matrix, or form part of the silica surface or remain inside the pores), the functional variety of organic chemistry can be combined with the advantages of an inorganic support mechanically and thermally stable and with a large surface area.

Usually, two different synthetic strategies are used to functionalize the surfaces of mesoporous silica materials: grafting and co-condensation. Whichever procedure is carried out, the incorporated organic group can have a function by itself (such as increasing the hydrophobicity / hydrophilicity of the surface, stabilizing it ...) or it can be used as a reactive group to further anchor new molecules through covalent bonds or electrostatic interactions.

- **Functionalization by grafting:**

In this method, the inorganic mesoporous silica material is first synthesized and, in a posterior step, it is functionalized with the selected organic groups. This strategy takes advantage of the high concentration of structural defects on the surface of mesoporous materials in the form of silanol (Si-OH) groups, which act as anchor points for organic modification. If the H group of silanol is replaced by a chemical species capable of covalently attaching a radical R group to the oxygen atom, a family of materials with different chemical composition of the R fragment can be obtained. The most common methodology to functionalize these supports is based on the reaction of silanol groups with trialkoxysilane derivatives, whose structure is (R'O) 3-Si-R (where R is an organic group). The reaction of superficial silanol groups with trialkoxysilanes can be considered as a simple condensation reaction or nucleophilic substitution (Figure 11).

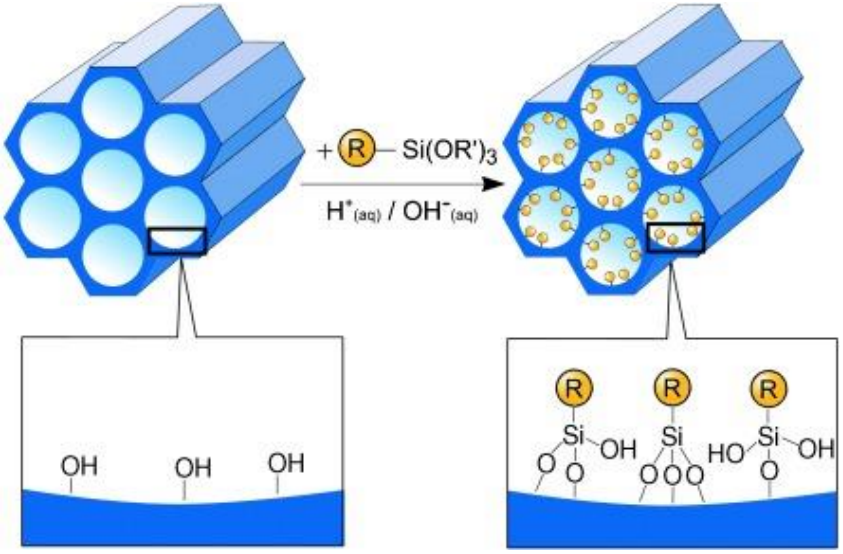

Figure 12. Schematic of the grafting procedure for functionalization of mesoporous pure silica materials with organotryalkoxysilanes of the type (R'O)3-Si-R. R represents an organic functional group. *Reprinted with permission from Angew. Chem. Int. Ed. 2006, 45, 3216. Copyright © 2006 Wiley-VCH.*

One of the advantages of this method is that the original structure of the mesoporous support is maintained after the functionalization step. Furthermore, the inorganic matrix can be easily obtained through standard procedures in large quantities to later carry out its modification with the selected organosilanes. It is also possible to achieve a regioselective functionalization by anchoring different organic groups on the internal and external surfaces. This can be done by first functionalizing the mesoporous material as it is obtained from the synthesis (i.e., with the pores still with the surfactant molecules), so that the organic groups will anchor on the outer surface. Once the surfactant is removed by extraction, the support can be re-functionalized with a different derivative that will anchor itself on the inner surface of the pores.

- **Functionalization by co-condensation:**

This method consists is the simultaneous condensation, in the presence of the structure directing agent, of the silica precursors (eg. TEOS) and the functional derivatives of interest, which takes place during the synthesis process itself (Figure 13). This strategy, carried out in a single step, normally allows the homogeneous distribution of organic molecules throughout the mesoporous support, both on its external surface and on the walls and channels. In this case, the removal of the surfactant from the pores must be carried out by extraction, since the calcination could affect the functional organic groups. It should also be noted that if the content of functional derivatives is too high in the reaction, it can prevent the mesoporous structure from forming. Since the presence of functional groups on the walls of the material can influence the mechanism of interaction with the surfactant, this functionalization strategy must be optimized for each particular case.

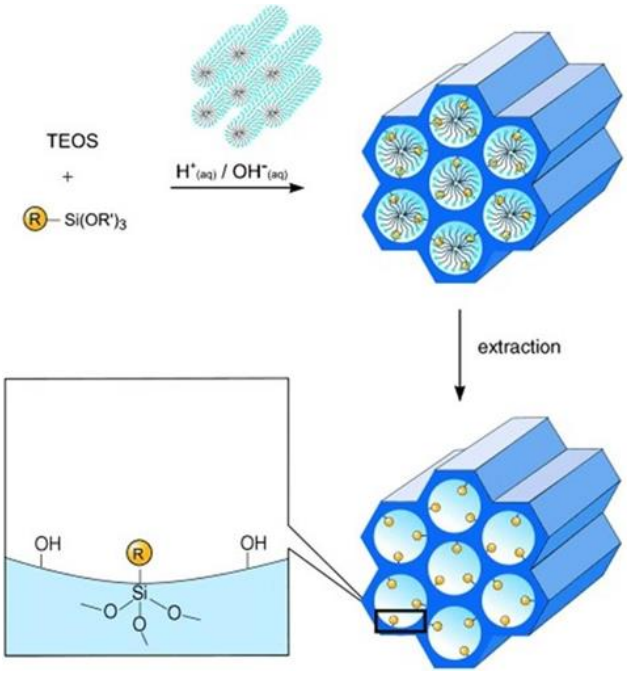

Figure 13. Schematic of the co-condensation method for organic functionalization of mesoporous silica materials. R represents an organic functional group. *Adapted with permission from Angew. Chem. Int. Ed. 2006, 45, 3216. Copyright © 2006 Wiley-VCH.*

1.4.2. Characterization of mesoporous silica materials

Several standard characterization techniques are used with the purpose of checking the formation of the mesoporous structure, its preservation along the different modification steps, and the incorporation of the different components. The structural properties and porous characteristics are mainly studied by power X-ray diffraction (PXRD), transmission electron microscopy (TEM) and N_2 adsorption-desorption analysis.

Powder X-Ray Diffraction (PXRD) is a non-destructive technique that allows to study the internal mesoporous structure of materials at an atomic scale, since diffractograms provide information on the periodicity and internal order of nanoparticles. The source of X-ray emits radiation at different incident angle over the sample and the diffracted light is collected by the detector to obtain the PXRD patterns. The intensity of diffracted light is function of the angle of incident radiation. The intensity peaks or reflections related for each angle are determined by the distance between the atomic planes in the ordered structure in accordance to Brag's law. Using this technique, it is possible to clearly distinguish between the different types of mesoporous materials MCM-41, MCM-48 and MCM-50 according to their hexagonal, cubic or laminar structure. For example, the typical XRD pattern of mesoporous nanoparticles shows a characteristic main peak between 2 and 2.5 degrees θ, indexed as Bragg peak (100); and three other secondary peaks at higher angles, indexed as (110), (200) and (210) (Figure 14). If the same diffraction pattern is maintained between the initial solid and the final hybrid solid, the technique confirms that the mesoporous structure of the material is maintained after the functionalization process.

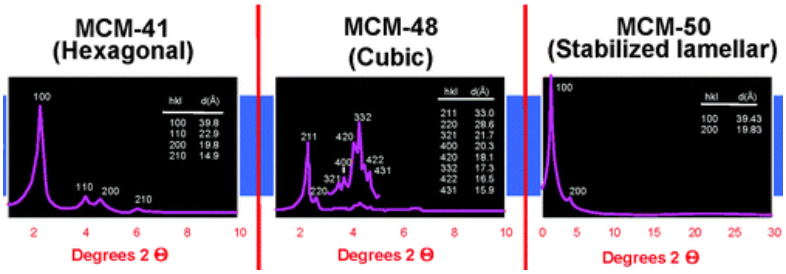

Figure 14. Characteristic PXRD patterns of the M41S family of mesoporous silica materials. *Adapted from Chem. Soc. Rev. 2013, 42, 3663. Copyright © 2013 The Royal Society of Chemistry.*

Nitrogen adsorption and desorption (porosimetry) is a fundamental technique in the characterization of mesoporous materials. It is used to demonstrate the effectiveness of the charging and functionalization processes, giving information about the specific surface area, pore size and specific pore volume.

When the mesoporous support is empty, the amount of nitrogen adsorbed inside the pores is high. Otherwise, if the pores are filled with a cargo or have not been properly formed, the amount of adsorbed nitrogen is significantly lower. Therefore, this technique allows determining the specific surface of the material, and this value provides information when comparing the calcined nanoparticle, with a high surface area, and the charged and functionalized nanoparticle, with a very low surface area.

Transmission electron microscopy (TEM) allows to visualize the size and morphology of the materials with high resolution. TEM can indicate the hexagonal arrangement where parallel lines observed in the micrographs are related to the hexagonal repeat between tubes and a uniform pore (size around 2-4 nm).

Finally, there are several techniques that can be used to qualitatively and / or quantitatively evaluate functionalization with organic molecules. Elemental analysis (EA) is based on the combustion of a small amount of sample and provides information on the percentage by weight of carbon, hydrogen, nitrogen and sulfur. This data can be related to the amount of functional organic molecules present in the material. On the other hand, thermogravimetric analysis (TGA) records the loss

in weight of the material as a function of temperature, thus allowing the calculation of the total percentage of organic matter in the solid. Finally, two general and well-known techniques are very useful when working with mesoporous materials: UV-visible spectrophotometry and fluorescence. They can be used, for instance, for monitoring the release of a fluorescent or colored cargo from the nanoparticles.

1.5 Stimuli-responsive gated materials

In the last ten years, anchoring organic molecules or supermolecules onto certain inorganic scaffoldings has led to the development of hybrid materials, which has resulted in cooperative functional supramolecular behaviors that are not found in unanchored molecules or in the un-functionalized solids alone. One appealing concept in this novel field relates with the development of gated nano-devices for delivery applications. These functional materials contain "molecular gates", which are the switchable entities controlling either the on-command release of confined guests or the on-command entrance of molecular species to certain sites (see Figure 15). These gated materials usually contain two components: (i) a switchable "gate-like" ensemble capable of being "opened" or "closed" upon the application of certain external stimuli and (ii) a suitable inorganic support acting as a nanocontainer (for loading the carrier), where gate-like molecules can be easily grafted.[50]

[50] C. Coll, A. Bernardos, R. Martínez-Máñez, F. Sancenón, *Acc. Chem. Res.*, **2013**, 46, 339−349.
[51] N. K. Mal, M. Fujiwara, Y. Tanaka, *Nature* **2003**, 421, 350−353.
[52] N. K. Mal, M. Fujiwara, Y. Tanaka, T. Taguchi, M. Matsutaka, *Chem. Mater.*, **2003**, 15, 3385−3394.
[53] H. M. Lin, W. K. Wang, P. A. Hsiung, S. G. Shyu, *Acta Biomater.* **2010**, 6, 3256−3263.
[54] J. Yang, W.-D. He, C. He, J. Tao, S.-Q. Chen, S.-M Niu, S.-L. Zhu, *J. Polym. Sci., Part A: Polym. Chem.* **2013**, 51, 3791−3799.
[55] D. P. Ferris, Y. – L. Zhao, N. M. Khashab, H. A., Khatib, J.F. Stoddart, J.I. Zink *J. Am. Chem. Soc.* **2009**, 131, 1686−1688.
[56] R. Casasús, M.D. Marcos, R. Martínez-Mañez, J.V. Ros-Lis, J. Soto, L.A. Villaescusa, P. Amorós, D. Beltran, C. Guillem, J. Latorre, *J. Am. Chem. Soc.*, **2004**, 126, 8612−8613.
[57] A. Bernardos, E. Aznar, C. Coll, R. Martínez-Mañez, J. M. Barat, M.D. Marcos, F. Sancenón, A. Benito, J. Soto, *J. Controlled Release* **2008**, 131 (3), 181− 189.

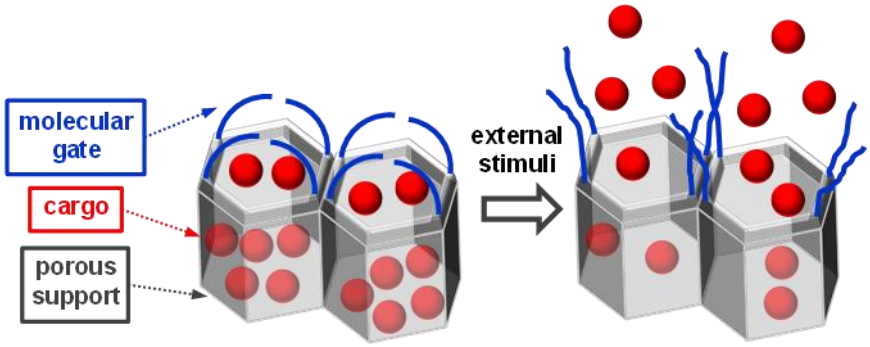

Figure 15. Schematic representation of a molecular gate. Reprinted with permission from *Chem. Rev.* 2016, *116, 2, 561–718 Copyright © 2016 American Chemical Society.*

Both components are important and their selection determines the controlled release performances of the hybrid support. In relation to the gated ensemble, several molecular and supramolecular systems have been developed which are able to trigger at will the delivery of the entrapped cargo using several external stimuli such as light,[51-55] pH,[56-60] changes in redox potential,[61-62] temperature,[63-64] and the presence of certain ions, molecules or biomolecules.[65-69]

[58] M. Mas, I. Galiana, S. Hurtado, L. Mondragón, A. Bernardos, F. Sancenoń, M.D. Marcos, P. Amorós, N. Abril-Utrillas, R. Martıńez- Máñez, et al. *Int. J. Nanomed.* **2014**, 9, 2597−2606.
[59] C. Acosta, E. Pérez-Esteve, C. A. Fuenmayor, S. Benedetti, M. S. Cosio, J. Soto, F. Sancenón, S. Mannino, J. Barat, M.D. Marcos, et al. *ACS Appl. Mater. Interfaces* **2014**, 6, 6453−6460.
[60] S. Angelos, Y. W.Yang, K. Patel, J .F. Stoddart, J.I. Zink, *Angew. Chem., Int. Ed*. **2008**, 47, 2222−2226.
[61] R. Hernandez, H. R. Tseng, J. W. Wong, J. F. Stoddart, J. I. Zink, *J. Am. Chem. Soc.* **2004**, 126, 3370−3371.
[62] C. Y. Lai, B. G. Trewyn, D. M. Jeftinija, K. Jeftinija, S. Xu, S. Jeftinija, V.S. Y. Lin, *J. Am. Chem. Soc.* **2003**, 125, 4451−4459.
[63] Q. Fu, G.V.R. Rao, L. K. Ista, Y. Wu, B. P. Andrzejewski, L. A. Sklar, T. L. Ward, G. P. Lopez, *Adv. Mater*. **2003**, 15, 1262−1266.
[64] C. Liu, J. Guo, W. Yang, J. Hu, C. Wang, S. Fu, *J. Mater. Chem.* **2009**, 19, 4764−4770.
[65] E. Aznar, R. Villalonga, C. Gimenez, F. Sancenón, M.D. Marcos, R. Martínez-Máñez, P. Diez, J.M.Pingarrón, P. Amorós, *Chem. Commun.* **2013**, 49, 6391−6393.
[66] R. Villalonga, P. Diez, A. Sanchez, E. Aznar, R. Martínez-Máñez, J.M. Pingarrón, *Chem. - Eur. J.* **2013**, 19, 7889−7894.
[67] P. Diez, A. Sanchez, M. Gamella, P. Martínez-Ruiz, E. Aznar, C. de la Torre, J. R. Murguia, R. Martínez-Máñez, R. Villalonga, J.M. Pingarrón, *J. Am. Chem. Soc.* **2014**, 136, 9116−9123.
[68] M. Domínguez, J. F. Blandez, B. Lozano-Torres, C.de la Torre, M. Licchelli, C. Mangano, V. Amendola, Félix Sancenón and RamónMartínez-Máñez, *Chem.Eur.J.* **2021**,27,1306 –1310.
[69] A. Ribes, E. Aznar, S. Santiago-Felipe, E. Xifre-Perez, M. A. Tormo-Mas, J. Pemán, L. F. Marsal and R. Martínez-Máñez, *ACS Sensors* **2019** 4 (5), 1291-1298.

Silica mesoporous materials bearing gate-like ensembles can be used for on-command delivery applications in the presence of different physical or (bio)-chemical stimuli. Moreover, very recently, gated materials capable of responding specifically to a certain target molecule has been prepared as a suitable method for developing new protocols for sensing applications.[70] The underlying idea here is that the coordination or reaction of the target analyte with the binding sites could modulate the transport of the dye from pores to the solution, and would result in a chromo-fluorogenic signal. In this sensing approach the starting material is capped and the presence of a target analyte induces pore opening and dye delivery (Figure 16). Given the possible use of different porous supports, diverse guest-selective gate-like systems and a wide range of indicator dyes, this strategy, which has still to be fully studied, displays enormous potential for the development of novel signaling systems.

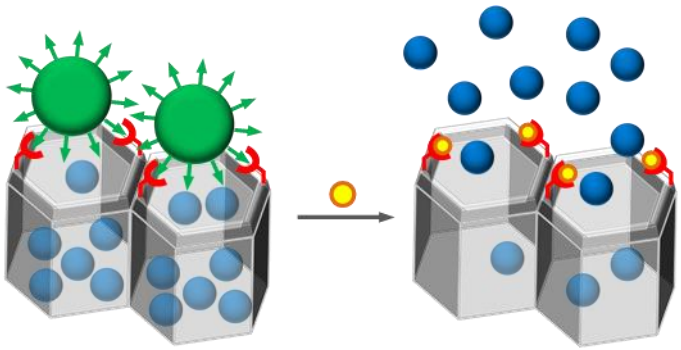

Figure 16. Scheme of the recognition paradigm using nanoscopic gate-like scaffoldings in which a selected analyte induced a displacement reaction with subsequent pore opening and the release of a dye/fluorophore.

In a very recent work, Pla and co-workers have reported a novel detection system of gluten based on a gated nano-porous material capped with an aptamer for gliadin (Figure 16).[71]

[70] E. Climent, M.D. Marcos, R. Martínez-Máñez, F. Sancenón, J. Soto, K. Rurack, P. Amorós, *Angew. Chem., Int. Ed.* **2009**, 48, 8519–8522.
[71] L. Pla, M. C. Martínez-Bisbala, E. Aznar, Félix Sancenón, Ramón Martínez-Máñeza, S. Santiago-Felipe, *Analytica Chimica Acta* 1147, 2021, 178-186.

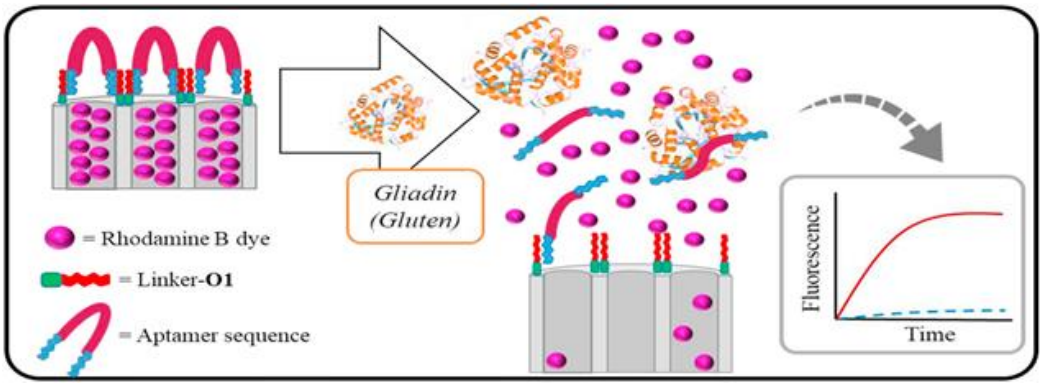

Figure 16. Schematic representation of the molecular gate based on the synergic combination of gluten aptamers and nano-porous anodic alumina (NAA) supports. Reprinted with permission from *Analytica Chimica Acta*, 1147, **2021**, 178-186. *Copyright © 2020 Elsevier B.V.*

Commercially available NAA supports were loaded with the fluorescent dye rhodamine B, then the external surface was functionalized and finally three different aptamers were used as caps. In the prepared final solids, the presence of the target gliadin protein was able to displace the capping oligonucleotide chains (**O2**–**O4**) allowing cargo release, which finally resulted in a fluorescence emission enhancement in the solution, whereas the final solids remain capped when the analyte is not present and were not able to release the cargo (See Figure 17).

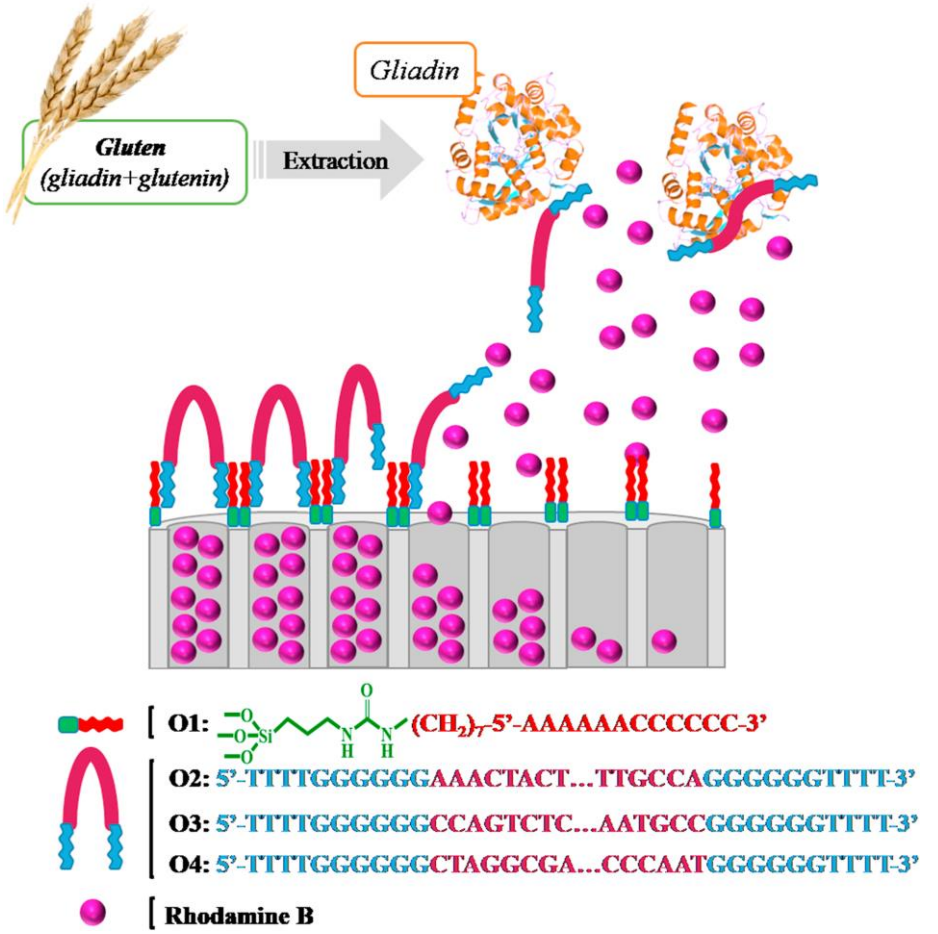

Figure 17. Schematic representation of the gated support. The material capped with the selected oligonucleotide sequences (O2, O3 and O4) deliver the entrapped dye in the presence of gliadin. Reprinted with permission from *Analytica Chimica Acta*, 1147, **2021**, 178-186. *Copyright © 2020 Elsevier B.V.*

With this new aptasensor the authors were able to detect gluten water soluble protein gliadin with low LOD using the displacement of the capping aptamer and in the subsequent pore opening and release of the entrapped fluorophore.

Recently Garrido and co-workers have developed a new nanosensor for sensitive detection of the new psychedelic drug 25I-NBOMe.[72] The system is based on mesoporous silica nanoparticles, loaded with a fluorescent dye, functionalized with a serotonin derivative and capped with the 5-HT2A receptor antibody. In the

presence of 25I-NBOMe the capping antibody is displaced, leading to pore opening and rhodamine B release (Figure 18). This delivery was ascribed to 5-HT2A receptor antibody detachment from the surface due to its stronger coordination with 25I-NBOMe present in the solution.

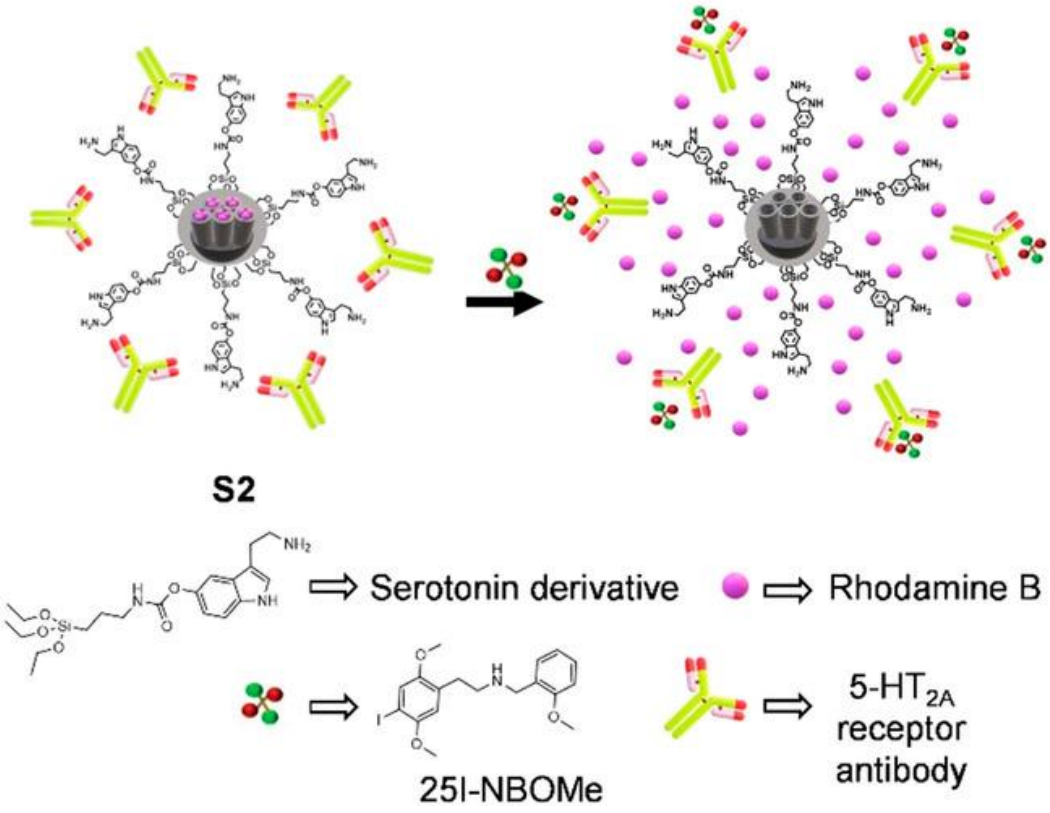

Figure 18. Schematic representation of the mechanism of release of solid S2 in the presence of 25I-NBOMe. Reprinted with permission from *Chem.Eur.J.2020,26,2813 –2816 Copyright © 2020 Wiley-VCHVerlag GmbH&Co. KGaA, Weinheim.*

[72] E. Garrido, M. Alfonso, B. Díaz de Greñu, B. Lozano-Torres, M. Parra, P. Gaviña, M. D. Marcos, R. Martínez-Máñez and Félix Sancenón, *Chem.Eur.J.***2020**,26,2813 –2816.

Chapter 2: Objectives

Considering the importance of the detection in water of chemical species of environmental and biological importance, the objectives of this PhD thesis have been centered on the preparation of molecular sensors and functionalized hybrid materials with molecular gates for sensing new chemosensors able to detect contaminating species and drugs in water.

The specific objectives are:

- To synthesize, purify and characterize a fluorescent chalcone-based chemodosimeter (1)
- To test the chromo-fluorogenic response of the chemodosimeter (1), able to selectively detect trivalent cations over monovalent, divalent cations and anions using a dehydration reaction in nearly pure water.
- To prepare a new BODIPY derivative electronically connected with a dithia-dioxa-aza macrocycle (2).
- To test the chromo-fluorogenic behaviour of probe (2), able to selectively detect Hg(II) cation in nearly pure water.
- To develop capped mesoporous silica nanoparticles for the optical (chromo-fluorogenic) detection of amantadine and berberine in water.

Chapter 3: Selective chromo-fluorogenic detection of trivalent cations in aqueous environments using a dehydration reaction

Selective chromo-fluorogenic detection of trivalent cations in aqueous environments using a dehydration reaction

Maria Lo Presti,[abc] Sameh El Sayed,[abc] Ramón Martínez-Máñez,*[abc]

Ana M. Costero,*[acd] Salvador Gil,[acd] Margarita Parra[acd] and Félix Sancenón[abc]

[a] Instituto Interuniversitario de Reconocimiento Molecular y Desarrollo Tecnológico (IDM), Unidad Mixta Universidad Politécnica de Valencia-Universidad de Valencia, Spain

[b] Departamento de Química, Universidad Politécnica de València, Camino de Vera s/n, 46022, Valencia, Spain. E-mail: rmaez@qim.upv.es

[c]CIBER de Bioingeniería, Biomateriales y Nanomedicina (CIBER-BBN)

[d]Departamento de Química Orgánica, Facultad de Ciencias Químicas, Universidad de Valencia, Doctor Moliner 50, 46100 Burjassot (Valencia), Spain. E-mail: ana.costero@uv.es

Published on 28 September 2016.
Received on 23rd June 2016,
Accepted on 27th September 2016.

(Reprinted with permission from **New J. Chem., 2016, 40, 9042-9045**

3.1 Abstract

Trivalent cations (Al^{3+}, Fe^{3+}, Cr^{3+}, As^{3+}, In^{3+} and Ga^{3+}) induced a dehydration reaction of a chemodosimeter in water that is coupled with colour and emission changes.

3.2 Introduction

The preparation of probes for the selective recognition of trivalent cations has received increased attention in the last few years due to the crucial roles played by these cations in many biological and environmental processes. For instance, Al^{3+} is the third most abundant element on earth and some aluminium derivatives are used in water purification, as food additives and in pharmaceutical formulations. Unfortunately, an overdose of Al^{3+} in human tissues and cells can induce diseases like Parkinson's, osteoporosis, headache, gastrointestinal problems and Alzheimer's.[1] Iron is the most abundant transition metal in cells. It is used as a cofactor in the electron transport system and in many biochemical processes at the cellular level.[2] Its deficiency can lead to anaemia, hemochromatosis, diabetes, liver and kidney damage, Parkinson's and heart diseases.[3] Chromium is one of the essential elements in human nutrition and plays a fundamental role in the metabolism of carbohydrates, proteins, lipids and nucleic acids.[4] Gallium exists in nature only in its Ga^{3+} oxidation state and it has no known biological role. However, because gallium and iron salts behave in a similar way in biological systems, gallium ions often mimic iron in some medical applications; for instance, certain drugs and radiopharmaceuticals containing gallium have been used.[5] All indium compounds should be regarded as highly toxic and are able to damage the heart, kidneys and the liver, and may be teratogenic.[6] Finally, arsenic is one of the most toxic elements known. Despite its toxic effect, inorganic arsenic can be found on earth naturally in small quantities. Humans can be exposed to arsenic through food, water and air. Exposure can also occur through skin contact with soil or water containing arsenic. High levels of arsenic can cause cardiovascular, neurological, dermatological and

carcinogenic effects.[7]

For these reasons, the development of optical chemosensors able to discriminate trivalent from divalent and monovalent cations[8] is especially appealing. In particular, there are relatively few probes able to detect simultaneously several trivalent cations[9–19] and we have found in the literature only one probe that recognizes Al^{3+}, Fe^{3+}, Cr^{3+}, As^{3+}, In^{3+} and Ga^{3+} at the same time.[20] Moreover, most probes for trivalent cations display sensing features in organic solvents and it is rare to find probes for these cations in pure water.[21] Taking into account these facts, and our experience in the synthesis of molecular and material-based sensors for the optical recognition of chemical species,[22] we report herein the synthesis, characterisation and chromo-fluorogenic behavior toward cations of the chalcone-based probe **3**.

3.3 Results and discussion

- ***Synthesis of probe 3***

The synthesis of **3** is shown in Fig. 1.

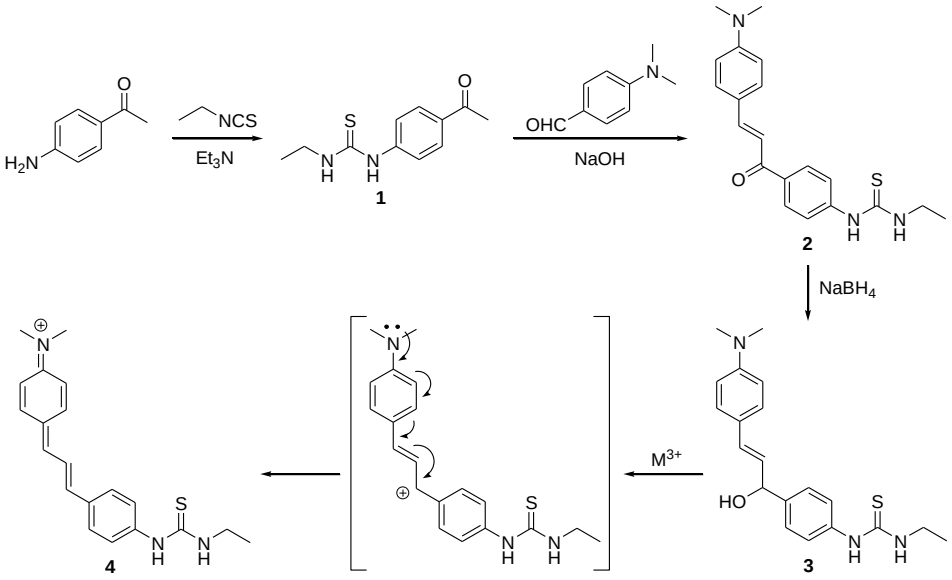

Fig. 1 Schematic representation of the synthetic route used to prepare probe **3** and structure of its dehydration product **4**.

In the first step, 4-aminoacetophenone was reacted with ethylisothiocyanate, yielding derivative **1**. Then, 4-(*N,N*-dimethylamino)benzaldehyde was condensed with **1** to give the chalcone-based product **2**. Finally, reduction of the α,β-unsaturated carbonyl moiety in **2**, using sodium borohydride, yielded probe **3**. The most characteristic ^{1}H NMR signals ($CDCl_3$) of probe **3** were one doublet (J = 4 Hz) centered at 5.3 ppm, which was ascribed to the proton in the carbon atom functionalized with an hydroxyl moiety and attached directly to the *trans* double

bond; one double doublet (*J* = 14, 4 Hz) at 6.1 ppm for the proton of the trans double bond linked directly to the carbon atom bearing the hydroxyl group; and another doublet (*J* = 14 Hz) at 6.5 ppm attributed to the other proton in the $C = C$ bond. Moreover, the aromatic protons appeared, as doublets, at 6.6, 7.1, 7.3 and 7.4 ppm, whereas the singlet at 2.8 ppm was ascribed to the *N,N*-dimethyl moiety.

Water–acetonitrile 95:5 v/v (pH 7.0) solutions of probe **3** were colorless and only intense absorption bands in the UV region were observed. The optical response of probe **3** was tested upon addition of 2 eq. of selected anions (*i.e.* F^-, Cl^-, Br^-, I^-, AcO^-, HS^-, CN^-, NO_3^-) and cations (*i.e.* Li^+, Na^+, K^+, Cu^+, Ag^+, Mg^{2+}, Ca^{2+}, Al^{3+}, Fe^{3+}, Fe^{2}+, Ba^{2+}, In^{3+}, As^{3+}, Zn^{2+}, Ni^{2+}, Ga^{3+}, Cd^{2+}, Hg^{2+}, Cr^{3+}, Co^{2+}, Cu^{2+}, Pb^{2+}, Eu^{3+}, Gd^{3+}, Ce^{3+}, Nd^{3+}).

Of all of them, only Al^{3}+, Fe^{3+}, Cr^{3+}, As^{3+}, In^{3+} and Ga^{3+} induced the appearance of a new absorption band after ca. 5 minutes in the visible region centered at 511 nm (see Fig. 2). The appearance of the new absorbance produced a marked color change from colorless to deep violet (see Fig. 3).

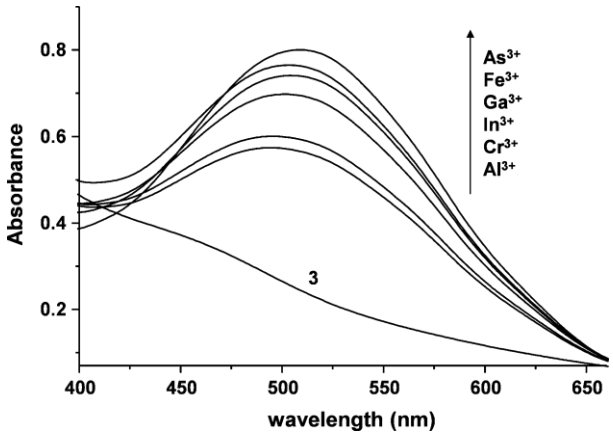

Fig. 2 UV-visible spectra of probe **3** (1.0×10^{-4} mol L^{-1}) in water– acetonitrile 95:5 v/v (pH 7.0) alone and in the presence of trivalent cations (2 eq.).

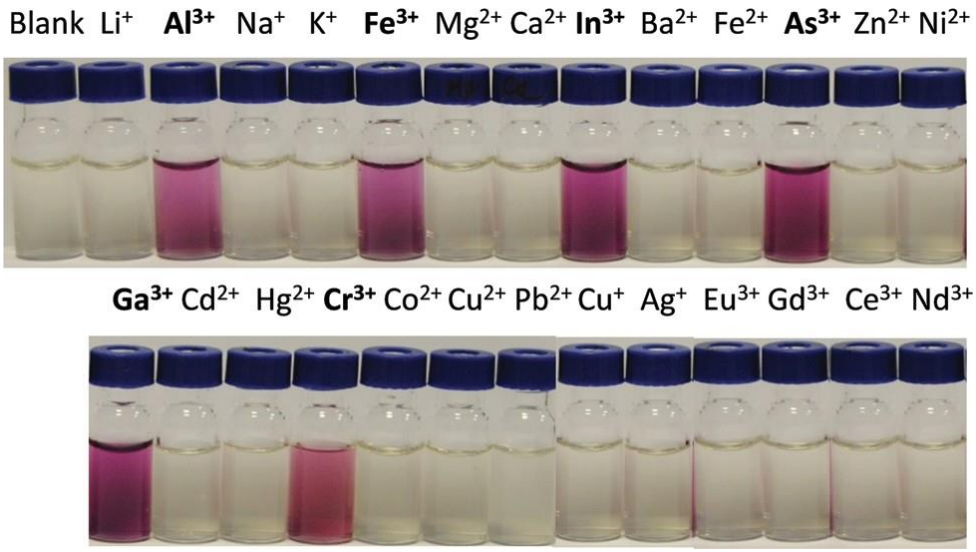

Fig. 3 Color changes observed for water–acetonitrile 95:5 v/v solutions of probe **3** (1.0×10^{-4} mol L^{-1}) at pH 7.0 upon addition of 1 eq. of selected metal cations.

Having assessed the highly selective response of **3** toward trivalent cations, the sensitivity of the probe was studied by monitoring UV-visible changes in water–acetonitrile 95:5 v/v at pH 7.0 upon the addition of increasing quantities of Cr^{3+}, Fe^{3+}, Al^{3+}, Ga^{3+}, In^{3+} and As^{3+}. The UV-visible titration profiles obtained in the presence of the six trivalent cations were quite similar and, as an example, the complete set of spectra obtained for probe **3** and Cr^{3+} cations is shown in Fig. 4 (for titrations with the other trivalent cations see the ESI). As seen in Fig. 4, upon addition of increasing quantities of Cr^{3+} to water–acetonitrile 95:5 v/v solutions of **3**, the absorbance at 516 nm progressively increased. Moreover, from these titration profiles with **3**, the limits of detection (LOD) were calculated (see Table 1). The LOD were in the mM range and were similar to those calculated for other recently published probes for trivalent cations.[9–21]

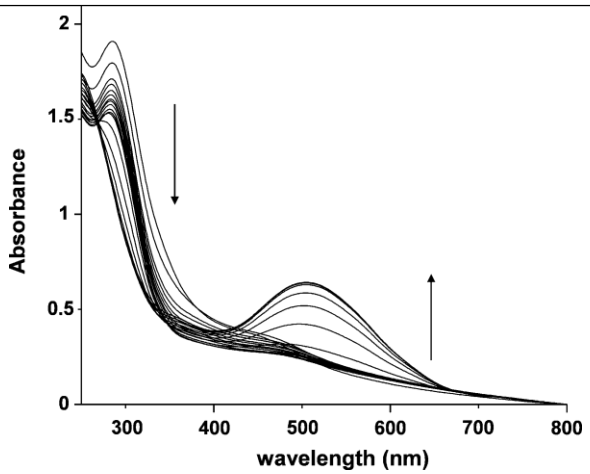

Fig. 4 UV-visible titration of probe **3** (1.0×10^{-4} mol L^{-1}) in water– acetonitrile 95:5 v/v at pH 7.0 upon addition of increasing quantities of Cr^{3+} cation.

Table 1 Detection Limits for probe **3** with trivalent cations.

Cation	UV-visible (μM)	Fluorescence (mM)
Al^{3+}	9.7	9.9
In^{3+}	10.6	10.4
Ga^{3+}	10.9	10.0
Fe^{3+}	10.8	9.2
As^{3+}	10.4	11.7
Cr^{3+}	9.3	10.2

Moreover, we also found that water–acetonitrile 95:5 v/v solutions of **3** showed, when excited at 300 nm, an intense emission band at 397 nm. From all the cations tested, only the addition of Cr^{3+}, Fe^{3+}, Al^{3+}, Ga^{3+}, In^{3+} and As^{3+} induced a marked emission quenching (see Fig. 5 for the set of spectra obtained upon addition of increasing quantities of Cr^{3+}). The LOD obtained from fluorescence titration profiles are also shown in Table 1.

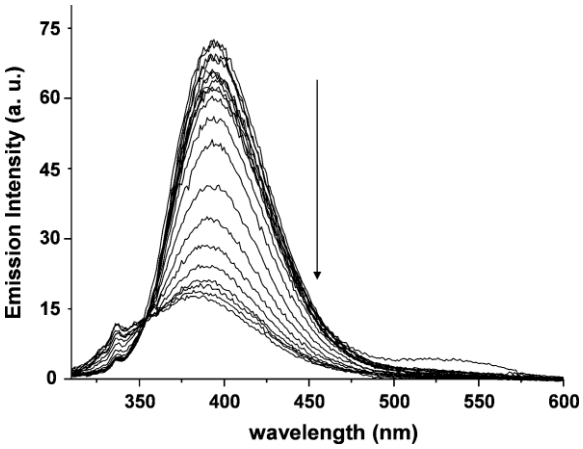

Fig. 5 Fluorescence titration of probe **3** (1.0×10^{-4} mol L^{-1}) in water– acetonitrile 95:5 v/v at pH 7.0 upon addition of increasing quantities of Cr^{3+} cation.

The fact that color and emission changes in the presence of Cr^{3+}, Fe^{3+}, Al^{3+}, Ga^{3+}, In^{3+} and As^{3+} were not instantaneous but time-dependent (*ca.* 5 min) pointed toward a chemical reaction as the mechanism for the chromo-fluorogenic response observed. Moreover, the appearance of the same visible band for the six trivalent cations seemed to indicate the occurrence of a similar chemical reaction in all cases. These trivalent cations are small, have a strong Lewis acid character and a high polarizing power. On the other hand, the appearance of a strong violet color upon reaction with Cr^{3+}, Fe^{3+}, Al^{3+}, Ga^{3+}, In^{3+} and As^{3+} indicated the formation of a final highly conjugated molecule. Taking into account both the facts, we proposed a cation-induced dehydration of probe **3** to yield the highly delocalized cationic molecule **4** (see Fig. 1) as the mechanism in control of the chromogenic modulations observed. This hypothesis was confirmed by the fact that addition of *p*-toluenesulfonic, hydrochloric or sulfuric acids (able to induce dehydration reactions) to water–acetonitrile solutions of probe **3** induced exactly the same chromo-fluorogenic changes (see the ESI). Moreover, HRMS carried out for the compound obtained through *p*-toluenenesulfonic acid-induced dehydration of **3** showed a molecular fragment at *m/z* 338.1687 indicative of the formation of **4** (m/z: 338.1691 calculated for $C_{20}H_{24}N_3S^+$). Chemical reactions that induced an extension of conjugation were recently used as a mechanism for the preparation of

fluorogenic probes for Hg^{2+} cations[23] and reactive oxygen species.[24]

Also, ^1H NMR measurements were carried out in order to assess the dehydration mechanism for the color changes observed in the presence of Cr^{3+}, Fe^{3+}, Al^{3+}, Ga^{3+}, In^{3+} and As^{3+}. In this respect, probe **3** was dissolved in CD_3CN and its ^1H NMR was registered before and after addition of 20 equivalents of Al^{3+} cations. The obtained results are shown in Fig. 6.

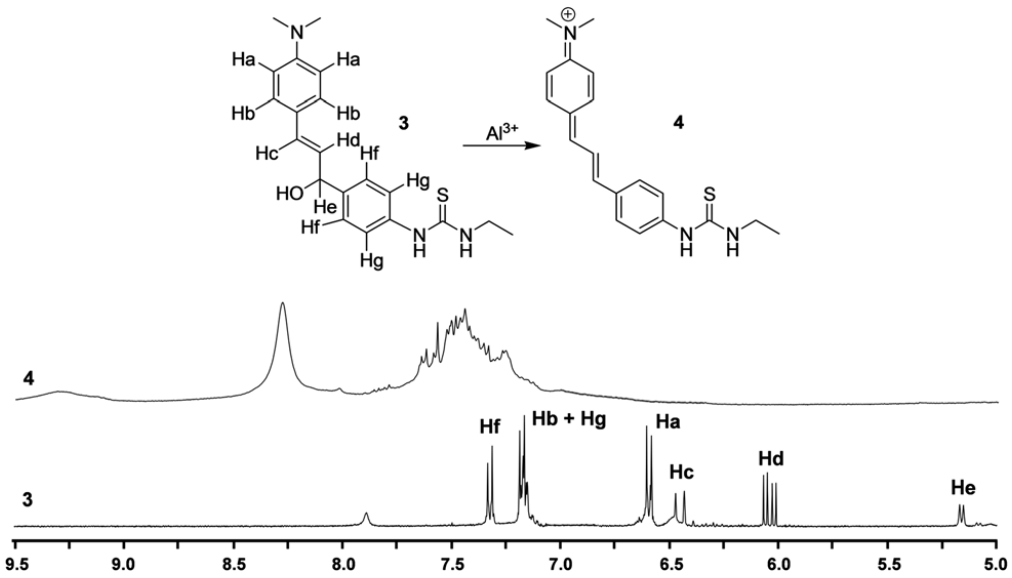

Fig. 6 ^1H NMR spectra of probe **3**, in CD_3CN, alone and in the presence of 20 eq. of Al^{3+} cations

As a general trend, all the resonances of probe **3** were downfield shifted upon addition of Al^{3+} cations. The most remarkable shift was that of methyl groups that in probe **3** appeared as a singlet centered at 2.8 ppm, which was displaced to 3.3 ppm in the presence of Al^{3+} (data not shown in Fig. 6). This remarkable shift could be ascribed to the fact that the methyl groups in the reaction product were directly linked to a positively charged nitrogen atom. Dealing with the signals of the aromatic protons of probe **3**, all resonances showed marked downfield shifts upon addition of Al^{3+} cations. In fact, most of the signals of the final product appeared as a broad multiplet in the 7.0–7.7 ppm interval. However, the most remarkable shifts

were suffered by protons He, Hd and Hc, located in the vicinity of the hydroxyl group of probe **3**. These shifts were ascribed to an Al^{3+}-induced dehydration reaction yielding compound **4**.

3.4 Conclusions

In summary, we reported herein the synthesis and characterization of a new simple probe able to selectively detect Al^{3+}, Fe^{3+}, Cr^{3+}, As^{3+}, In^{3+} and Ga^{3+} over monovalent, divalent and lanthanide trivalent cations and anions in nearly pure water. Trivalent cations were able to induce a dehydration reaction of **3** that resulted in color changes from colorless to deep violet. Moreover, the addition of Cr^{3+}, Fe^{3+}, Al^{3+}, Ga^{3+}, In^{3+} and As^{3+} induced quenching of the emission of free **3**. The probe was also quite sensitive with LOD in the mM range. As far as we know, probe **3** displays a different sensing mechanism from those already reported for the detection of trivalent metal cations; moreover, this is also one of the few probes able to display sensing features for these cations in an aqueous environment.

3.5 Experimental section

- **Synthesis of 1**

4-Aminoacetophenone (2.61 g, 19.31 mmol) was dissolved in THF (25 mL) and then ethyl isothiocyanate (1.75 mL, 19.38 mmol) and triethylamine (2.84 g, 19.31 mmol) were added to the initial solution. The resultant mixture was refluxed for 16 h. Later, the solvent was removed under reduced pressure and the residue was diluted with dichloromethane (30 mL), washed with HCl 10% (3 × 20 mL), dried with $MgSO_4$ and, finally, the organic solvent was evaporated to yield 1 (3.43 g, 15.44 mmol, 80%) as a pale-yellow solid. The ^{1}H and ^{13}C NMR data are coincident with those previously published.[20]

- **Synthesis of 2**

4-(Dimethylamino)benzaldehyde (738.73 mg, 4.95 mmol) and compound **1** (1100 mg, 4.95 mmol) were dissolved in ethanol (16 mL). Then, NaOH 40% solution in H_2O–EtOH 4 : 1 v/v (3.24 mL) was added and the mixture was stirred at room temperature for 18 h. The crude was poured over 100 mL of water. The precipitate was filtered off and dried at 60 ^{o}C. Finally, the solid was recrystallized from MeOH to yield probe **2** (0.78 g, 2.22 mmol, 45%) as red crystals. The ^{1}H and ^{13}C NMR data are coincident with those previously published.[20]

- **Synthesis of 3**

Compound **2** (356 mg, 1 mmol) and sodium borohydride (272.13 mg, 7.19 mmol) were dissolved in acetonitrile–MeOH 2.8 : 1 v/v (380 mL) and stirred for 21 hours. Later, the solvent was evaporated and the crude extracted with water and ethyl acetate (3 × 20 mL). The organic phases were collected, washed with saturated NaCl solution (3 × 20 mL), dried with $MgSO_4$ and, finally, the organic solvent was evaporated to yield **3** (213 mg, 0.6 mmol, 60%) as a yellow-orange solid. ^{1}H NMR (400 MHz, $CDCl_3$): δ 1.10 (t, *J* = 6–5 Hz, 3H), 2.80 (s, 6H), 4.0 (q, *J* = 6.5 Hz, 2H), 5.30 (d, *J* = 4 Hz, 1H), 5.85 (br s, 1H), 6.10 (dd, *J* = 14, 4 Hz, 1H), 6.55 (d, *J* = 14 Hz, 1H), 6.60 (d, *J* = 6.1 Hz, 2H), 7.10 (d, *J* = 6.3 Hz, 2H), 7.25 (d, *J* = 6.1 Hz, 2H), 7.40 (d, *J* = 6.3 Hz, 2H), 7.75 (br s, 1H). ^{13}C NMR (101 MHz, $CDCl_3$): δ 14.0, 40.1, 74.5, 105.6, 125.8, 127.5, 128.0, 130.8, 142.5, 151.2, 181.4. Calcd. for $C_{20}H_{25}N_3OS$: 355.1718; found: 356.1787 ($M + H^+$).

3.6 Acknowledgements

Financial support from the Spanish Government and FEDER funds (Project MAT2015-64139-C4-1) and the Generalitat Valencia (Project PROMETEO II/2014/047) is gratefully acknowledged.

M. L. P. is grateful to the Generalitat Valenciana for her Santiago Grisolia grant.

3.7 References

1. T. P. Flaten, *Brain Res. Bull.*, 2001, **55**, 187.

2. W. E. Winter, L. A. Bazydlo and N. S. Harris, *Lab. Med.*, 2014, **45**, 92.

3. S. Von Haehling and S. D. Anker, *Dtsch. Med. Wochenschr.*, 2014, **139**, 841.

4. S. Wallach, *J. Am. Coll. Nutr.*, 1985, **4**, 107.

5. (a) R. E. Caffey-Nolan and K. L. McCoy, *Toxicol. Appl. Pharmacol.*, 1998, **151**, 330; (*b*) S. M. Kennedy, D. C. Walker, A. S. Belzberg and J. C. Hogg, *J. Nucl. Med.*,1985, **26**, 1195.

6. (a) G. Gabbiani, H. Selye and B. Tuchweber, *Br. J. Pharmacol.*, 1962, **19**, 508; (*b*) J. R. Buscombe, M. E. Caplin and A. J. W.Hilson, *J. Nucl. Med.*, 2013, **44**, 1.

7. N. V. Solenkova, J. D. Newman, J. S. Berger, G. Thurston, J. S. Hochman and G. A. Lamas, *Am. Heart J.*, 2014, **168**, 812.

8. L. E. Santos-Figueroa, M. E. Moragues, E. Climent, A. Agostini, R. Martínez-Máñez and F. Sancenón, *Chem. Soc. Rev.*, 2013, **42**, 3489.

9. A. Barba-Bon, A. M. Costero, S. Gil, M. Parra, J. Soto, R. Martínez-Máñez and F. Sancenón, *Chem. Commun.*, 2012, **48**, 3000.

10. C. Marín-Hernández, L. E. Santos-Figueroa, M. E. Moragues, M. M. M. Raposo, R. M. F. Batista, S. P. G. Costa, T. Pardo, R. Martínez-Máñez and F. Sancenón, *J. Org. Chem.*, 2014, **79**, 10752.

11. S. Goswami, K. Aich, A. Kumar Das, A. Manna and S. Das, *RSC Adv.*, 2013, **3**, 2412.

12. H. Liua, X. Wana, T. Liub, Y. Lib and Y. Yaob, *Sens.Actuators, B*, 2014, **200**, 191.

13. S. Goswami, K. Aich, S. Das, A. K. Das, D. Sarkar, S. Panja, T. K. Mondal and S. Mukhopadhyay, *Chem. Commun.*, 2013, **49**, 10739.

14. X. Wan, T. Liu, H. Liu, L. Gub and Y. Yao, *RSC Adv.*, 2014, **4**, 29479.

15. M. Venkateswarulu, S. Sinha, J. Mathew and R. R. Koner, *Tetrahedron Lett.*, 2013, **54**, 4683.

16. X. Chen, X. Y. Shen, E. Guan, Y. Liu, A. Qin, J. Z. Sun and B. Z. Tang, *Chem. Commun.*, 2013, **49**, 1503.

17. S. Samanta, S. Goswami, A. Ramesh and G. Dasa, *Sens.Actuators, B*, 2014, **194**, 120.

18. M. Venkateswarulu, T. Mukherjee, S. Mukherjee and R. R. Koner, *Dalton Trans.*, 2014, **43**, 5269.

19. L. Wang, F. Li, X. Liu, G. Wei, Y. Cheng and C. Zhu, *J. Polym.Sci., Part A: Polym. Chem.*, 2013, **51**, 4070.

20. L. E. Santos-Figueroa, A. Llopís-Lorente, S. Royo, F. Sancenón, R. Martínez-Máñez, A. M. Costero, S. Gil and M. Parra, *ChemPlusChem*, 2015, **80**, 800.

21. S. Tao, Y. Wei, C. Wang, Z. Wang, P. Fan, D. Shi, B. Ding andJ. Qiu, *RSC Adv.*, 2014, **4**, 46955.

22. See for example: (*a*) L. Pascual, I. Baroja, E. Aznar, F. Sancenón, M. D. Marcos, J. R. Murguía, P. Amorós, K. Rurack and R. Martínez-Máñez, *Chem. Commun.*, 2015, **51**, 1441; (*b*) S. El Sayed, M. Milani, M. Licchelli, R. Martínez-Máñez and F. Sancenón, *Chem. – Eur. J.*, 2015, **21**, 7002; (*c*) M. E. Moragues, A. Toscani, F. Sancenón, R. Martínez-Máñez, A. J. P. White and J. D. E. T. Wilton- Ely, *J. Am. Chem. Soc.*, 2014, **136**, 11930; (*d*) L. E. Santos-Figueroa, C. Giménez, A. Agostini, E. Aznar, M. D. Marcos, F. Sancenón, R. Martínez-Máñez and P. Amorós, *Angew. Chem., Int. Ed.*, 2013, **52**, 13712; (*e*) M. Oroval, E. Climent, C. Coll,

R. Eritja, A. Aviñó, M. D. Marcos, F. Sancenón, R. Martínez-Máñez and P. Amorós, *Chem. Commun.*, 2013, **49**, 5480; (*f*) E. Climent, D. Gröninger, M. Hecht, M. A. Walter, R. Martínez-Máñez, M. G. Weller, F. Sancenón, P. Amorós and K. Rurack, *Chem. – Eur. J.*, 2013, **19**, 4117.

23. W. Xuan, C. Chen, Y. Cao, W. He, W. Jiang, K. Liu andW. Wang, *Chem. Commun.*, 2012, **48**, 7292.

24. K. Kundu, S. F. Knight, N. Willet, S. Lee, W. R. Taylor and

25. N. Murthy, *Angew. Chem., Int. Ed.*, 2009, **48**, 299.

3.8 Supporting Information

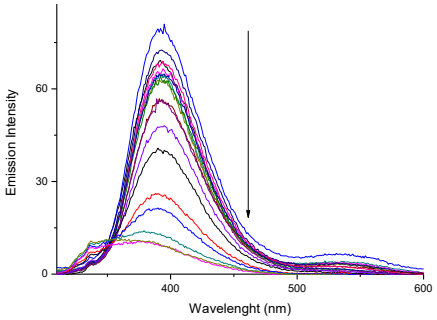

Figure S-1 Uv-visible titration of 3 (1.0 x 10^{-4} mol L^{-1}) in water-acetonitrile 95:5 v/v solution at pH 7.0 upon addiction of increasing quantities of Fe^{3+}.

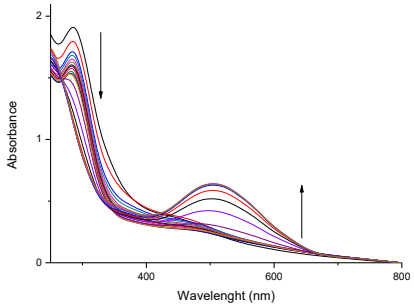

Figure S-2 Fluorescence titration of **3** (1.0 x 10^{-4} mol L^{-1}) in water-acetonitrile 95:5 v/v solution at pH 7.0 upon addiction of increasing quantities of Fe^{3+}.

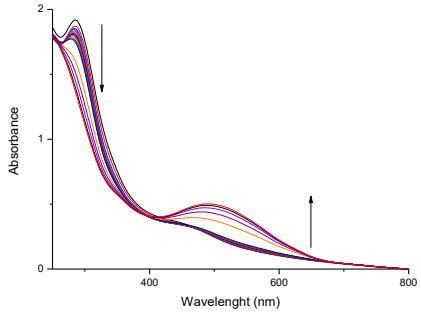

Figure S-3 Uv-visible titration of **3** (1.0 x 10^{-4} mol L^{-1}) in water-acetonitrile 95:5 v/v solution at pH 7.0 upon addiction of increasing quantities of Al^{3+}.

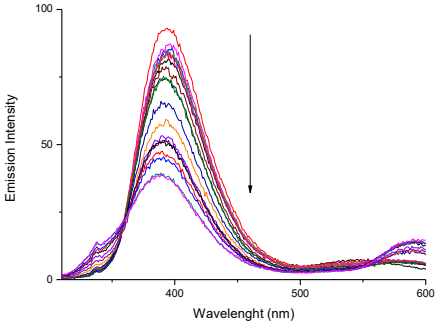

Figure S-4 Fluorescence titration of **3** (1.0 x 10^{-4} mol L^{-1}) in water-acetonitrile 95:5 v/v solution at pH 7.0 upon addiction of increasing quantities of Al^{3+}.

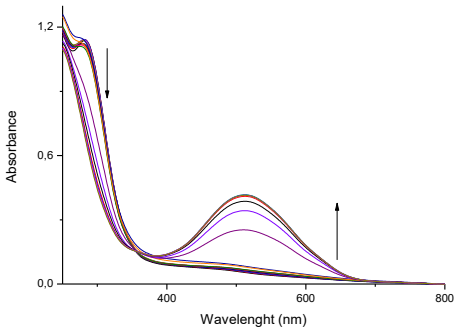

Figure S-5 Uv-visible titration of **3** (1.0 x 10^{-4} mol L^{-1}) in water-acetonitrile 95:5 v/v solution at pH 7.0 upon addiction of increasing quantities of Ga^{3+}.

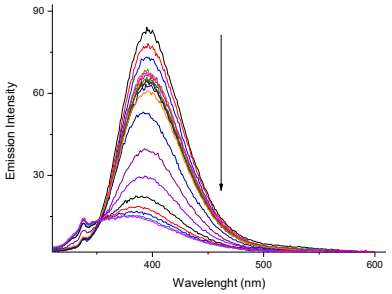

Figure S-6 Fluorescence titration of **3** (1.0 x 10^{-4} mol L^{-1}) in water-acetonitrile 95:5 v/v solution at pH 7.0 upon addiction of increasing quantities of Ga^{3+}.

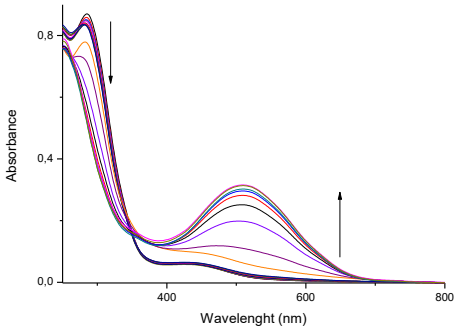

Figure S-7 Uv-visible titration of **3** (1.0 x 10^{-4} mol L^{-1}) in water-acetonitrile 95:5 v/v solution at pH 7.0 upon addiction of increasing quantities of In^{3+}.

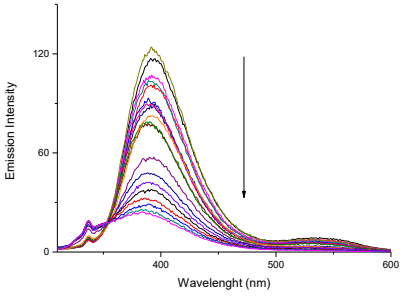

Figure S-8 Fluorescence titration of **3** (1.0 x 10^{-4} mol L^{-1}) in water-acetonitrile 95:5 v/v solution at pH 7.0 upon addiction of increasing quantities of In^{3+}.

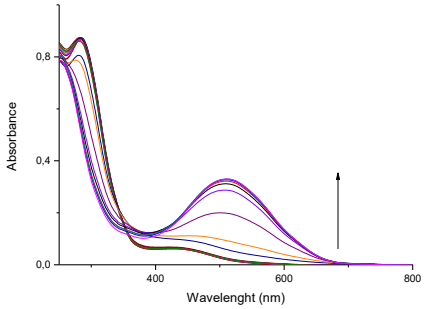

Figure S-9 Uv-visible titration of **3** (1.0 x 10^{-4} mol L^{-1}) in water-acetonitrile 95:5 v/v solution at pH 7.0 upon addiction of increasing quantities of As^{3+}.

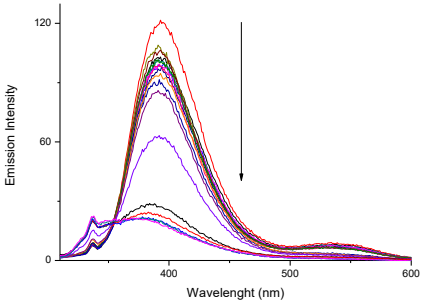

Figure S-10 Fluorescence titration of **3** (1.0 x 10^{-4} mol L^{-1}) in water-acetonitrile 95:5 v/v solution at pH 7.0 upon addiction of increasing quantities of As^{3+}.

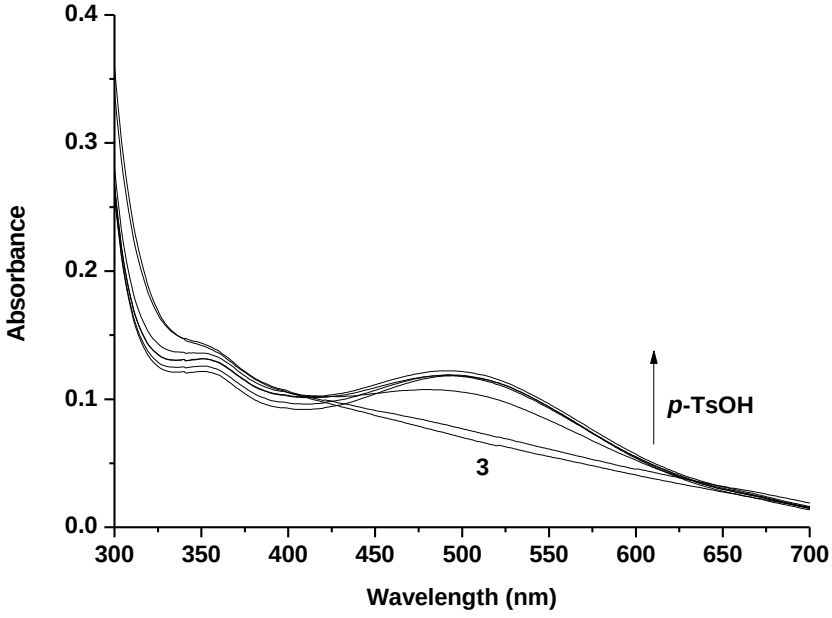

Figure S-11 UV-visible titration of probe **3** (1.0 x 10^{-4} mol L^{-1}) in water-acetonitrile 95:5 v/v at pH 7.0 upon addition of increasing quantities of *p*-toluenesulfonic acid.

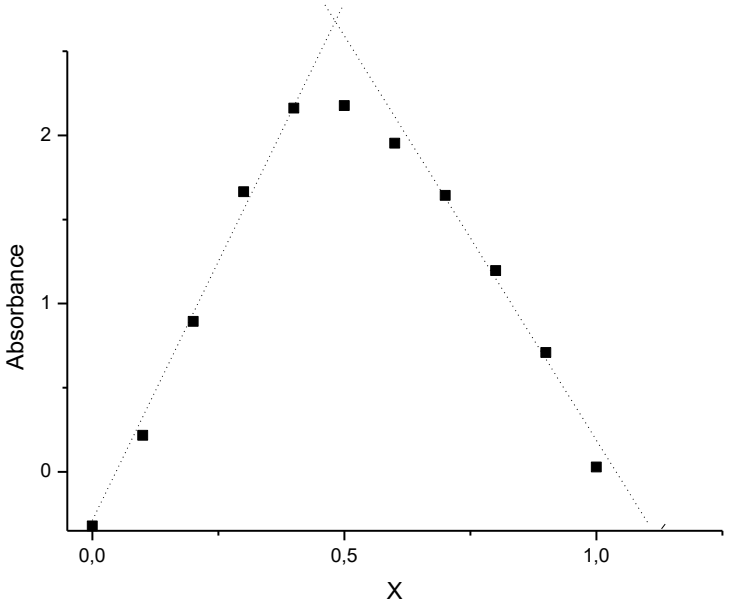

Figure S-12 Job's plot for probe **3** (1.0 x 10^{-3} mol L^{-1}) and Ga^{3+} cation in water-acetonitrile 95:5 v/v solution at pH 7.0.

Chapter 4. A dual channel sulphur-containing a macrocycle functionalised BODIPY probe for the detection of Hg(II) in a mixed aqueous solution

A dual channel sulphur-containing a macrocycle functionalised BODIPY probe for the detection of Hg(II) in a mixed aqueous solution

Maria Lo Presti,[a] Ramón Martínez-Máñez,*[ab] José V. Ros-Lis,[bc] Rosa M. F. Batista,[d] Susana P. G. Costa,[d] M. Manuela M. Raposo*[d] and Félix Sancenón[ab]

[a] Instituto Interuniversitario de Investigación de Reconocimiento Molecular y Desarrollo Tecnológico Universitat Politècnica de València – Universitat de València, Camino de Vera s/n, 46022, Valencia, Spain. E-mail: rmaez@qim.upv.es

[b] CIBER de Bioingeniería, Biomateriales y Nanomedicina (CIBER-BBN), Spain

[c] Inorganic Chemistry Department, Universitat de València, Doctor Moliner 50, 46100, Burjassot, Valencia, Spain

[d] Centro de Química, Universidade do Minho, Campus de Gualtar, 4710-057, Braga, Portugal

Received 30th November 2017
Accepted 24th January 2018

(Reprinted with permission from **New J.Chem., 2018, 42, 7863**

4.1 Abstract

We report herein the synthesis and chromo-fluorogenic behaviour of a new probe **1** containing a boron-dipyrromethene (BODIPY) unit electronically connected with a dithia-dioxa-aza macrocycle. Acetonitrile and water–acetonitrile 95:5 v/v solutions of the probe showed an ICT band in the visible zone and are nearly non-emissive. When acetonitrile was used as a solvent, addition of Hg(II) and trivalent metal cations induced an hypsochromic shift of the absorption band and moderate emission enhancements. A highly selective response was obtained when using competitive media such as water– acetonitrile 95:5 v/v. In this case only Hg(II) induced a hypsochromic shift of the absorption band and a marked emission enhancement.

4.2 Introduction

In the past few decades, the detection and quantification of transition metal cations has attracted great interest in different areas, such as environmental chemistry and clinical toxicology, because of their polluting nature.[1,2] Among them, mercury is one of the most toxic metal ions, even at very low concentrations. Accumulation of mercury over time in humans leads to cognitive and motion disorders and Minamata disease.[3–13] Taking into account the above mentioned facts, the detection of mercury contamination in drinking water, food, air and soil is a matter of concern.

Among the strategies employed to detect and quantify metal cations in general and mercury in particular, the development of optical probes based on supramolecular and coordination concepts has been widely studied and in fact there are a number of publications dealing with the synthesis and characterization of optical probes for Hg(II). Moreover, very recently, two review papers have been published by Lippard[14] and Chen.[15]

Most of the described probes are formed by two subunits, namely, a binding site and a signalling reporter, connected through a covalent bond. The binding site

is responsible for the interaction with the metal cation and is usually designed bearing in mind coordination chemistry principles in order to achieve a high degree of complementarity between both components. In these probes, the interaction between the binding site and Hg(II) is transformed into an easy-to-observe output by the signalling subunit. In the case of optical sensors the signal is based on variations in the emission (fluorescence) or absorption properties of the probe. However, although preferred, systems able to combine both properties (*i.e.* fluorescence and colour change) are less common, in particular if they are accompanied by a ''switch on'' of the emission.

Regarding fluorescent signalling subunits, the boron- dipyrromethene moiety (BODIPY) has received great attention in recent years because of their advantageous features, such as photochemical stability, sharp absorption with high intensity in the visible to NIR region and high fluorescence quantum yields.[16,17] Furthermore, the BODIPY core can be chemically modified in order to fine tune the optical properties or add new functionalities, such as receptor groups selective to analytes in the case of sensors.[18]

In most published probes the BODIPY core is chemically modified at the *meso* position. In general, benzene rings added to this position appear twisted with respect to the difluoro boron dipyrromethene core, and therefore are not part of the conjugated system. Interaction of these probes with selected analytes induces changes in the fluorescence through a reductive or oxidative PET mechanism that can be turned on or off depending on the functional groups.[16] Other probes are constructed by the functionalization at the 3 and 5 positions of the BODIPY core. In this case, the attached groups are conjugated with the BODIPY core and the recognition event induces variations not only in the absorbance but also in the emission. Besides, in the case of functionalization with benzene rings directly linked to a nitrogen atom, an ICT process is active that red shifts the absorption band of the BODIPY core and also quenches the fluorescence. Blocking the nitrogen electron pair (by coordination or protonation), usually results in a recovery of the spectroscopic properties of the original BODIPY framework turning on its emission.[19]

Among the binding sites, sulphur containing macrocycles are particularly well suited for the recognition of Hg(II) in a selective way due to the preferential and

strong nature of the S–Hg interaction.[14] In particular, *N*-phenyl-1-aza-4,13-dithia-7,10-dioxacyclopentadecane has been reported to display a high binding affinity toward Hg(II) over other transition metal cations even in water or mixed aqueous environments. Besides, Hg(II) coordination with the macrocycle modulates the electron donor character of the nitrogen atom, a fact that was reflected in the ICT character of the UV-vis bands.[20,21]

Taking into account the above mentioned facts we report herein the synthesis and chromo-fluorogenic behaviour toward transition metal cations of a new, easy to prepare, BODIPY probe (**1**) which contained a *N*-phenyl-1-aza-4,13-dithia-7,10-dioxacyclopentadecane macrocycle attached to the 3 position to the BODIPY fluorophore. Probe **1** showed an unselective behaviour in acetonitrile, and Hg(II) and other trivalent cations induced changes in the UV-visible and emission spectra. However, a Hg(II) selective response was observed on changing to a more competitive solvent such as water–acetonitrile 95:5 v/v.

4.3 Results and discussion

•Synthesis and characterization of probe 1

Probe **1** consists of a BODIPY core functionalized with a macrocycle (containing sulphur, nitrogen and oxygen atoms) at position 3 of the fluorophore core (see Scheme 1). Probe **1** was prepared by the piperidine-induced condensation between aldehyde **1a** and the BODIPY derivative **1b** (see Scheme 1 and Experimental section for details). The syntheses of **1a** and **1b** were published elsewhere.19,22

Probe **1** contains in its structure a methoxy group linked to a benzene ring at the meso position that was included with the aim to increase its solubility in aqueous environments. Besides, it also contains a N-phenyl-1-aza-4,13-dithia-7,10-dioxacyclopenta- decane macrocycle as the cation binding site. The ^{1}H NMR of probe **1** confirmed the proposed structure.

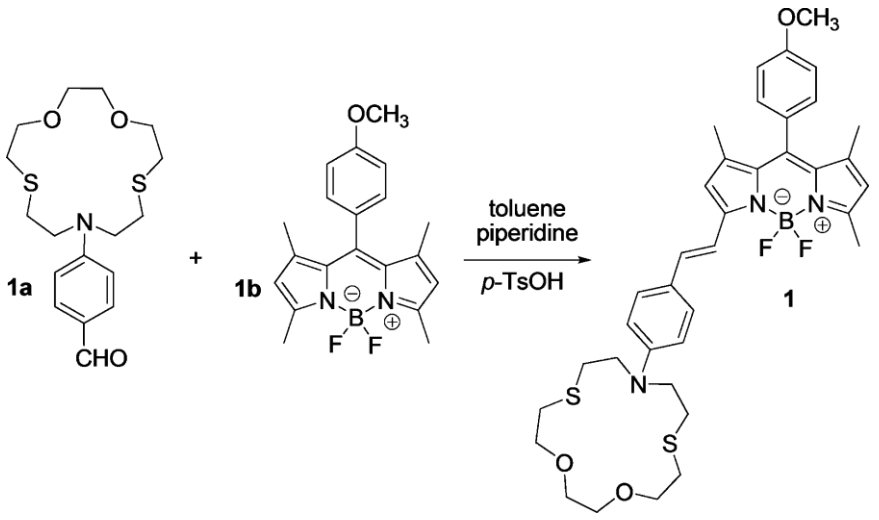

Scheme 1 Synthesis of probe **1**.

•Spectroscopic studies in acetonitrile

In a first step, we studied the chromo-fluorogenic behaviour of **1** in an organic solvent of medium polarity such as acetonitrile. As could be seen in Fig. 1, the UV-visible spectra of probe **1** in acetonitrile is characterised by the presence of an

absorption band centred at *ca.* 600 nm. This absorption band is attributed to the 0–0 vibrational band of an S_0–S_1 transition, from the donor nitrogen atom to the acceptor BODIPY core, with a strong charge-transfer nature.[16] Also a shoulder at *ca.* 550 nm was observed and assigned to the 0–1 vibrational band of the same transition.[19] The ICT nature of the visible bands suggested that the interactions of metal cations with the nitrogen atom of the macrocycle could modulate the HOMO and LUMO levels of the probe which could be reflected in marked colour changes.

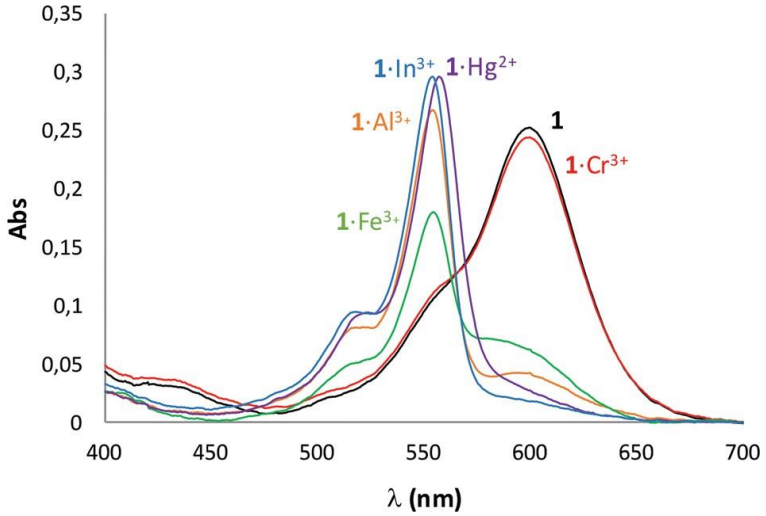

Fig. 1 UV-visible spectra of probe **1** in acetonitrile (1.0 × 10—5 M) alone and in the presence of 1 eq. of Hg(II) and trivalent metal cations.

Bearing in mind the above mentioned facts, in a second step, changes in the colour of probe **1** upon the addition of 1 eq. of selected metal cations was studied. Addition of alkaline (Li(I), Na(I), K(I)) or alkaline-earth (Ca(II) Ba(II), Mg(II)) cations to acetonitrile solutions of **1** induced negligible changes in the UV-visible spectrum of the probe. On the other hand, among certain transition metal cations tested (Hg(II), Al(III), In(III), Cr(III), Fe(III), Co(II), Zn(II), Ni(II), Pb(II), Ag(I)) only Hg(II) and the trivalent cations In(III), Al(III) and Fe(III) were able to induce hypsochromic shifts (*ca.* 45 nm) of the visible band (see Fig. 1) together with marked colour modulation from blue to magenta (see ESI for details). The observed changes in the visible band of **1** are attributed to cation coordination with the donor nitrogen atom of the macrocycle that inactivates the ICT contribution. The spectra obtained after metal cation coordination is similar to that of the BODIPY core with a narrower band

width.[16]

However, it was apparent from these studies that the shifts of the absorption band of **1** observed for Hg(II) and the trivalent cations were slightly different. As can be seen in Fig. 1, Hg(II) induced a slightly lower shift (42 nm) when compared with that obtained in the presence of Al(III), Fe(III) or In(III) (45 nm). This subtle difference could be ascribed to a stronger coordination of Hg(II) with the macrocycle when compared with the strength of the Al(III), Fe(III) or In(III) interaction.

Although the response of **1** in the presence of Hg(II) was expected, since the probe contains a macrocycle that selectively coordinates with this thiophilic cation, **1** also responded to trivalent cations in a medium solvating solvent such as acetonitrile. However, we can observe (see again Fig. 1) that the intensity of the new absorption band, formed upon coordination, varies in the order In(III) > Al(III) >> Fe(III). The observed order is most likely a consequence of the Lewis acidity of the cation and of its affinity towards coordination with the amine in the macrocycle, this last factor being additionally modulated by the interaction with the sulphur and oxygen atoms in the crown ether.

In spite of the fact that **1** was designed to coordinate with cationic species, the UV-visible response of acetonitrile solutions of the probe in the presence of 1 eq. of selected anions (F^-, Cl^-, Br^-, I^-, CN^-, HS^-, HCO_3^-, NO_3^-, AcO^-, BzO^-) was also tested. As expected none of the anions tested induced changes in the UV-visible spectrum of probe **1**.

On the other hand, probe **1** was slightly emissive. Upon excitation of acetonitrile solutions of probe **1** (1.0×10^{-5} M) at 540 nm, a very weak emission band at *ca.* 560 nm was observed (see Fig. 2). The shape and intensity of this band is a direct consequence of the strength of the internal conversion processes and the non-radiative transitions induced by the polar nature of the solvent and the large change in dipole moment between the ground and the excited state derived from the partial CT between the strongly coupled BODIPY core and the aniline group in the macrocycle.[19]

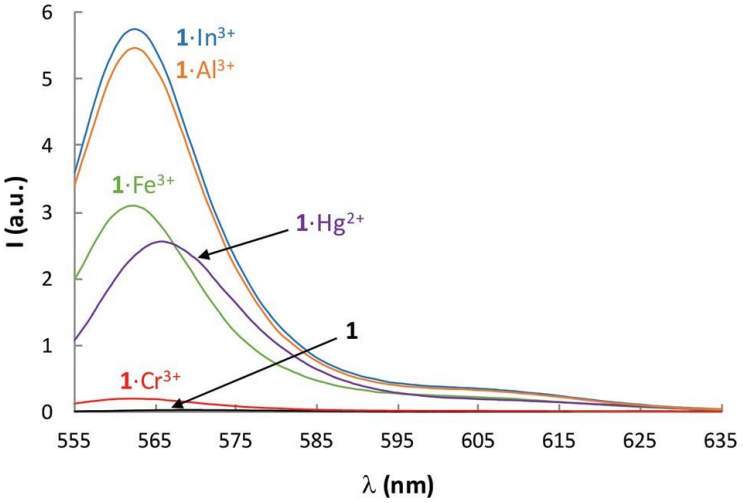

Fig. 2 Emission spectra of probe **1** in acetonitrile (excitation at 540 nm) alone (1.0×10^{-5} M) and in the presence of 1 eq. of Hg(II), In(III), Al(III), Fe(III) and Cr(III).

Moreover, emission changes in the presence of selected metal cations (the same used in the UV-visible experiments) were studied. Again, only Hg(II), Fe(III), In(III) and Al(III) induced marked emission enhancements (see Fig. 2) whereas Cr(III) was able to induce a small emission enhancement.

The intense emission band, which appeared at *ca.* 560 nm, was due to a partial inhibition of the ICT band upon cation coordination with the macrocycle. In the case of trivalent metal cations, the new emission band appeared at 562 nm whereas for Hg(II) the fluorescence was red-shifted to 566 nm (the same effect was observed in the UV-visible measurements, see Fig. 1). Besides, the Stokes' shifts moved from 1069 to 285 and 257 cm^{-1} for the free probe, Hg(II) and trivalent cations complex, respectively, in agreement with the lesser differences in the dipolar moment between the ground and excited states upon complexation with **1**. Regarding intensity, although probe **1** presented a very weak fluorescence, upon complexation with In(III) the emission experienced a 700-fold enhancement. For the trivalent cations, comparing Fig. 1 and 2, it was clear that the emission intensity is proportional to the absorbance measured at 550 nm. This fact could suggest that the trivalent metal cations and probe **1** interacted in a similar fashion (although the intensity of the complexation strength varies between them). Again Hg(II)

presented a different behaviour, when compared with the response obtained with trivalent cations. As could be observed in Fig. 1 the intensity of the absorption band of the complex formed between probe **1** and Hg(II) is almost the same as that in the case of In(III), but the intensity of emission reaches only 44% (see Fig. 2).

In order to assess the site of interaction of metal cations with probe **1**, ^{1}H NMR studies with Hg(II) in deuterated aceto- nitrile were carried out (see Fig. 3).

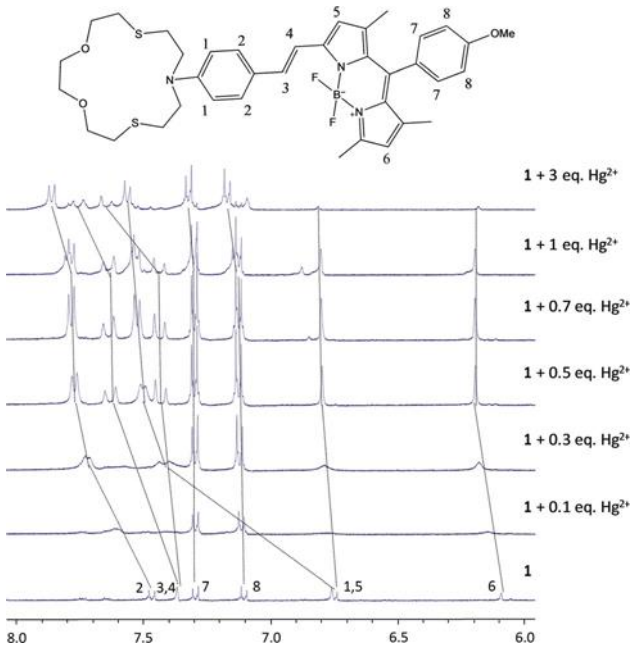

Fig. 3 ^{1}H NMR titration of probe **1** in deuterated acetonitrile in the presence of increasing quantities of Hg(II) cation.

The ^{1}H NMR spectrum of **1** showed the expected signals of the aniline and methoxy phenyl moieties, the vinyl double bond and the BODIPY core protons in the aromatic region (one of them overlapped with the aniline doublet at 6.75 ppm). Probe **1** showed a strong coordination with the Hg(II) cation reflected in the remarkable downfield shifts (0.7 ppm upon addition of 0.5 Hg(II) eq.) suffered by the *ortho* aromatic protons of the 1,4-disubstituted aniline ring. Also, other hydrogens of the aniline ring and the vinyl double bond (all of them close to the macrocycle) showed moderate shifts. In contrast, protons of the 1,4-disubstituted ring at the *meso* position (containing the methoxy subunit) centred at 7.1 and 7.3 ppm experienced negligible shifts. This fact could be explained bearing in mind the

twisted conformation of this 1,4-disubstituted benzene ring with respect to the BODIPY core. As a consequence of this conformation this benzene ring did not participate in the conjugated system of **1** and the coordination with Hg(II) was reflected in insignificant changes. More- over, addition of 1 eq. of the Hg(II) cation induced moderate downfield shifts of the methylene protons adjacent to sulfur atoms from 2.78 and 2.92 ppm to 3.00 and 3.18 ppm together with a marked broadening (see ESI).[23] All these facts suggested that Hg(II) coordinated with the macrocyclic subunit present in probe **1**. Besides, the peaks of the conjugated system broadened or even disappeared upon addition of 0.1–0.3 eq. of Hg(II) indicating a fluxional **1**-Hg(II) system and reinforced the assumption that coordination occurred through the macro- cyclic binding site.

•Spectroscopic studies in the presence of water

Taking into account the response obtained with **1** in acetonitrile and in order to assess its possible application for the detection of transition metal cations in environmental applications the response of the probe in aqueous media was tested. The presence of important amounts of water is expected to modulate the selectivity of the probe toward certain cations[21,24] due to the high solvation energy of these species.

Probe **1** was not fully water soluble and, for this reason, water (pH 7.0)–acetonitrile 95:5 v/v mixtures were used to assess the sensing behaviour toward metal cations. The UV-visible spectrum of **1** in water (pH 7.0)–acetonitrile 95:5 v/v changed markedly when compared to that observed in acetonitrile. The single relatively narrow band at 600 nm in acetonitrile was replaced by a broad absorption with two relative maxima centred at 583 and 613 nm (see Fig. 4). These changes in the shape of the bands may tentatively be ascribed to the formation of aggregates that induced red shifts in the absorption.[25]

The changes in the UV-visible spectrum of **1** in water (pH 7.0)–acetonitrile 95:5 v/v in the presence of 10 eq. of selected metal cations (*i.e.* Na(I), K(I), Li(I), Mg(II), Ca(II), Ba(II), Hg(II), Al(III), In(III), Cr(III), Fe(III), Co(II), Zn(II), Ni(II), Pb(II), Ag(I)) and anions (*i.e.* F^-, Cl^-, Br^-, I^-, CN^-, HS^-, HCO_3^-, NO_3^-, AcO^-, BzO^-) were studied.

The observed response was remarkably selective and only Hg(II) induced remarkable changes. As could be seen in Fig. 4, addition of increasing amounts of Hg(II) induced a decrease of the broad absorptions at 613 and 583 nm together with the appearance of a narrow band centred at 560 nm (similar to that obtained in acetonitrile for the free probe in the presence of Hg(II)). Besides, the colour of the solution changed from blue to pink (see inset in Fig. 4). As expected, water improves the selectivity through the competition of the highly coordinating water solvating sphere with the macrocyclic binding site in probe **1**.

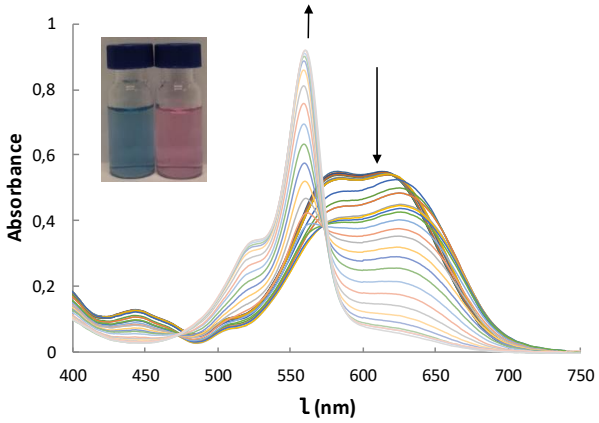

Fig. 4 UV-visible titration spectra of water–acetonitrile 95:5 v/v solutions of probe 1 ($5.0\ 10^{-5}$ M) upon addition of increasing quantities of the Hg^{2+} cation (0–25 eq.). Inset: Colour changes observed in the absence (left) and in the presence (right) of 10 equivalents of Hg(II) cation to the water–acetonitrile 95:5 v/v solutions of probe **1** (5.0×10^{-5} M).

A closer look at the set of spectra shown in Fig. 4 indicates a complex coordination pattern between **1** and the Hg(II) cation (reflected in the absence of isosbestic points). Low amounts of Hg(II) induced a moderate decrease of the bands at 583 and 613 nm, while at high cation concentration, these bands continue to decrease and the narrow absorption band, centred at 561 nm, typical of BODIPY cores, was observed. This behaviour is ascribed to cation coordination with the donor nitrogen atom of the macrocycle that inactivates the ICT contribution active in **1**.

On the other hand, water (pH 7.0)–acetonitrile 95:5 v/v solutions of probe **1** were practically non-emissive upon excitation at 550 nm. Moreover, it was

observed that the response obtained upon addition of target cations and anions was also selective in this solvent mixture since only Hg(II) induced a remarkable emission enhancement at 570 nm (see Fig. 5).[26] As could be seen, the addition of increasing amounts of Hg(II) cation to probe **1** induced a progressive enhancement in emission intensity (300-fold enhancement after addition of 20 eq. of Hg(II)). Furthermore, from the fluorescence titration profile a limit of detection of 99 ppm of Hg(II) was determined. Finally, and taking into account the fact that BODIPY derivative **1** appears to aggregate in aqueous environments, the stability of water–acetonitrile 95:5 v/v solutions of the probe was tested. In this regard, we carried out Hg(II) detection measurements with a freshly prepared solution of probe **1** in water–acetonitrile 95:5 v/v and then, after 72 h, we used the same solution and observed an identical chromo-fluorogenic sensing behaviour. Solutions of probe **1** are quite stable for at least 1 week. After this period of time, a precipitate of the probe begins to appear and the solution loses part of its detection characteristics.

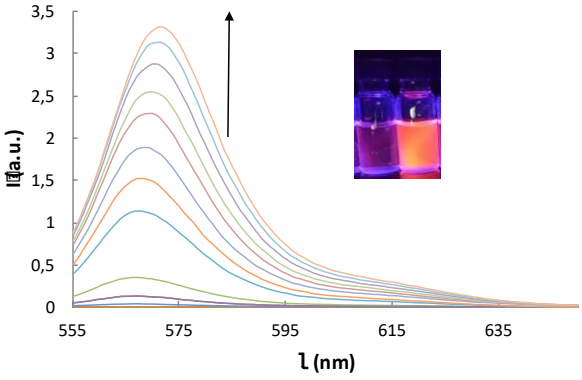

Fig. 5 Set of emission spectra of probe **1** (5.0×10^{-5} M) titration in water (pH 7.0)–acetonitrile 95:5 v/v solutions upon addition of increasing quantities of Hg(II) cation (0–16 eq.). Inset: Fluorescence changes observed in the absence (left) and in the presence (right) of 10 equivalents of Hg(II).

4.4 Conclusions

In summary, we presented herein the synthesis and chromo- fluorogenic behaviour toward metal cations and anions of a new BODIPY derivative. Probe **1** contains a BODIPY core and an aza-dithia-dioxa macrocycle as the binding unit. **1** showed a charge-transfer transition in the visible zone that was blue shifted in acetonitrile in the presence of Hg(II), In(III), Al(III) and Fe(III). The same cations induced marked emission enhancements (*ca.* 700-fold enhancement for In(III)) upon coordination with probe **1**. Moreover, the selectivity of **1** was dramatically improved on changing the solvent to a more competitive media such as water (pH 7.0)–acetonitrile 95:5 v/v. In this medium, only Hg(II) induced a hypsochromic shift (together with a marked colour change) of the visible band of **1** and a marked emission enhancement. The simplicity of the presented probe indicated that this or similar compounds could be of interest for the detection of the Hg(II) cation in environmental or biological applications.

4.5 Experimental section

•Materials and methods

Piperidine, *p*-toluenesulfonic acid, $MgSO_4$, dry toluene and all the perchlorates (Na(I), K(I), Li(I), Mg(II), Ca(II), Ba(II), Hg(II), Al(III), In(III), Cr(III), Fe(III), Co(II), Zn(II), Ni(II), Pb(II), Ag(I)) were purchased from Aldrich and Acros. Acetonitrile was purchased from Scharlab. All commercially available reagents and solvents were used as received. The precursors BODIPY **1b**[19] and crown ether **1a**[22] were synthesized using the experimental procedures reported before. The reaction progress was monitored by thin layer chromatography, 0.25 mm thick pre-coated silica plates (Merck Fertigplatten Kieselgel 60 F254), and the spots were visualised under UV light. Purification was achieved by silica gel column chromatography (Merck Kieselgel, 230–400 mesh). NMR spectra were obtained on a Brucker Avance II 400 at an operating frequency of 400 MHz for ^1H and 100.6 MHz for ^{13}C, using the

solvent peak as internal reference. The solvents are indicated in parenthesis before the chemical shifts values (δ relative to TMS). Peak assignments were made by comparison of chemical shifts, peak multiplicities and *J* values, and were supported by spin decoupling-double resonance and bidimensional heteronuclear techniques. NMR spectroscopy titration was performed in a 400 MHz magnet (Bruker Ascend 400) equipped with an ATM 5 nm probe (BBO 400 MHz 5 mm Z-Grad). Melting points were determined on a Gallenkamp apparatus. Infrared spectra were recorded on a BOMEM MB 104 spectrophotometer. LR-Mass spectra were recorded on a TripleTOF^{TM} 5600 LC/MS/MS System, (AB SCIEX), a triple quadrupole time-of-flight mass spectrum, the MS was measured using the method of direct infusion. Data was evaluated using the PeakView^{TM}eter. High resolution mass spectrometry (HRMS) data were obtained with a TRIPLETOF T5600 (AB SCIEX, USA) spectrometer.

The absorption spectra were recorded with a JASCO V-650 Spectrophotometer. Fluorescence spectra were measured with a JASCO FP-8500 Spectrophotometer (λ_{exc} = 550 nm). The analysis was performed by adding aliquots of Hg(II) perchlorate hydrate to 5.0×10^{-5} M water (pH 7.0)–acetonitrile 95:5 v/v solutions of probe **1**. The UV-vis and fluorescence titrations were measured at room temperature (25 ^{o}C).

•Synthesis of compound 1

The previously prepared BODIPY **1b** (50 mg, 0.14 mmol) was reacted with the formylated crown ether **1a** (50 mg, 0.14 mmol) in dry toluene (10 mL) in a round bottomed flask fitted with a Dean–Stark apparatus and a condenser, in the presence of piperidine (0.12 mL, 1.21 mmol) and a trace amount of *p*-toluenesulfonic acid. The reaction mixture was heated at reflux under a nitrogen inert atmosphere for 2 h. After cooling, the mixture was transferred to a separation funnel and washed with water (10 mL). The organic phase was dried with anhydrous $MgSO_4$, filtered and the solvent was evaporated. The crude residue was subjected to preliminary dry flash chromatography followed by column chromatography on silica, both using ethyl acetate/ petroleum ether (1:2) as eluent. The product was obtained as a blue greenish solid (45 mg, 30%). Mp = 211–213 1C. ^{1}H NMR (400 MHz, $CDCl_3$): δ = 1.44 (s, 3H, CH_3-1), 1.48 (s, 3H, CH_3-7), 2.59 (s, 3H, CH_3-3), 2.78 (t,

J = 5.2 Hz, 4H, S–CH_2–CH_2–O), 2.92 (t, *J* = 7.6 Hz, 4H, N–CH_2–CH_2–O), 3.66 (s, 4H, O–$(CH_2)_2$–O), 3.69 (t, *J* = 7.6 Hz, 4H, N–CH_2–CH_2–O), 3.82 (t, *J* = 5.2 Hz, 4H, S–CH_2–CH_2–O), 3.88 (s, 3H, OCH_3), 5.97 (s, 1H, H-2), 6.59 (s, 1H, H-6), 6.63 (d, *J* = 8.8 Hz, 2H, H-3'' and H-5''), 7.01 (dd, *J* = 8.8 Hz, 2H, H-3' and H-5'), 7.17–7.21 (m, 3H, Hβ, H-2' and H-6'), 7.47–7.51 (m, 3H, Hα, H-2'' and H-6'') ppm. ^{13}C NMR (100.6 MHz, $CDCl_3$): δ = 14.4 (CH_3-1), 14.6 (CH_3-3), 14.9 (CH_3-7), 29.6 (N–CH_2–CH_2–O), 31.3 (S–CH_2–CH_2–O), 51.9 (N–CH_2–CH_2–O), 55.3 (OCH_3), 70.7 (O–$(CH_2)_2$O), 74.3 (S–CH_2–CH_2–O), 111.8 (C-3'' and C-5''), 114.4 (C-3' and C-5'), 114.6 (Ca), 117.5 (C-6), 120.4 (C-2), 124.8 (C-1''), 127.4 (C-1'), 129.5 (C-2' and C-6'), 129.6 (C-2'' and C-6''), 131.6 (C-8a), 133.4 (C-7a), 137.2 (Cβ), 139.0 (C-8), 140.9 (C-1), 142.8 (C-7), 147.7 (C-4''), 152.9 (C-3), 154.5 (C-5), 160.0 (C-4') ppm. IR (liquid film): *υ* 2922, 2856, 1737, 1591, 1539, 1520, 1501, 1467, 1413, 1353, 1295, 1247, 1200, 1177, 1119, 1076, 1030, 985, 813 cm^{-1}. HRMS-EI *m*/*z*: calcd for $C_{37}H_{44}BF_2N_3O_3S_2$ + H^+: 692.2963; measured: 692.2958. Elemental analysis calcd for $C_{37}H_{44}BF_2N_3O_3S_2$ 64.25% C, 6.41% H, 6.07% N, 9.27% S; measured 64.17% C, 6.44% H, 6.03% N, 9.31% S.

4.6 Acknowledgements

We thank the Spanish Government (MAT2015-64139-C4-1-R) and Generalitat Valenciana (PROMETEOII/2014/047). M. L. P. thanks Generalitat Valenciana for her Grisolia fellowship. Thanks are also due to Fundação para a Ciência e Tecnologia (Portugal) for financial support to the Portuguese NMR network (PTNMR, Bruker Avance III 400-Univ. Minho), FCT and FEDER (European Fund for Regional Development)-COMPETEQREN- EU for financial support to the research centre CQ/UM [PEst-C/ QUI/UI0686/2013 (FCOMP-01-0124-FEDER-037302)], and a post-doctoral grant to R. M. F. Batista (SFRH/BPD/79333/2011).

4.7 References

1. G. K. Walkup and B. Imperiali, *J. Am. Chem. Soc.*, 1996, **118**, 3053.

2. A. Miyawaki, J. Llopis, R. Helm, J. M. McCaffery, J. A. Adams, M. Ikura and R. Y. Tsien, *Nature*, 1997, **388**, 882.

3. D. Zeller and S. Booth, *Science*, 2005, **310**, 777.

4. L. A. Broussard, C. A. Hammett-Stabler, R. E. Winecker and J. D. Ropero-Miller, *Labor-Med.*, 2002, **33**, 614.

5. A. Curley, V. A. Sedlak, E. F. Girling, R. E. Hawk, W. F. Barthel, P. E. Pierce and W. H. Likosky, *Science*, 1971, **172**, 65.

6. T. W. Clarkson, L. Magos and G. J. Myers, *N. Engl. J. Med.*,2003, **349**, 1731.

7. C. M. Carvalho, E. H. Chew, S. I. Hashemy, J. Lu and A. Holmgren, *J. Biol. Chem.*, 2008, **283**, 11913.

8. F. Schurz, M. Sabater-Vilar and J. Fink-Gremmels, *Mutagenesis*, 2000, **15**, 525.

9. M. T. Solis, E. Yuen, P. S. Cortez and P. J. Goebel, *Am.J. Emerg. Med.*, 2000, **18**, 599.

10. D. Mozaffarian, P. Shi, J. S. Morris, P. Grandjean, D. S.Siscovick, D. Spiegelman, W. C. Willett, E. B. Rimm, G. C. Curhan and J. P. Forman, *Hypertension*, 2012, **60**, 645.

11. N. Takahata, H. Hayashi, S. Watanabe and T. Anso, *Folia Psychiatr. Neurol. Jpn.*, 1970, **24**, 59.

12. A. Franzblau, H. D'Arcy, M. B. Ishak, R. A. Werner, B. W. Gillespie, J. W. Albers, C. Hamann, S. E. Gruninger, H. N. Chou and D. M. Meyer, *Neurotoxicology*, 2012, **33**, 299.

13. B. Fernandes Azevedo, L. Barros Furieri, F. M. Peçanha, G. A. Wiggers, P. Frizera Vassallo, M. Ronacher Simõ es, J. Fiorim, P. Rossi de Batista, M. Fioresi, L. Rossoni, I. Stefanon, M. J. Alonso, M. Salaices and D. ValentimVassallo, *J. Biomed. Biotechnol.*, 2012, **2012**, 949048.

14. E. M. Nolan and S. J. Lippard, *Chem. Rev.*, 2008, **108**, 3443.

15. G. Chen, Z. Guo, G. Zeng and L. Tanga, *Analyst*, 2015, **140**, 5400.

16. A. Loudet and K. Burgess, *Chem. Rev.*, 2007, **107**, 4891.

17. R. Ziessel, G. Ulrich and A. Harriman, *New J. Chem.*, 2007, **31**, 496.

18. (*a*) G. Ulrich, R. Ziessel and A. Harriman, *Angew. Chem., Int. Ed.*, 2008, **47**, 1184; (*b*) A. Barba-Bon, A. M. Costero, S. Gil, F. Sancenón and R. Martínez-Máñez, *Chem. Commun.*, 2014, **50**, 13289; (*c*) T. Ozdemir, Z. Kostereli, R. Guliyev, S. Yalcin, Y. Dede and E. U. Akkaya, *RSC Adv.*, 2014,**4**, 14915; (*d*) A. Coskun, M. D. Yilmaz and E. U. Akkaya, *Org. Lett.*, 2007, 9, 607; (*e*) T. Ozdemir, F. Sozmen, S. Mamur, T. Tekinay and E. U. Akkaya, *Chem. Commun.*, 2014, **50**, 5455;(*f*) M. Isik, T. Ozdemir, I. S. Turan, S. Kolemen andE. U. Akkaya, *Org. Lett.*, 2013, **15**, 216.

19. M. Baruah, W. Qin, C. Flors, J. Hofkens, R. A. L. Valle, D. Beljonne, M. Van der Auweraer, W. M. De Borggraeve andN. Boens, *J. Phys. Chem. A*, 2006, **110**, 5998.

20. (*a*) A. B. Descalzo, R. Martínez-Máñez, R. Radeglia, K. Rurack and J. Soto, *J. Am. Chem. Soc.*, 2003, **125**, 3418; (*b*) T. Ábalos, D. Jiménez, M. Moragues, S. Royo, R. Martínez-Máñez, F. Sancenón, J. Soto, A. M. Costero, M. Parra and S. Gil, *Dalton Trans.*, 2010, **39**, 3449; (*c*) T. Ábalos, M. Moragues, S. Royo, D. Jiménez, R. Martínez-Máñez, J. Soto, F. Sancenón, S. Gil and J. Cano, *Eur. J. Inorg. Chem.*, 2012, 76.

21. (*a*) J. V. Ros-Lis, R. Martínez-Máñez, K. Rurack, F. Sancenón, J. Soto and M. Spieles, *Inorg. Chem.*, 2004, **43**, 5183; (*b*) J. V.Ros-Lis, R. Martínez-Máñez, F. Sancenón, J. Soto, M. Spieles and K. Rurack, *Chem. – Eur. J.*, 2008, 14, 10101; (*c*) S. Atilgan, T. Ozdemir and E. U. Akkaya, *Org. Lett.*, 2010, **12**, 4792.

22. M. Yuan, Y. Li, J. Li, C. Li, X. Liu, J. Lv, J. Xu, H. Liu, S. Wangand D. Zhu, *Org. Lett.*, 2007, **9**, 2313.

23. M. Zhu, M. Yuan, X. Liu, J. Xu, J. Lv, C. Huang, H. Liu, Y. Li, S. Wang and D. Zhu, *Org. Lett.*, 2008, **10**, 1481.

24. J. V. Ros-Lis, R. Martínez-Máñez, F. Sancenón, J. Soto, K. Rurack, M. Spieles and H. Weißhoff, *Eur. J. Org. Chem.*, 2007, 2449.

25. B. Wu, L. Xu, S. Wang, Y. Wang and W. Zhang, *Polym.Chem.*, 2015, **6**, 4279.

26. X.-J. Jiang, C.-L. Wong, P.-C. Lo and D. K. P. Ng, *DaltonTrans.*, 2012, **41**, 1801.

4.8 Supporting Information

•Materials and methods

4-Methoxybenzaldehyde (**I**), 2,4-dimethyl pyrrole (**II**), dry CH_2Cl_2 and dry toluene were purchased from Aldrich and Acros. All commercially available reagents and solvents were used as received. The precursors BODIPY **1b** [1], crown ether **III** [2] and **1a** [3] were synthesized using the experimental procedures reported before. Reaction progress was monitored by thin layer chromatography, 0.25 mm thick pre-coated silica plates (Merck Fertigplatten Kieselgel 60 F254), and spots were visualized under UV light. Purification was achieved by silica gel column chromatography (Merck Kieselgel, 230-400 mesh). NMR spectra were obtained on a Brucker Avance II 400 at an operating frequency of 400 MHz for ^1H and 100.6 MHz for ^{13}C, using the solvent peak as internal reference. The solvents are indicated in parenthesis before the chemical shifts values (δ relative to TMS). Peak assignments were made by comparison of chemical shifts, peak multiplicities and *J* values, and were supported by spin decoupling-double resonance and bidimensional heteronuclear HMBC (heteronuclear multiple bond coherence) and HMQC (heteronuclear multiple quantum coherence) techniques. Melting points were determined on a Gallenkamp apparatus and are uncorrected. Infrared spectra were recorded on a BOMEM MB 104 spectrophotometer.

•Synthesis of BODIPY derivatives 1b and 1

The precursor BODIPY derivative **1b** was synthesized through reaction of 4-methoxybenzaldehyde (**I**) and 2,4-dimethyl pyrrole (**II**) in the presence of a catalytical amount of TFA, followed by oxidation with DDQ and treatment with BF_3-OEt_2 in 33 % yield. Earlier the synthesis of compound **1b** was reported in in 38 % yield by Boens *et al* [1]. On the other hand, the precursor crown ether **III** was prepared by the Richman-Atkins reaction using the synthetic procedure described by some of us [2], in which the mesylated *N,N´*-phenylethanolamine was initially synthesized by reaction of *N,N'*-phenylethanolamine with methanesulfonyl chloride in 96 % yield. In a second step, the mesylated precursor obtained above reacted with the 3,6-dioxaoctane-1,8-dithiol, yielding the crown ether **III** as a

colorless solid in 40 % yield. Vilsmeier formylation of compound **III** with $POCl_3$ in DMF gave the formylated crown ether **1a** [3], in 80 % yield (see Scheme S1).

The target BODIPY **1** was prepared by a condensation reaction of **1b** and crown ether **1a**, in toluene, at reflux, under a N_2 atmosphere using piperidine-*p*-toluenesulfonic acid as catalyst (see Scheme S2). Purification of the crude product **1** by preliminary dry flash chromatography followed by column chromatography on silica, both using ethyl acetate/petroleum ether (1:2) as eluent afford the pure compound as a blue greenish solid in 30% yield. The new BODIPY derivative **1** was completely characterized by the usual spectroscopic techniques.

The most characteristic signals in the ^{1}H NMR spectra for compound **1** were those corresponding to the BODIPY nucleus such as the singlets assigned to H-2 and H-6 at 5.97 and 6.59 ppm respectively, and the singlet at 3.88 ppm assigned to the OCH_3 group in 4´ position. Functionalization of the BODIPY **1b** with the crown ether moiety in order to obtained compound **1** can be also confirmed by ^{1}H NMR. Therefore it was observed the substitution of two singlets at 1.44 ppm (s, 6H, CH_3-1 and CH_3-7) and 2.56 ppm (s, 6H, CH_3-3 and CH_3-5) in the ^{1}H NMR spectra of **1b** by three singlets at 1.44, 1.48 and 2.59 ppm assigned to the *N,N*-dimethylamino groups in positions 1, 7 and 3 respectively. Additionally, five new signals at 2.78 ppm (t, J = 5.2 Hz, 4H, S-CH_2-CH_2-O), 2.92 ppm (t, J = 7.6 Hz, 4H, N-CH_2-CH_2-O), 3.66 ppm (s, 4H, O-$(CH_2)_2$-O), 3.69 ppm (t, J = 7.6 Hz, 4H, N-CH_2-CH_2-O) and 3.82 ppm (t, J = 5.2 Hz, 4H, S-CH_2-CH_2-O), assigned to the protons of the crown ether moiety were also observed in the ^{1}H NMR spectra of **1**.

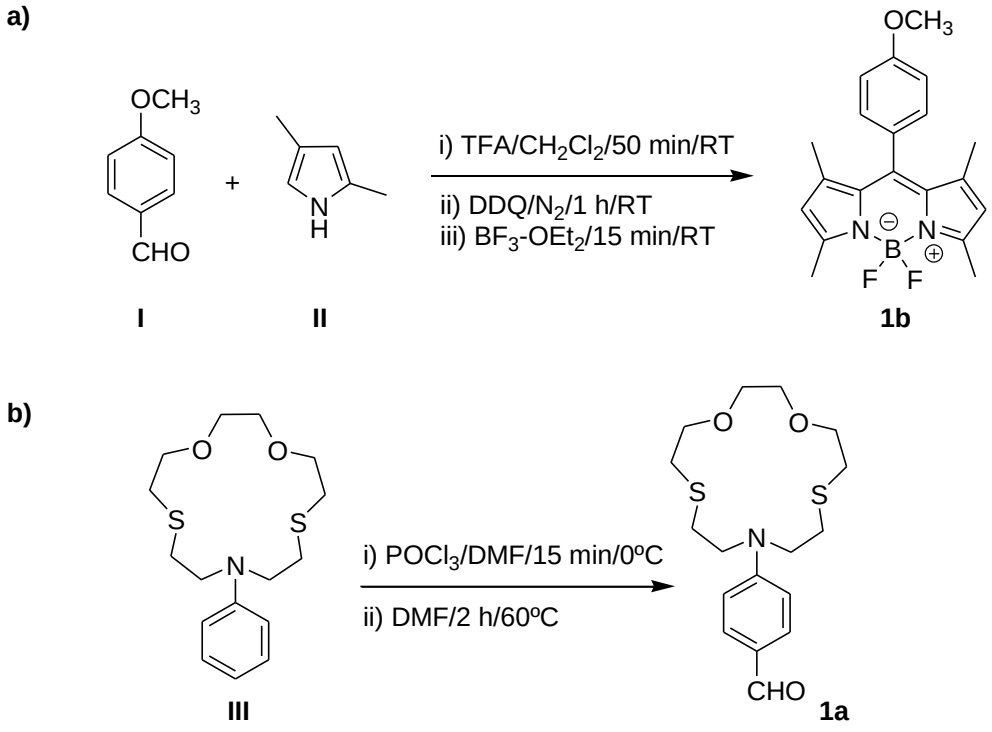

Scheme S1. (a) Synthesis of BODIPY **1b** and **(b)** crown ether **1a**.

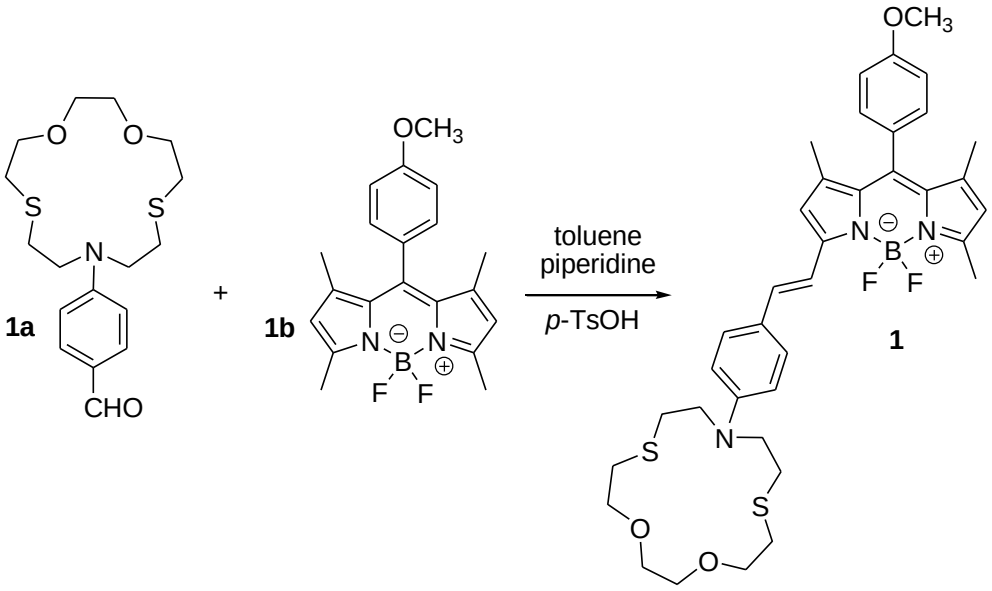

Scheme S2. Synthesis of BODIPY derivative **1**.

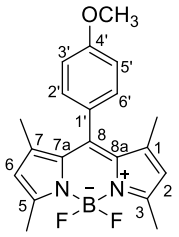

1b

*Synthesis of BODIPY **1b***: 2,4-Dimethyl pyrrole (**II**, 559 mg, 5.80 mmol) and 4-methoxybenzaldehyde (**I**, 400 mg, 2.9 mmol) were dissolved in anhydrous dichloromethane (990 mL). One drop of trifluoracetic acid was added in catalytic amount and the mixture was allowed to stir for 50 min at room temperature under N_2 atmosphere. A solution of DDQ (2.62 g, 7.6 mmol) in dichloromethane (50 mL) was added to the mixture. Stirring was continued for another 45 min and then triethylamine (13.3 mL, 95.2 mmol) was added. After stirring for 15 min $BF_3.OEt_2$ (13.3 mL, 161.1 mmol) was added and further stirred for 30 min. The mixture was evaporated under reduced pressure and the crude residue was subjected to a preliminary dry flash chromatography (petroleum ether/ethyl acetate, 4:1), followed by column chromatography on silica gel (petroleum ether/ethyl acetate, 4:1). The compound was obtained as reddish solid (337 mg, 33 %). Mp = 221–223 ºC (lit.[1] 214-216 ^oC). ^1H NMR (400 MHz, $CDCl_3$): δ = 1.44 (s, 6H, CH_3-1 and CH_3-7), 2.56 (s, 6H, CH_3-3 and CH_3-5), 3.88 (s, 3H, OCH_3), 5.98 (s, 2H, H-2 and H-6), 7.02 (dd, *J* = 7.2 and 2.4 Hz, 2H, H-3'and H-5'), 7.17 (dd, *J* = 7.2 and 2 Hz, 2H, H-2' and H-6') ppm. ^{13}C NMR (100.6 MHz, $CDCl_3$): δ = 14.5 (CH_3-1, CH_3-3, CH_3-5 and CH_3-7), 55.3 (OCH_3), 114.5 (C-3' and C-5'), 121.0 (C-2 and C-6), 126.9 (C-1'), 129.2 (C-2' and C-6'), 131.8 (C-7a and C-8a), 141.8 (C-8), 143.1 (C-1 and C-7), 155.2 (C-3 and C-5), 160.1 (C-4') ppm.

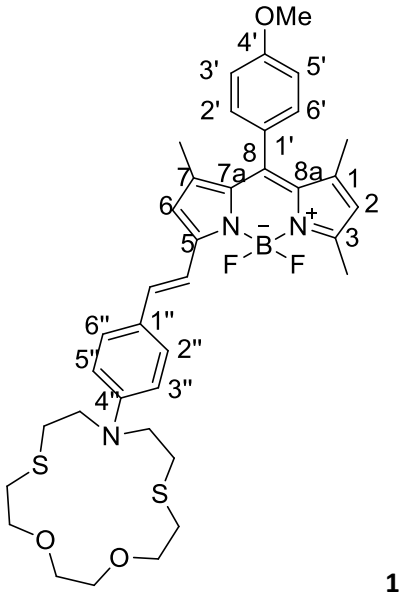

1

*Synthesis of BODIPY **1***: The previously prepared BODIPY **1b** (50 mg, 0.14 mmol) was reacted with the formylated crown ether **1a** (50 mg, 0.14 mmol) in dry toluene (10 mL) in a round bottomed flask fitted with a Dean-Stark and a condenser, in the presence of piperidine (0.12 mL, 1.21 mmol) and a trace amount of *p*-toluenesulfonic acid. The reaction mixture was heated at reflux under nitrogen inert atmosphere for 2 h. After cooling, the mixture was transferred to a separation funnel and washed with water (10 mL). The organic phase was dried with anhydrous $MgSO_4$, filtered and the solvent was evaporated. The crude residue was subjected to a preliminary dry flash chromatography followed by column chromatography on silica, both using ethyl acetate/petroleum ether (1:2) as eluent. The product was obtained as a blue greenish solid (45 mg, 30 %). Mp = 211–213 °C. ^{1}H NMR (400 MHz, $CDCl_3$): δ = 1.44 (s, 3H, CH_3-1), 1.48 (s, 3H, CH_3-7), 2.59 (s, 3H, CH_3-3), 2.78 (t, *J* = 5.2 Hz, 4H, S-CH_2-CH_2-O), 2.92 (t, *J* = 7.6 Hz, 4H, N-CH_2-CH_2-O), 3.66 (s, 4H, O-$(CH_2)_2$-O), 3.69 (t, *J* = 7.6 Hz, 4H, N-CH_2-CH_2-O), 3.82 (t, *J* = 5.2 Hz, 4H, S-CH_2-CH_2-O), 3.88 (s, 3H, OCH_3), 5.97 (s, 1H, H-2), 6.59 (s, 1H, H-6), 6.63 (d, *J* = 8.8 Hz, 2H, H-3'' and H-5''), 7.01 (dd, *J* = 8.8 Hz, 2H, H-3' and H-5'), 7.17–7.21 (m, 3H, Hβ, H-2'and H-6'), 7.47–7.51 (m, 3H, Hα, H-2''and H-6'') ppm. ^{13}C NMR (100.6 MHz, $CDCl_3$): δ= 14.4 (CH_3-1), 14.6 (CH_3-3), 14.9 (CH_3-7), 29.6 (N-CH_2-CH_2-O), 31.3 (S-CH_2-CH_2-O), 51.9 (N-CH_2-CH_2-O), 55.3 (OCH_3), 70.7 (O-$(CH_2)_2$O), 74.3 (S-CH_2-CH_2-O), 111.8 (C-3'' and C-5''), 114.4 (C-3' and C-5'), 114.6 (Cα), 117.5 (C-6), 120.4 (C-2), 124.8 (C-1''), 127.4

(C-1'), 129.5 (C-2' and C-6'), 129.6 (C-2'' and C-6''), 131.6 (C-8a), 133.4 (C-7a), 137.2 (Cβ), 139.0 (C-8), 140.9 (C-1), 142.8 (C-7), 147.7 (C-4''), 152.9 (C-3), 154.5 (C-5), 160.0 (C-4') ppm. IR (liquid film): υ 2922, 2856, 1737, 1591, 1539, 1520, 1501, 1467, 1413, 1353, 1295, 1247, 1200, 1177, 1119, 1076, 1030, 985, 813 cm^{-1}. HRMS-EI m/z: calcd for $C_{37}H_{44}BF_2N_3O_3S_2 + H^+$: 692.2963; measured: 692.2958.

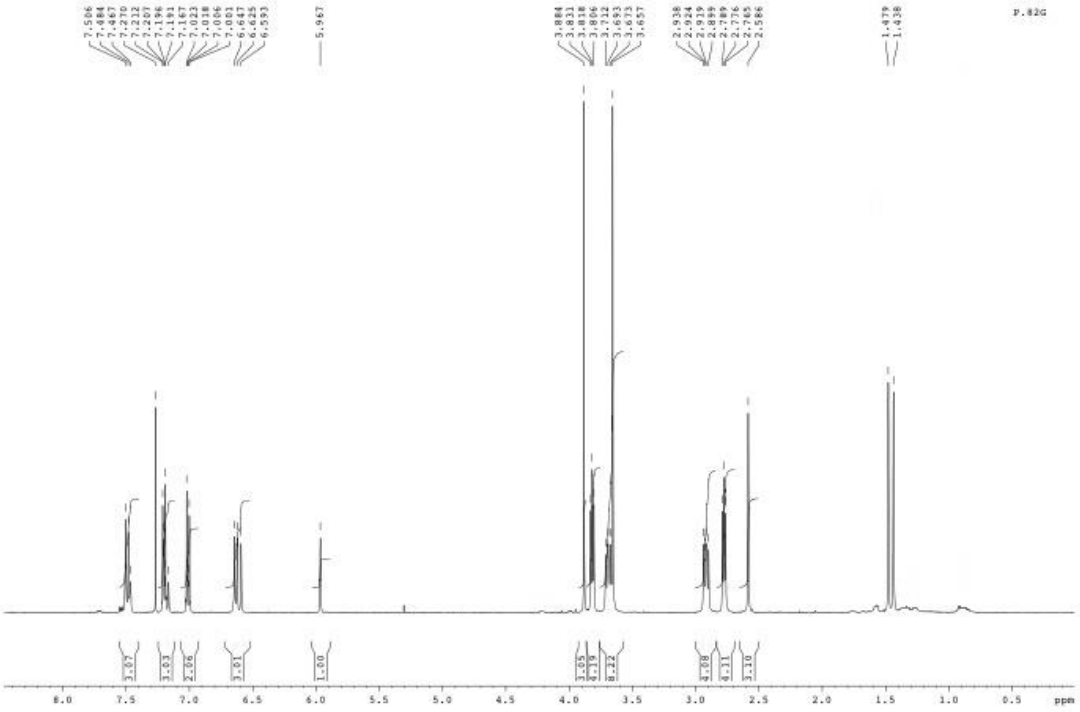

Figure S1. ^1H NMR spectrum of probe **1** in $CDCl_3$.

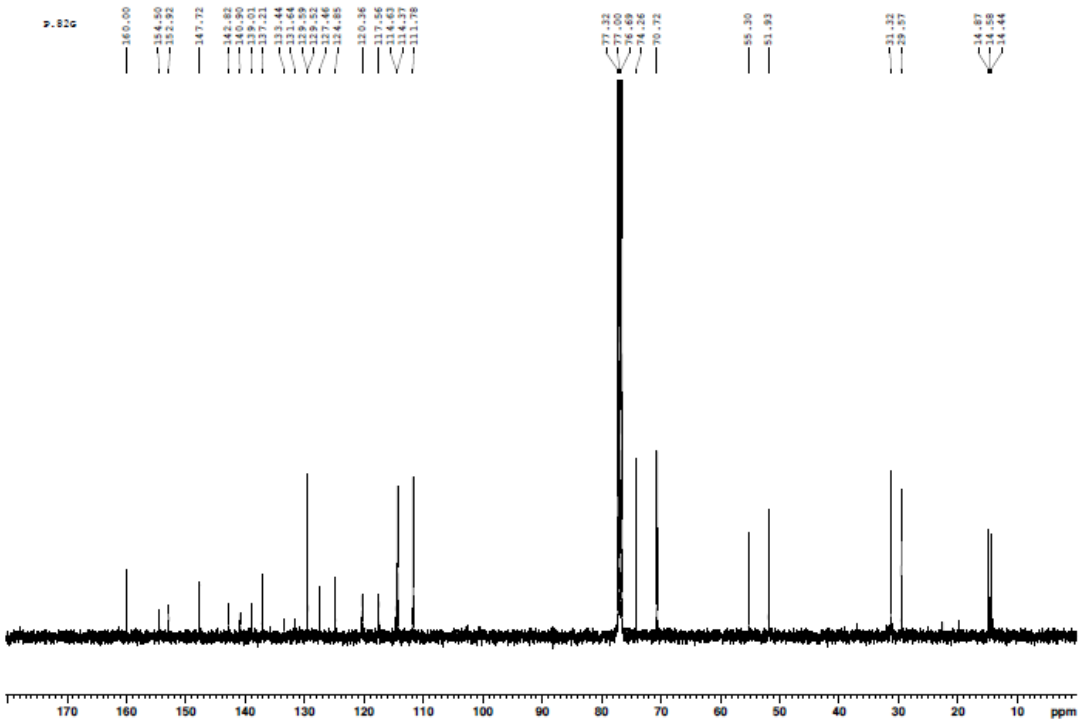

Figure S2. ^{13}C NMR spectrum of probe **1** in $CDCl_3$

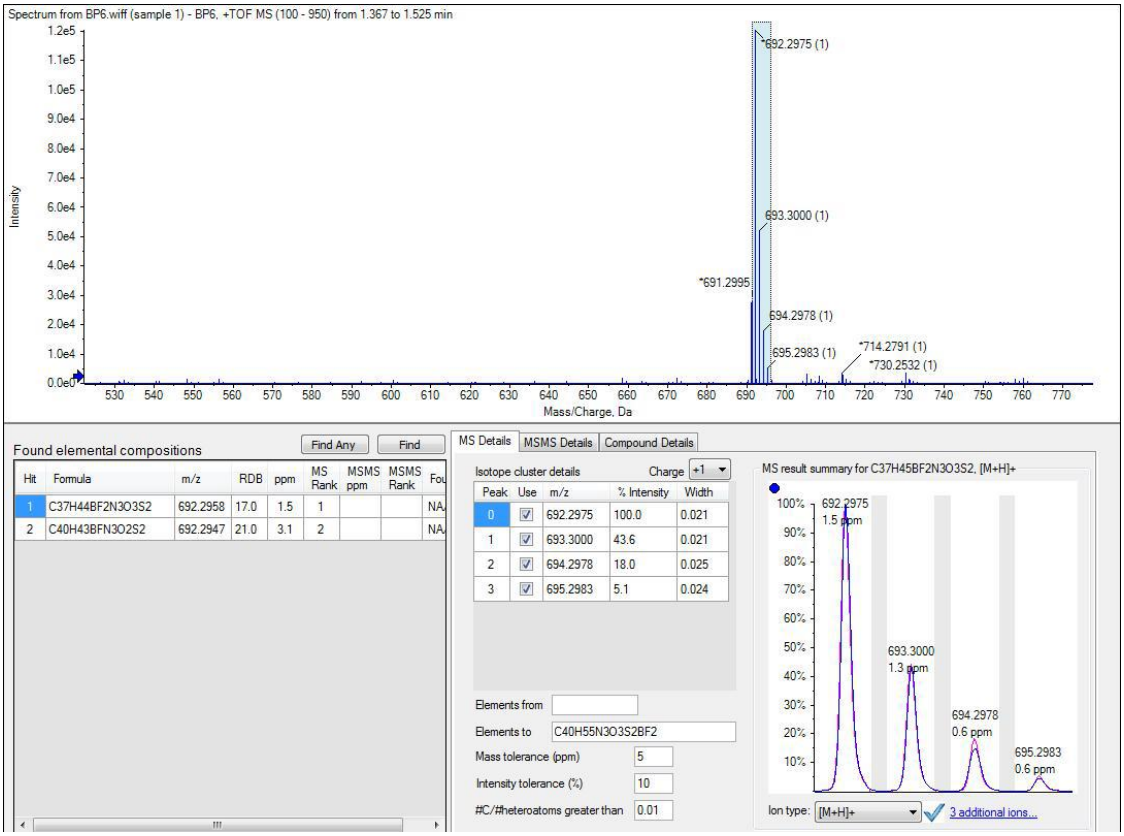

Figure S3. HRMS of probe **1**.

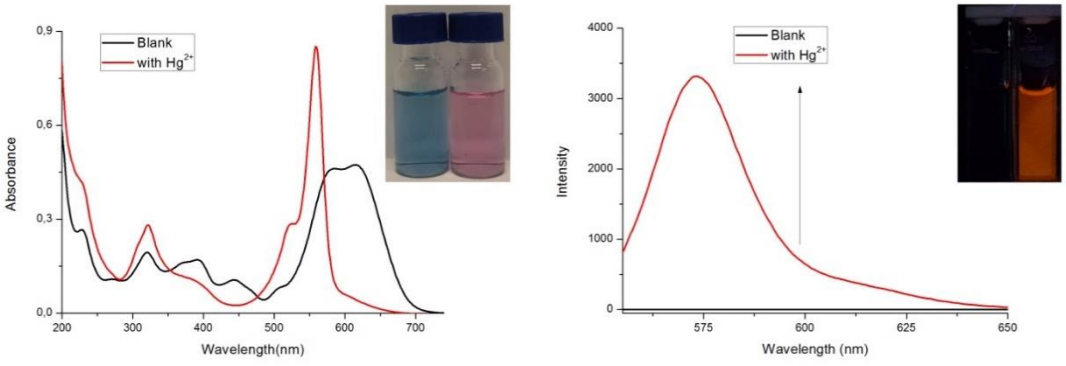

Figure S4. UV-visible and fluorescence spectra of **1** (5.0 x 10^{-5} mol L^{-1}) in water-acetonitrile 95:5 v/v solution at pH 7.0 upon addition of Hg(II) (20 eq.).

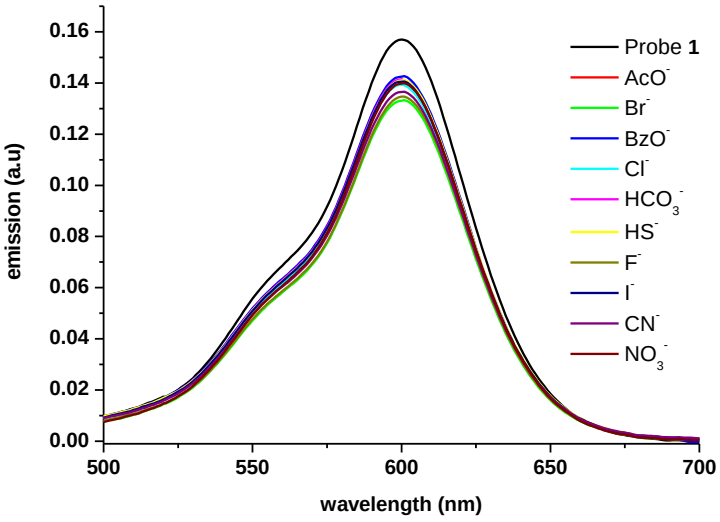

Figure S5. Fluorescence spectra of **1** (5.0 x 10^{-5} mol L^{-1}) in water-acetonitrile 95:5 v/v solution at pH 7.0 upon addition of selected anions (10 eq.).

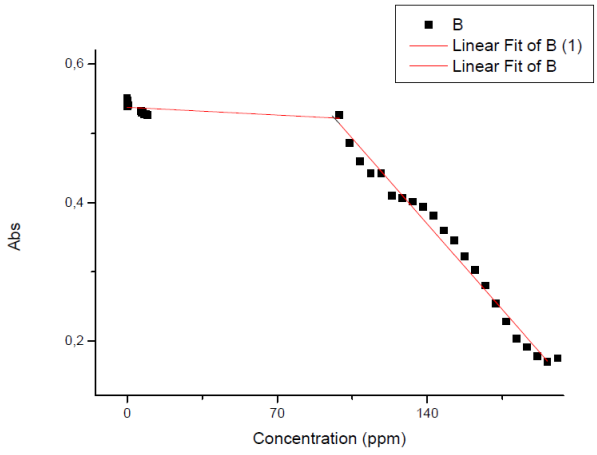

Figure S6. Calibration curve for probe **1** (5.0 x 10^{-5} mol L^{-1}) in water-acetonitrile 95:5 v/v solution at pH 7.0 upon addition of increasing concentrations of Hg(II).

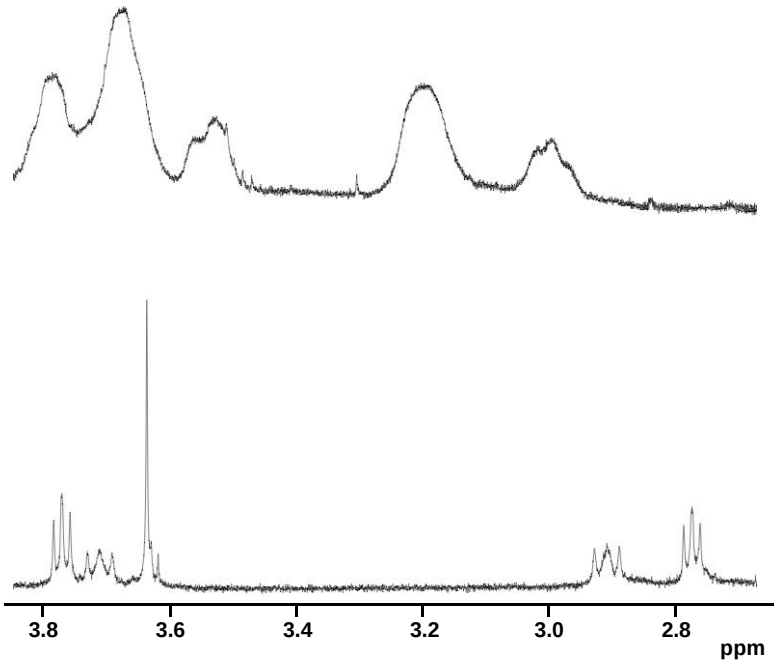

Figure S7. ^{1}H NMR fragment of probe **1** (deuterated acetonitrile) showing the macrocycle signals in the absence (down) and in the presence (up) of Hg(II) cation (1 eq).

References

[1] M. Baruah, W. Qin, C. Flors, J. Hofkens, R. A. L. Valle, D. Beljonne, M. Van der Auweraer, W. M. De Borggraeve, N. Boens, *J. Phys. Chem. A* **2006**, *110*, 5998.

[2] A. B. Descalzo, R. Martínez-Máñez, R. Radeglia, K. Rurack, J. Soto, *J. Am. Chem. Soc.* **2003**, *125*, 3418.

[3] B. García-Acosta, M. Comes, J. L. Bricks, M. A. Kudinova, V. V. Kurdyukov, A. I. Tolmachev, A. B. Descalzo, M. D. Marcos, R. Martínez-Máñez, A. Moreno, F. Sancenón, J. Soto, L. A. Villaescusa, K. Rurack, J. M. Barat, I. Escriche, P. Amorós, Chem. Commun. **2006**, 2239.

Chapter 5: Cucurbituril capped materials as tools for the determination of molecules of medicinal interest

Cucurbituril capped materials as tools for the determination of molecules of medicinal interest

Maria Lo Presti[1], José V. Ros-Lis[2,3], Félix Sancenón[1,2], Andreas Hennig[4], Werner Nau[5], Ramón Martínez-Máñez[1,2]

[1] *Instituto Interuniversitario de Investigación de Reconocimiento Molecular y Desarrollo Tecnológico. Universitat Politècnica de València - Universitat de València. Camino de Vera s/n, 46022, Valencia, Spain.*

[2] *CIBER de Bioingeniería, Biomateriales y Nanomedicina (CIBER-BBN).*

[3] *Inorganic Chemistry Department, Universitat de València. 46100, Burjassot, Valencia Spain.*

[4] *Institute of Chemistry of New Materials, Universität Osnabrück, Germany.*

[5] *School of Engineering and Science, Jacobs University Bremen, Bremen, Germany.*

NOTE: The experimental studies of this chapter are currently under development.

5.1 Abstract

Berberine and amantadine are two molecules of biological interest due to their use as drugs. In the present work, three sensing systems based on gated materials are prepared. Specifically, MCM-41 nanoparticles are loaded with Rhodamine B as a signalling unit, functionalized with different amines and capped with cucurbituril CB7. The amines used are cyclohexylamine, benzylamine and amantadine. The materials obtained are characterized by X-ray diffraction techniques and transmission electron microscopy, confirming the mesoporous structure of the nanoparticles. The prepared materials show a response to berberine and amantadine, which are able to remove the cucurbituril CB7 and release the fluorescent dye to the medium. The response of the materials to the two substances of interest (berberine and amantadine) depends on the chemical structure of the capping ensemble and is a function of the affinity constants between the analyte and CB7. The results obtained open the way to the use of molecular gates as berberine and amantadine probes.

5.2 Introduction

Berberine is a significant natural alkaloid widely used in traditional Chinese Medicine. It is a quaternary ammonium salt found in the bark, rhizomes, roots, and stems of Berberis vulgaris L. (Berberidaceae). It owns several therapeutic properties to treat several pathologies including heart and intestinal disorders, cancer, diabetes or infectious diseases due to its anti-inflammatory, anti-lipase, antioxidant, cholesterol-lowering, antihyperglycemic, antidepressant effects and antibacterial activity [1]. Moreover, amantadine, with its diamond-like structure, is applied in diseases such as Parkinson and viral infections, but it also offers a high potential for the treatment of depression, cancer, autism, diabetes, attention deficit hyperactivity, obesity, schizophrenia, recovery after spinal cord injury and cutaneous pain [2].

The wide applications of this drugs have generated a great interest in the development of novel methods of analysis of the content of these active substances. Reported methods for berberine detection include high performance liquid chromatography (HPLC) [3] capillary electrophoresis [4] and electrochemical analysis [5]. These methods have advantages of high sensitivity and selectivity, yet need complicated extraction processes, use of organic solvents and/or require expensive instruments or complicated procedures. Optical methods offer a suitable alternative, due to the advances derived from the application of electronics to the optical instrumentation and the advances in the software of analysis. Some examples of optical methods have been developed, including absorbance and emission techniques [6]. In addition, there are some reported methods for the detection of berberine using nanoparticles. Thus, the interaction of silica nanoparticles with berberine was studied to generate a spectrofluorimetric method in aqueous solution [7]. Also, a visual colorimetric method for the detection of berberine was proposed based on the aggregation of silver nanoparticles (AgNPs) resulting in colour change from yellow to green and to blue depending on the concentration of berberine [8].

Also, several examples of methods for the detection of amantadine have been reported, including high-performance liquid chromatography [9-12], gas chromatography [13, 14], capillary electrophoresis [15], potentiometry [16], and fluorimetry [17]. Due to the absence of chromophores in the amantadine molecule, it shows no distinct absorption in the UV region above 200 nm. Thus, direct UV spectrophotometry is not useful for its determination and only few spectrophotometric methods [18-21] have been reported for its determination. Unfortunately, these methods were sophisticated to perform and/or time consuming. Other interesting methods were reported, based on the oxidation of the drug and a charge-transfer complexation reaction, [22], a label-free piezoelectric immunosensor [23] or a Surface Plasmon Resonance Immunochip for the analysis of foods of animal origin [24]. In addition, there are some reported methods for amantadine detection using gold nanoparticles, [25-26] flower-like gold nanoparticles (AuNFs) and magnetic beads [27].

Controlled release systems based on molecular gates as platforms for the

development of optical sensors are a topic of interest due to its novelty, versatility and potency [28]. These gated materials can be constructed to finely tune the delivery of chemical or biochemical species from the mesopores to a solution in response to predefined stimuli, in the case of the chemosensors, the analyte. Such gated materials are composed of three modules: the support that contains the cargo and holds the recognition unit in the surface, the cargo to be released (typically a dye of fluorescent molecule) and molecular or supramolecular recognition entities (the recognition unit) that are activated by the analyte inducing cargo delivery.

Among capping units, the use of macrocycles such as cyclodextrins, crown ethers, calixarenes, pillarenes or cucurbiturils have been employed in gated materials [29]. Most of these systems using macrocycles rely on the formation of host complexes with guest molecules attached to the silica surface that, upon a chemical change in the guest (for instance protonation) or the presence of molecules able to form stronger complexes with the macrocycle induce the rupture of the host-guest complex and release of the entrapped molecule.

Berberine and amantadine have been reported to form strong inclusion complexes with cucurbiturils [30]. This ability has been used for example for the preparation of chromatographic columns functionalised with cucurbiturils [31]. However, the use of this capability has not been explored before for the preparation of gated materials for their detection. Based on the above we report herein a nanoparticulated mesoporous silica nanoparticles loaded with rhodamine B as optical signaling unit, functionalized with different coordinating units (i.e. bencil amine, adamantane amine and cyclohexyl amine) and capped with cucurbiturils. The materials were characterized and their ability to detect berberine and/or amantadine studied.

5.3 Materials and methods

- ***Reagents***

The chemicals tetraethyl orthosilicate (TEOS), n-cetyltrimethylammonium bromide (CTABr), sodiumhydroxide (NaOH), 3- iodopropyl)trimethoxysilane, triethylamine, (3-mercaptopropyl)- triethoxysilane, Rhodamine B, benzylamine, cyclohexanemethylamine, 1-Adamantanemethylamine, amantadine hydrochloride, cucurbit[7]uril hydrate, berberine chloride, methyl viologen dichloride hydrate, cadaverine, anthracene, epinephrine, were purchased from Sigma-Aldrich.

- ***Synthesis***

*Synthesis of the MCM-41 mesoporous silica nanoparticles (**S1**)*

1.00 g (2.74 mmol) of *n*-cetyltrimethylammonium bromide (CTABr) was dissolved in 480 mL of deionized water. Then, the pH, was basified by adding 3.5 mL of a 2 mol·L^{-1} NaOH solution and the temperature was increased to 80 °C. Then, TEOS (5.00 mL, 22.4 mmol) was added dropwise to this solution. Magnetic stirring was kept for 2 hours to give a white precipitate. Finally, the solid was isolated by centrifugation, washed several times with water and dried at 70 °C overnight (as-synthesized MCM-41). To obtain the final mesoporous nanoparticles (MCM-41), the as-synthesized solid was calcined at 550 °C using an oxidant atmosphere for 5 hours in order to remove the surfactant.

*Synthesis of iodine functionalized particles (**S2**).*

To prepare **S2**, first 200 mg of calcined MCM-41 nanoparticles **S1** and rhodamine B (76.64 mg, 0.16 mmol, 0.8 mmol/g solid) were suspended in H_2O (16 mL). The suspension was stirred at room temperature for 24 h. The resulting pink solid (**S1-loaded**) was isolated by centrifugation and dried at 37°C. Then, 250 mg of **S1-loaded** were suspended in 9.5mL of DCM, an excess of (3-iodopropyl)trimethoxysilane (293 µl, 1.5 mmol, 6 mmol/g solid) and of Rhodamine B (0.02 mmol, 9.5mg) were added, and the final mixture was stirred at room temperature for 5.5 h. The final solid **S2** was filtered, washed with 5mL of DCM and dried at 60°C overnight.

Synthesis of the uncapped materials

20 mg of **S2** were suspended in 1.6 mL of a saturated solution of the corresponding amine (benzylamine, cyclohexanmethylamine, amantadine) in toluene at 80 °C and 4.8 mL of triethylamine (1:3 v/v toluene-triethylamine ratio). The mixture was stirred and heated at 80 °C for three days. After this, the resulting solid was centrifuged, washed with acetonitrile and dried at 70 °C overnight. Depending on the amine used the materials obtained are **BEN-UC** (containing benzylamine), **CYC-UC** (containing cyclohexanmethylamine) and **ADA-UC**

(containing amantadine).

Synthesis of the capped materials

20 mg of the uncapped material (**BEN-UC**, **CYC-UC** or **ADA-UC**) were suspended in 5mL of 50 mM sodium phosphate buffer (pH 7.2) with an excess of Rhodamine B (0.76 mg, 0.0016 mmol) and 30 mg of CB7 and the suspension was stirred at room temperature for 21 hours. The resulting solid was filtered and washed with 50 mM sodium phosphate buffer obtaining the loaded capped materials **BEN**, **CYC** or **ADA.**

- ***Characterization of the materials***

The characterization of the tested materials was carried out by low-angle X-ray powder diffraction (XRD) with a Bruker D8 Advance diffractometer using CuKα radiation and by transmission electron microscopy (TEM, JEOL–jem-1010).

- ***Controlled release studies in solution***

Controlled release studies from **BEN**, **CYC** and **ADA** were performed in the presence of berberine (10 mM) or amantadine (2 mM). In a typical experiment, 2 mg of the corresponding solid were suspended in water and aliquots were taken at given times and filtered to remove the solid before analyzing. The solutions were measured with a Jasco FP-8500 Spectrophotometer (λ_{ex} = 546 nm, λ_{em} = 568 nm).).

5.4 Results and discussion

- ***Synthesis and characterization of the materials***

Following the approach of nanogated based sensors, a family of MCM-41 materials loaded with a fluorescent dye, functionalized with different amines having different affinity constants for CB7 and capped with cucurbituril units were prepared. MCM-41 in the nanometric range was selected due to their versatility and the possibility to induce cargo-controlled release in solution or in the cellular

media. The material was loaded with Rhodamine B, a fluorescent dye with high quantum yield widely used in sensing applications. The mesoporous material was functionalized with the amines benzylamine, cyclohexylamine and 1-adamantanemethylamine and capped with cucurbit[7]uril, via the formation of host-guest complexes with the attached amines (Scheme 1). Cucurbit[7]uril is a compound with strong binding constants with the two molecules of interest: berberine (Ka = 10^6) and amantadine (Ka = 10^{12}).

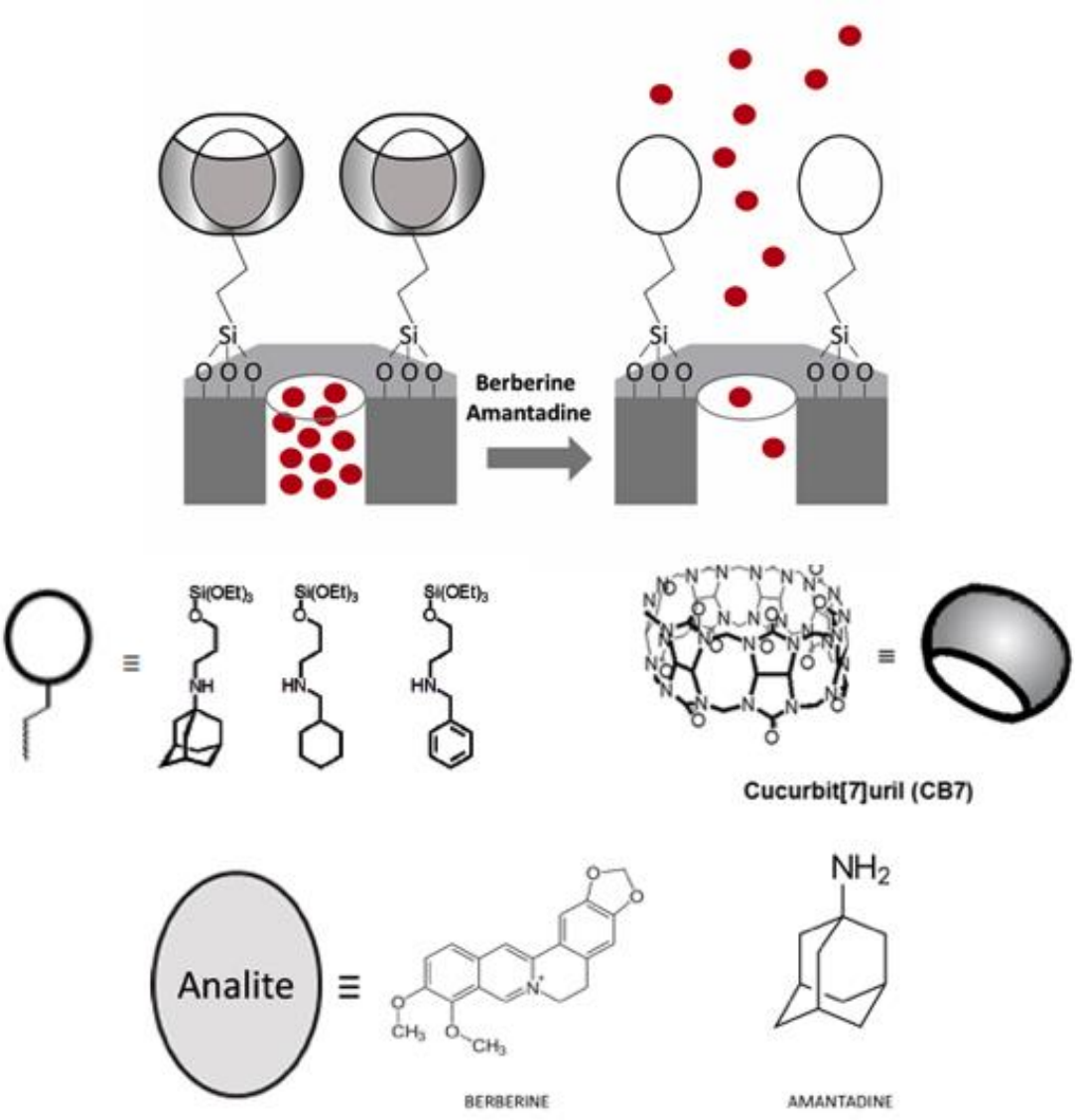

***Scheme 1**. Illustration of the controlled release mechanism and the main chemical blocks involved in the sensing process.*

More in detail the nano-MCM-41 particles were loaded with Rhodamine B in water and further modified with alkyl iodine groups in dichloromethane. The iodine group was displaced by the primary amines (benzylamine, cyclohexylamine or amantadine and further capped with cucurbituril CB7. The capping of the materials

was performed in presence of an excess of Rhodamine B to avoid a release of the fluorescent dye (Scheme 2).

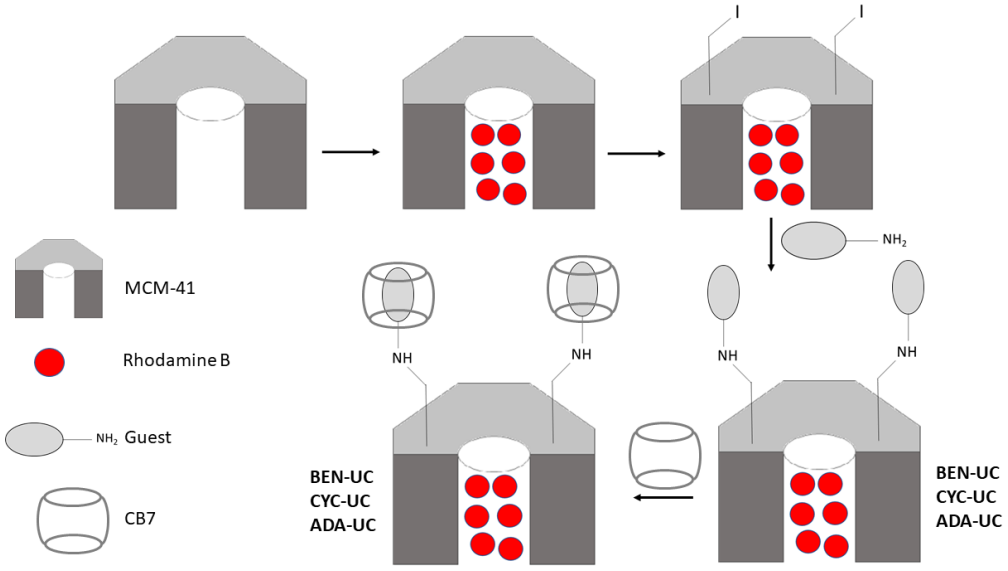

Scheme 2. *Summary of the synthesis procedure.*

The materials were characterized by TEM, XRD and controlled release assays. TEM of the MCM-41 support (Figure 1a) reveals that S1 is a material formed by particles in the nanometric range (80-100 nm). This structure is maintained during the loading and functionalization processes (Figure 1b). The XRD (Figure 1c) confirms the typical hexagonal distribution of the pores of the MCM-41 mesoporous system.

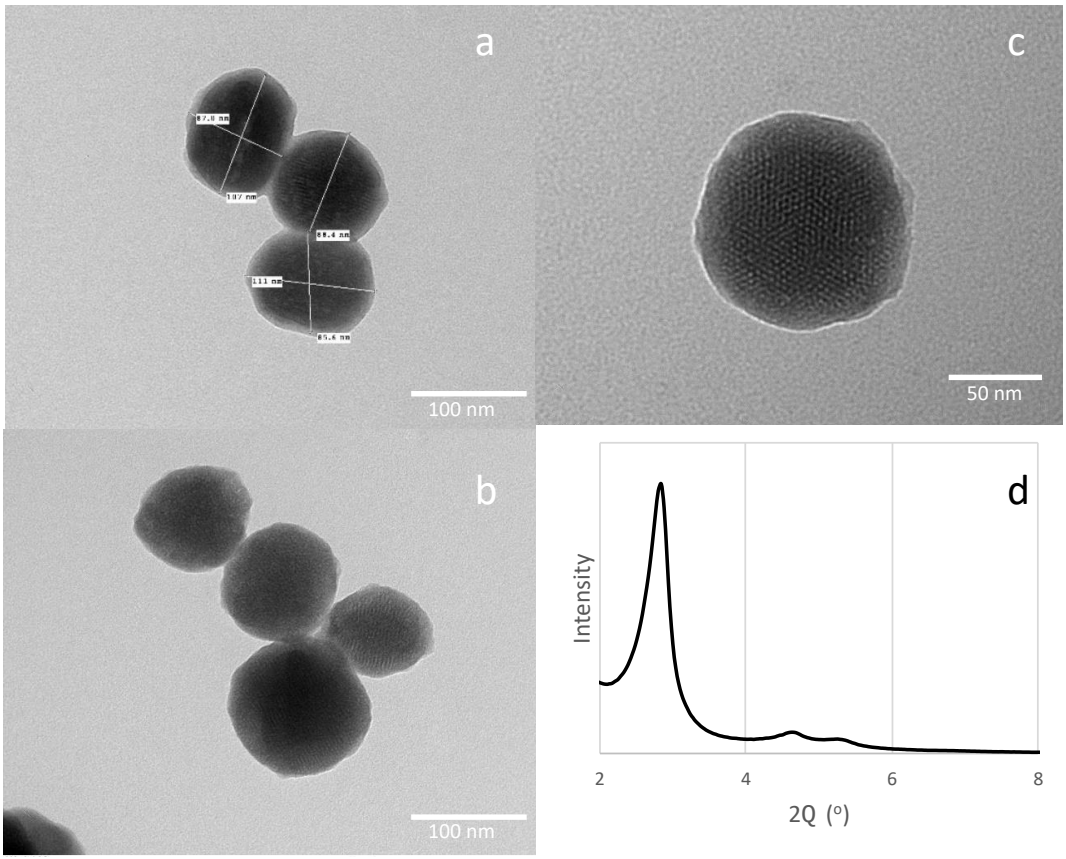

Figure 1**. a) TEM image of the calcined material **S1**, b) TEM image of the material loaded with Rhodamine B **S1-loaded**, c) TEM image of the functionalised material **S2**, d) XRD of **S1

As a final test to verify that the preparation of the nanogated system was successful, the three materials were exposed to 1-Adamantanemethylamine (AMADA). AMADA is a compound with a strong biding constant with CB7 (K = 1.0 x 10^{15}) [32], thus able to displace the cap. Also, cargo release in absence of AMADA was monitored and carried out as control. As can be seen in the Figure 2, all the materials (i.e **BEN**, **CYC** and **ADA**) showed increased fluorescent emission in presence of AMADA. The results also confirm that the materials offer a very low cargo release in PBS solution at neutral pH in the absence of AMADA.

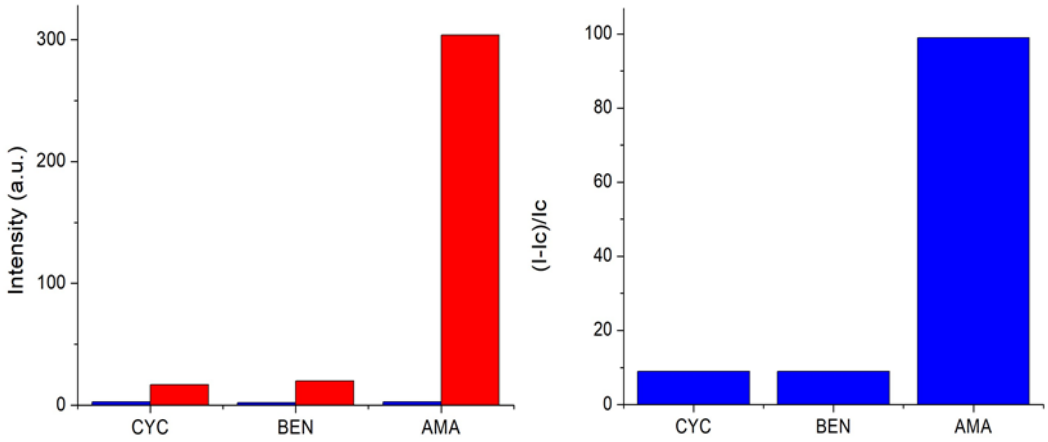

***Figure 2**. Left: fluorescence intensity measured after 3 h of contact of the materials in presence (orange) or absence (blue) of ADAMA. Right: relative fluorescence in presence of ADAMA. I: fluorescence intensity in presence ADAMA, Ic: fluorescence in absence of ADAMA.*

- ***Response to berberine and amantadine in solution***

Once it was verified that the materials were capped and that they could be uncapped by an analyte with a high affinity towards CB7, some other analytes of interest were tested using **BEN** as a model capped material. In particular experiments of cargo delivery in the presence of cadaverine, methyl viologen, anthracene, epinephrine, perfluorinated compounds (perfluoro-1,8-diiodooctane; 1,4-iiodoperfluorobutane; 1,6-diiodoperfluorohexane), berberine and adamantine were carried out. Only berberine and adamantine were able to uncap the materials. Encouraged with the promising results obtained in these studies a further analysis was performed for the three materials (i.e. **BEN**, **ADA** and **CYC**) with berberine and amantadine.

Berberine induced a poor cargo delivery for **ADA**. By contrast, **BEN** and **CYC** showed a high emission intensity in presence of berberine and very low cargo release in its absence. As can be seen in the Figure 3, the control (PBS) offers a flat line during the experiment (5h) with **BEN** and **CYC**, whereas the addition of

berberine induces a remarkable release of Rhodamine that grows over time. The behavior observed for **BEN** and **CYC** (cargo delivery in the presence of berberine) opposite to **ADA** (poor cargo delivery in the presence of berberine) could be explained by the binding constants. The constant amantadine-CB7 in solid **ADA** is the strongest thus is expected that this material present difficulties to be displaced by berberine.

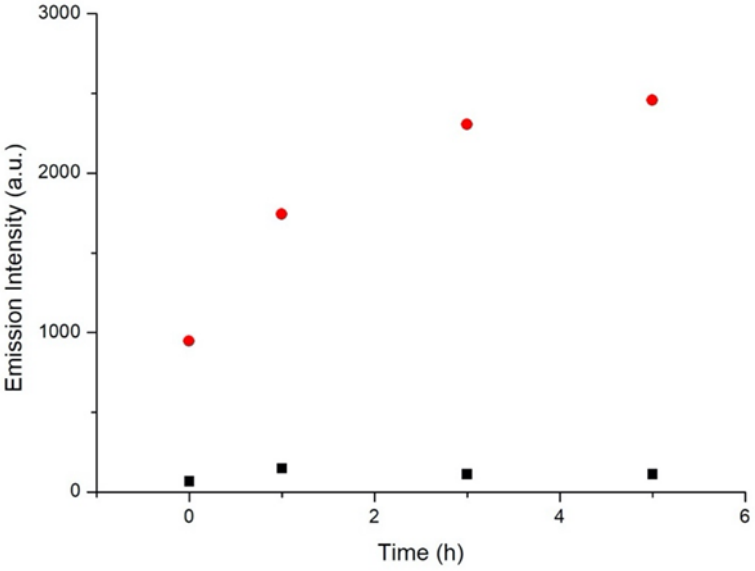

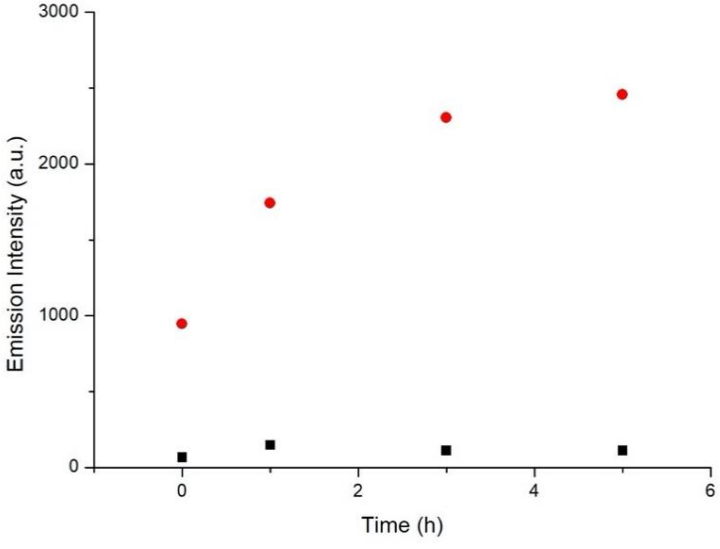

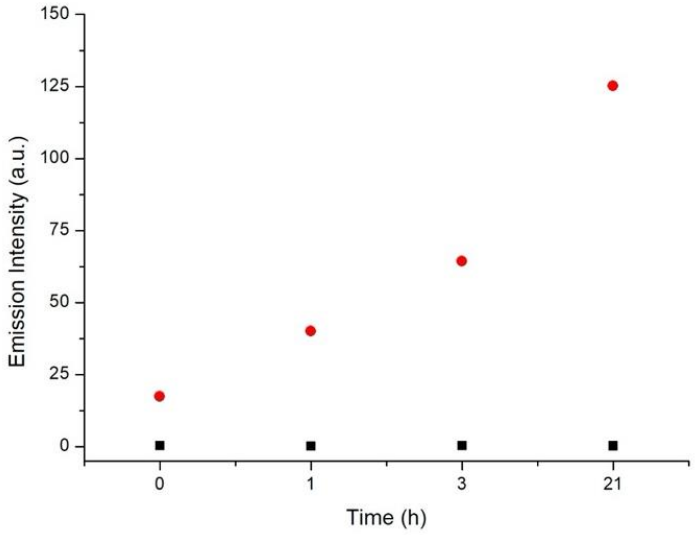

***Figure 3**. Fluorescence emission of **CYC** (up) or **BEN** (down) in presence of berberine 10 mM (red dots) or simply water (black squares).*

Adamantine was also able to induce the release of the encapsulated dyes (Figure 4). However, in this case both **ADA** and **BEN** responded to the analyte. Results from **CYC** were not reproducible and are not included here. The fluorescence intensity at 60 minutes shows that the **BEN** material offers a higher fluorescence intensity than **ADA**. This is in contrast to the response observed when both materials were exposed to AMADA, where the RhB release was substantially greater for **ADA** than for **BEN**. Further studied will be carried out in the future to explain this behavior.

Overall, the results above show that the capped materials **ADA**, **BEN** and **CYC** could be suitable chemosensors for the detection of amantadine and berberine.

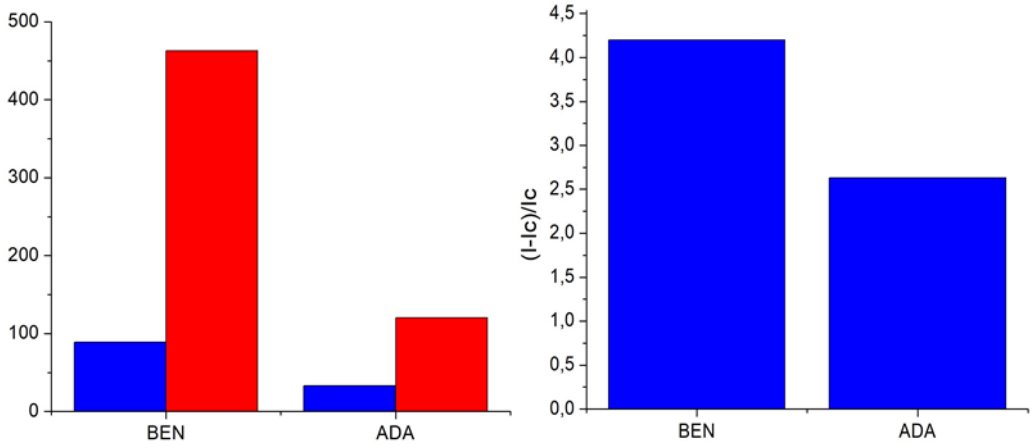

***Figure 4**. Left: fluorescence intensity measured after 1 h of contact of the materials in presence (orange) or absence (blue) of Amantadine (2mM). Right: relative fluorescence in presence of Amantadine. I: fluorescence intensity in presence Amantadine, Ic: fluorescence in absence of Amantadine.*

5.5 Conclusions

A family of nanogated materials capped with cucurbituril groups have been prepared. They respond to berberine and amantadine, two compounds of medicinal interest with good selectivity against other organic derivatives. The cyclohexylamine and benzylamine functionalized material show a good response against berberine. The benzylamine material responds also to amantadine reaching a fluorescence intensity 4 times higher than the control. These results suggest that these capped materials could be suitable probes for the fluorometric detection of adamantine or berberine in real samples and cells.

5.6 References

[1] X.J. Zeng, X.H. Zeng, Biomed. Chromatogr. 13 (1999) 442–444; S. Bandyopadhyay, P. H. Patra, A. Mahanti, D. K. Mondal, P. Dandapat, S. Bandyopadhyay, I. Samanta, C. Lodh, A. K. Bera, D. Bhattacharyya, M. Sarkar and K. K. Baruah, Asian Pac. J. Trop. Med., 2013, 6, 315–319; R. Gautam and S. M. Jachak, Med. Res. Rev., 2009, 29, 767– 820; L. M. Xia and

M. H. Luo, Chronic Dis. Transl. Med., 2015, 1, 231–235; C.M. Tian, X. Jiang, X. X. OuYang, Y. O. Zhang and W. D. Xie, Chin. J. Nat. Med., 2016, 14, 518–526; H. P. Kuo, T. C. Chuang, M. H. Yeh, S. C. Hsu, T. D. Way, P. Y. Chen, S. S. Wang, Y. H. Chang, M. C. Kao and J. Y. Liu, J. Agric. Food Chem., 2011, 59, 8216–8224.

[2] W. Danysz, A. Dekundy, A. Scheschonka, P. Riederer, J. Neural Transmission, 2021, 128(2),127-169.

[3] G. H. Liu, W. He, H. Cai, X. M. Sun, W. E. Hou, M. N. Lin, Z. Y. Xie and Q. F. Liao, Anal. Methods, 2014, 6, 2998–3008; P. L. Tsai and T. H. Tsai, J. Chromatogr. A, 2002, 961, 125–130; K. Suto, S. Kakinuma, Y. Ito, J. Chromatogr. A 786 (1997) 371–376.

[4] S. Uzasci and F. B. Erim, J. Chromatogr. A, 2014, 1338, 184–187.

[5] A. Geto, M. Pita, A. L. De Lacey, M. Tessema and S. Admassie, Sens. Actuators, B, 2013, 183, 96–101; J. F. Song, Y. Y. He and W. Guo, J. Pharm. Biomed. Anal., 2002, 28, 355–363.

[6] T. Sakai, Analyst 108 (1983) 608–614; Y. Liu, C.Z. Huang, Y.F. Li, Anal. Chem. 74 (2002) 5564–5568; X.-B. Zhang, Z.-Z. Li, C.-C. Guo, S.-H. Chen, G.-L. Shen, R.-Q. Yu, Anal. Chim. Acta 439 (2001) 65–71; T. Sakai, Analyst, 1991, 116, 187–190; Z. W. Hu, M. S. Xie, D. T. Yang, D. Chen, J. Y. Jian, H. B. Li, K. S. Yuan, Z. J. Jiang and H. B. Zhou, RSC Adv., 2017, 7, 34746–34754; P. Biparva, S. M. Abedirad, S. Y. Kazemi and M. Shanehsaz, Sens. Actuators, B, 2016, 234, 278–285.

[7] Q. Liu, Z. Xie, T. Liu and J. Fan, RSC Adv., 2018, 8, 6075–6082.

[8] J. Ling, Y. Sang, C.Z. Huang, J. Pharm. Biomed. Anal. 47 (2008) 860–864.

[9] F.A. Van der Horst, J. Teeuwsen, J.J. Holthuis, U.A. Brinkman, J. Pharm. Biomed. Anal., 8 (1990) 799-804.

[10] H. Yoshida, R. Nakao, T. Matsuo, H. Nohta, M. Yamaguchi, J. Chromatogr. A, 907 (2001) 39-46.

[11] R.F. Suckow, M.F. Zhang, E.D. Collins, M.W. Fischman, T.B. Cooper, J. Chromatogr. B: Biomed. Sci. Appl., 729 (1999) 217-224.

[12] H. Fujino, I. Ueno, S. Goya, Yakugaku Zasshi, 113 (1993) 391-395.

[13] H.J. Leis, G. Fauler, W. Windischhofer, J. Mass. Spectrom., 37 (2002) 477-480.

[14] D. Rakestraw, J. Pharm. Biomed. Anal., 11 (1993) 699-703.

[15] N. Reichova, J. Pazourek, P. Polaskova, J. Havel, Electrophoresis, 23 (2002) 259-262.

[16] N.T. Abdel-Ghani, A.F. Shoukry, S.H. Hussein, J. Pharm. Biomed. Anal., 30 (2002) 601-611.

[17] The United States Pharmacopeia 25, The National Formulary 20, US Pharmacopeial Convention Inc, Rockville MD, (2002) 101-103, 2256-2259.

[18] I.A. Darwish, A.S. Khedr, H.F. Askal, R.M. Mahmoud, IL Farmaco, 90 (2005) 555-562.

[19] J. Zhang, X.S. Zhang, G.P. Xue, Y. Guang, P.F. Xi, Anal. Chem., 22 (2002) 665-666.

[20] M. Sultan, Anal. Chem., 4 (2004) 103-109.

[21] M.S. Rizk, M.Sultan, Microchim. Acta, 143 (2003) 281-285.

[22] I. A. Darwish, A. S. Khedr, H. F Askal, R. M. Mahmoud, Journal of Applied Spectroscopy volume 73, pages 792–797 (2006).

[23] Y.G. Yun, M.F. Pan, LL. Wang, SJ. Li, YA. Wang, Y. Gu, JY. Yang, S. Wang, Anal. Bioanal. Chem., 2019, 411, 22, 5745-5753.

[24] MF. Pan, JY. Yang, SJ. Li, WJ. Wen, JP. Wang, YM. Ding, S. Wang, S. Food Anal. Methods, 2019, 12(4), 1007-1016.

[25] F. Zhu, J. Peng, Z. Huang, L. Hu, G. Zhang, D. Liu, K. Xing, K. Zhang, W. Lai, Food Chem., 257 (2018), pp. 382-387.

[26] W.B. Yu, T.T. Zhang, M.F. Ma, C.C. Chen, X. Liang, K. Wen, et al., Analytica Chimica Acta, 1027 (2018), pp. 130-136.

[27] M. Ma, J. Sun, Y. Chen, K. Wen, Z. Wang, J. Shen, S. Zhang, Y. Ke, Z. Wang, Food & Chemical Toxicology, 118 (2018), pp. 589-594.

[28] E. Aznar, M. Oroval, Ll. Pascual, J.R. Murguía, R. Martínez-Máñez, and F. Sancenón, Chem. Rev. 2016, 116, 561−718.

[29] BR. Tian, YM. Liu, JY. Liu, C*arbohydrate Polymers,* 2021, 116871; S. Alberti, G. Soler-Illia, O. Azzaroni, *Chem. Commun.* 2015, 51(28)*,* 6050-6075.

[30] Z. Miskolczy and L. Biczók, J. Phys. Chem. B 2014, 118, 2499−2505; Z. Miskolczy, L. Biczók and G. Lendvay, Phys.Chem.Chem.Phys., 2018, 20, 15986.

[31] L. Ma, S-M. Liu, L. Yao, L. Xu, J. Chromatograph. A, 1376 (2015) 64–73).

[32] S.J. Barrow, S. Kasera, M.J. Rowland, J. del Barrio, and O.A. Scherman, Chem. Rev. 2015, 115, 12320−12406.

Chapter 6: Conclusions

The preparation of optical chemosensors for chemical species of environmental and biological relevance is one of the most promising sub-areas within the supramolecular chemistry field. In particular, among chemosensors, those with optical properties are most interesting, since they allow rapid recognition using small amounts of samples, usually allowing in situ detection and in real-time measurements, avoiding the use of more complex and expensive techniques. This PhD thesis is an original scientific contribution to the evolution of this dynamic field and the studies have resulted in two articles published in high impact factor journals.

Organic, analytical and inorganic chemistry were combined in order to prepare molecular and hybrid probes for the optical detection of chemical species of environmental and biological relevance. We have designed, synthesized and evaluated two chemosensors that show very low LODs and are all capable of operating in water; this supposes a great advantage and novelty. Both were found to be selective with respect to the analyte of interest, trivalent cations and mercury.

In addition, a family of nanogated materials capped with cucurbituril groups have been prepared. They respond to berberine and amantadine, two compounds of medicinal interest.

The ***first chapter*** of this PhD thesis has been dedicated to introducing the fundamental principles of the supramolecular chemistry, especially about molecular recognition chemistry and about mesoporous silica materials.

In ***chapter 2***, the objectives attempted in the following experimental chapters have been stated.

In ***chapter 3***, a novel fluorescent chalcone-based chemodosimeter has been reported. It selectively detects Al^{3+}, Fe^{3+}, Cr^{3+}, As^{3+}, In^{3+} and Ga^{3+} over monovalent, divalent and lanthanide trivalent cations and anions in nearly pure water. Trivalent cations were able to induce a dehydration reaction on the dye that resulted in color changes from colorless to deep violet. Moreover, the addition of Cr^{3+}, Fe^{3+}, Al^{3+}, Ga^{3+}, In^{3+} and As^{3+} induced quenching of the emission of the ligand. The probe was also quite sensitive with LOD in the mM range.

Chapter 4 was devoted to the synthesis and characterization of a new BODIPY derivative electronically connected with a dithia-dioxa-aza macrocycle has been synthetized. The ligand showed a charge-transfer transition in the visible zone that was blue shifted in acetonitrile in the presence of Hg(II), In(III), Al(III) and Fe(III). The

same cations induced marked emission enhancements *(ca*. 700-fold enhancement for In(III)) upon coordination with the probe. Moreover, the selectivity was dramatically improved on changing the solvent to a more competitive media such as water (pH 7.0)–acetonitrile 95:5 v/v. In this medium, only Hg(II) induced a hypsochromic shift (together with a marked colour change) of the visible band and a remarkable emission enhancement.

In ***chapter 5***, a family of nanogated materials capped with cucurbituril groups have been prepared. They respond to berberine and amantadine, two compounds of medicinal interest. The cyclohexyl amine and benzylamine functionalized material show a good response against berberine. The benzylamine material responds also to adamantine reaching a fluorescence intensity 4 times higher than the control. These results suggest that this kind of materials could be suitable probes for the fluorometric detection of adamantine or berberine.

The results obtained during this PhD thesis provided new insights into the optical detection of chemical species of environmental and biological interest. Besides, our successful results in sensing of specific targets in aqueous media, also provide several potential applications that address some real problems, such as mercury pollution of water and suggests a possible use in living cells and real samples. On the other end, there are plenty of combinations of amines that could be used to prepare other nanogated materials capped with cucurbituril groups and also other analytes with high affinity towards cucurbiturils to be tested in aqueous media.

It is our hope that the results presented in this PhD thesis will inspire the development of new nanomaterials with application in different areas such as nanomedicine and sensing.

*Gracias a la **Generalitat Valenciana** por concederme una beca **SANTIAGO GRISOLÍA**.*